UNIVERSITÉ DE SHERBROOKE

Faculté de génie
Département de génie Mécanique

Simulation numérique de transfert de masse dans une cellule d'électrolyse d'aluminium

Numerical simulation of mass transfer in high temperature aluminium electrolysis cell

Thèse de doctorat
Spécialité: génie mécanique

Mohsen Ariana

Jury: Martin Désilets (directeur)
Pierre Proulx (co-directeur)
Marcel Lacroix
Gervais soucy
Laurent Birry

Sherbrooke (Québec) Canada January 2015

To my parents

To my brother and sisters, Hossein, Nahid, Afsaneh, and Leila

And to Mohammad

"Science may be described as the art of systematic oversimplification."

— *Karl Popper*

RÉSUME

L'étude des mécanismes de transfert de masse des ions dans le bain électrolytique dans une cellule d'électrolyse d'aluminium se heurte aux conditions sévères qui y sont rencontrées: haute température, milieu corrosif, etc.. Cependant, il est important de connaitre ces mécanismes de transfert en raison de leurs grands impacts sur les paramètres indicatifs du procédé d'électrolyse, par exemple l'efficacité du courant. Le calcul numérique est une façon de surmonter ces difficultés et d'éclairer les aspects moins connus du procédé de production d'aluminium. L'électrolyte utilisé pour l'électrolyse est composé par différents ions qui se déplacent dans un champ électromagnétique. Ce dernier est généré par le courant électrique intense qui passe par la couche d'aluminium et le bain. Le comportement dynamique des ions est sujet à leur gradient de concentration (la diffusion), à l'écoulement du bain (la convection) et au champ électrique (la migration). Dans le cadre de cette étude, le mouvement des ions est analysé et l'importance relative de la diffusion et de la migration est comparée en régime transitoire pour deux classes d'espèces électroactives et non-électroactives. Pour ces deux types d'espèces, on observe que la migration est le mécanisme dominant de transfert de masse dès les premières phases de l'électrolyse. Cependant, la diffusion devient graduellement le mécanisme le plus important aux électrodes pour des espèces électroactives comme $Al_2OF_6^{-2}$ et AlF_4^-. Le champ électrique et le champ de concentration ont été simulés à partir d'un modèle 2-D. Les résultats montrent qu'il y a un gradient de concentration entre l'espace inter-électrodes et la région proche de la couche de gelée. Par conséquent, il y a diffusion des espèces entre ces deux régions qui vient diminuer le gradient de concentration et ainsi éviter l'épuisement des ions $Al_2OF_6^{-2}$ ou la surconcentration des ions AlF_4^-. En outre, un code libre a été développé et implémenté sur OpenFOAM (une plateforme libre de librairies C++). Ce code est capable de résoudre simultanément les équations du champ électrique, du transfert de masse et de Navier-Stokes. Les principaux apports de cette thèse, tel que les modèles et résultats obtenus, peuvent éclairer les mécanismes de transfert de masse dans le bain et aux électrodes et ainsi améliorer leur compréhension.

Mots clés : Aluminium, électrolyse, transfert de masse, études numériques

ABSTRACT

The harsh conditions of electrolytic bath in aluminium electrolysis cell have been an obstacle against the understanding of mass transfer that is at the origin of the aluminium production process. This knowledge is of great importance due to the impact that it could have on the functional parameters of the cell like current efficiency. Numerical modelling is a way to overcome the difficulties and to shed light over the hidden aspects of the electrochemical process. The electrolyte typically used in an aluminum electrolysis cell is composed of different ions moving in the electromagnetic field generated by the high intensity current needed for this industrial application. The behaviour of these ions is under the influence of concentration gradients (diffusion) and depends also on other phenomena in the cell like bath flow (convection) and electric field (migration). In this study, the coupling between these fields is treated for 1D and 2D models of the cell. The relative importance of migration and diffusion are compared for two different categories of electroactive and electroinactive ions in a transient model. For both categories of ions, migration is the dominant form of mass transfer in the very first stages of electrochemical process. However, diffusion becomes the dominant mechanism of mass transfer for electroactive ions in developed boundary layers. In 2D model, there is a concentration gradient between interelectrode and near sidewalls region. Consequently, there is a diffusion of ions in and out of the interelectrode space to diminish the depletion or overconcentration of certain electroactive ions like $Al_2OF_6^{-2}$ and AlF_4^- at the electrodes. Furthermore, the impact of convection and bath equilibrium in addition to a more suitable mass transfer model has been studied on a parallel plate electrodes reactor. Finally, an open source library is developed and built on OpenFoam (an open source C++ CFD platform) that is capable of solving mass transfer equations for different models. The description and findings of this thesis will shed light on the mass transfer mechanisms in both bulk region and boundary layers, and can be used for further studies in this field.

Key words: aluminium, electrolysis, mass transfer, numerical simulation

ACKNOWLEDEGMENTS

First and foremost, I wish to express my sincere thanks to my advisor Martin Désilets for all of his supports during this period. These past five years were full of the desperate moments in which I have lost my confidence and motivation, and I survived those moments by his hopeful advices and encouraging and enlightening comments. I would also like to appreciate another great collaborator, my co-advisor Pierre Proulx, whose ideas were always great source of inspiration. The joy and enthusiasm he had during our long scientific discussions were so motivational and contagious for me. I will be always grateful for what I learnt from you both during these years.

I would like to thank thesis committee members, Dr. Laurent Birry, Prof. Gervais Soucy and Prof. Marcel Lacroix for their time and helpful comments to improve the quality of this work.

I would also like to give a heartfelt, special thanks to Dr. Brahim Selma and Nicolas Laroche for their great help and contribution in developing OpenFOAM models. The long working sessions was a memorable experience of teamwork and collaboration.

At the end, I would like to send special thanks and love to my friends, Mohammad Gholami, Barzin Rajabloo, Dr. Amir Masoud Abdollahzadeh, Behnam Norrizadeh, Reza Saghaee, Dr. Ali Shahverdi, Dr. Alireza Hekmat, Pierre Lecomte, Lou Lecuyer, and Geneviève Lajoie and all other friends that helped me in pursuit of my scientific and daily life during these years.

At the end, no word can describe how grateful I am to my family and especially to my parents for supporting me during my PhD studies and also for tolerating the distance between us during these past five years. I found still no way to describe how my brother, Hossein, and my Sisters Nahid, Afsaneh and Leila have been helpful and inspiring to me during my whole life. I feel blessed to have such a family, and will be always grateful to them.

TABLE OF CONTENTS

LIST OF FIGURES

LIST OF TABLES

1. INTRODUCTION

1.1 Production of aluminium

Aluminum has become one of the most important metals used in many aspects and different fields. The special particularities of aluminum and its alloys like its low density, flexibility, thermal, and electrical conductivity have made it one of the most appealing metals. Due to increasing demand for aluminium in various fields, the aluminium production industry has become an outstanding industry.

The most developed method, and still the only industrial process in operation, to produce aluminium is through the electrolysis of the aluminium oxide, alumina, in a cell containing a molten salt called bath between two electrodes. This process is called the Hall-Héroult process. There are generally two major industrial electrolysis cells that use this process, the Söderberg cells and the Hall-Héroult cells. Söderberg cells use a continuous anode created by addition of pitch continuously to the top of the submerged anode. In contrary to Söderberg cells, Hall-Héroult cells use prebaked anodes which lead to better product quality and less environmental effects [1]. Nowadays, the prebaked cells are more developed and more common. In this study, the general term of electrolysis cell refers to prebaked Hall-Héroult cell, and Söderberg cells are not included in this study.

1.2 Aluminium electrolysis cell

Hall-Héroult cell is the industrially scaled aluminium production cell, and is composed of two electrodes and a molten solution between them. The Hall-Héroult process uses the electrical energy to reduce alumina (Al_2O_3) to the pure aluminium by means of reactions taking place at the electrodes. This process occurs at high temperature (≈965˚C) and the solid alumina is injected and dissolved into the molten bath for the continuity of the process. Figure 1.1 shows schematically the prebaked aluminium electrolysis cell.

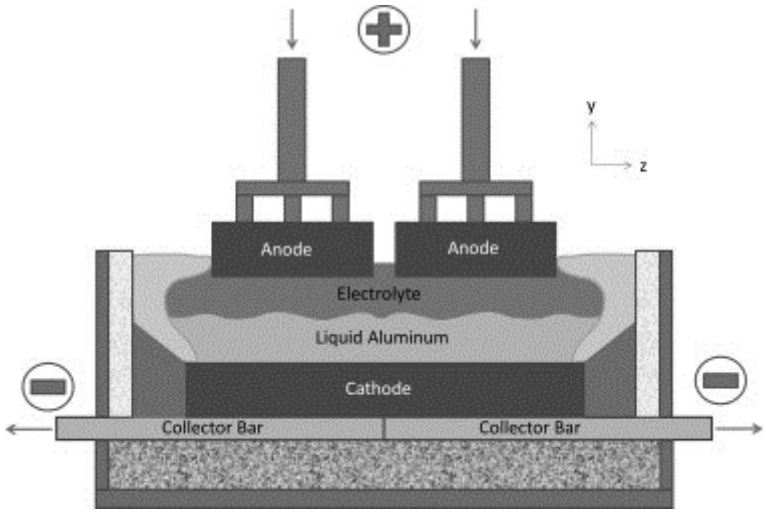

Figure 1.1Schematic of modern aluminium reduction cell [2]

1.2.1 Bath

Electrolytic bath or more briefly bath is the technical term that is used for the solution of alumina into cryolite (Na_3AlF_6) in addition to other additives. The purpose of adding these additives like AlF_3, CaF_2, MgF_2 and LiF into bath is to control thermophysical properties of the bath in the favorable range [3].

Aluminium is produced from alumina that is fed into the bath each 3 to 5 minutes to keep alumina concentration in favorable range. As it is given in reaction 1.1, carbon dioxide is the other product of the cell reaction.

$$2Al_2O_3(dissolved) + 3C(s) \rightarrow 4Al(l) + 3CO_2(g) \qquad 1.1$$

The above reaction presents the simplified overall reaction that leads to aluminium production. However, the production of aluminium and carbon dioxide are the last steps of a series of homogeneous and heterogeneous reactions that takes place in the bath and at both electrodes, respectively [1]. In other words, the dissolution of alumina in the molten bath results in different ions and complexes. These ions need to be transferred to

the electrodes in order to participate in electrochemical reactions. These electrochemical reactions produce aluminium and carbon dioxide and other ions that affect the initial composition of the cell [1]. However, the alumina is injected into the bath continuously to prevent the bath of being depleted of alumina and to keep the bath composition almost uniform. This leads to keep the electrochemical and thermophysical properties of the cell constant and helps to prevent the probable instabilities in the cell.

The movement of these ions and species in the bath is at the origin of macroscopic transport phenomena in the cell like electrical current and bubble flows. Generally speaking, the transport phenomena in the cell can be classified into four major categories of:

1. Mass transfer (ion transfer in bath)
2. Momentum transfer (bath and metal flow)
3. Heat transfer (energy balance)
4. Charge transfer (electric current)

In spite of the fact that each of the four transport phenomena refers to a particular physical phenomena, they are highly coupled to each other. In other words, the profile of concentration, velocity, temperature and current density in the cell affects the other fields and is affected by any change in other fields. Figure 1.2 illustrates schematically the mutual interaction of these four fields in the high temperature electrolysis cell of aluminium.

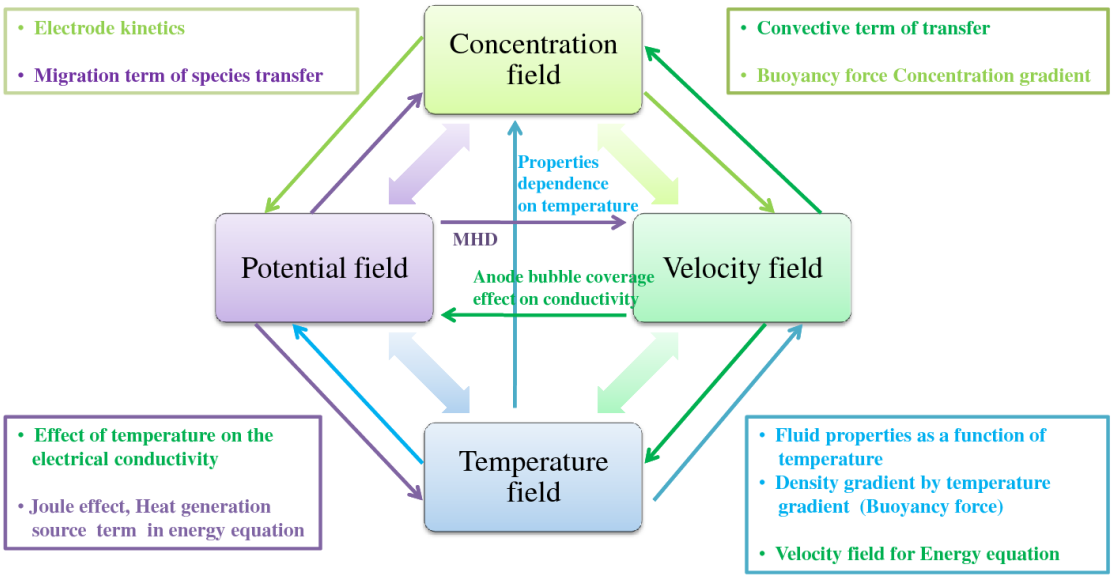

Figure 1.2 The fields and their mutual couplings in aluminium electrolysis cell

The electric current that passes through the bath is the source of the energy and cause of electrochemical reactions in the cell. The high amperage electric current which enters from anode and passes through electrically resistive bath generates the main heat source in the cell by Joule heating. This heat source provides the enthalpy of fusion of molten electrolytic bath. The electric current through molten salt is conducted by the movement of ions and is called ionic conductivity [4, 5]. Unlike the conductivity in solids, the importance of free electron in bath conductivity is limited and negligible for many cases [6, 7].

The other aspect of the cell is the flow of the bath in the inter-electrodes space. The current passes through aluminium layer after leaving the bath. The aluminium layer is formed by the produced aluminium at cathode that is sedimented under the bath due to its higher density. The electric current flow through this highly conductive layer in addition to the magnetic field generates the so-called Lorentz force. Lorentz force is the source of hydrodynamic flow in the aluminium layer which is transferred to the bath, and is one of the sources of momentum in bath. This interaction between electromagnetic field and

velocity field is called magnetohydrodynamic effect (MHD). MHD is one source of hydrodynamic instability in the cells and is a limiting parameter in the design of the cells [8].

There are other sources that affect flow pattern in the bath. The bubbly flow under the anode and Marangoni effect are two other sources of momentum transfer in the bath. As mentioned previously, CO_2 and Al are two major products of electrolysis cell. The CO_2 is produced at the anode by oxidation of carbonaceous anode. The rate of production of this species in gaseous state is high enough to be followed by CO_2 nucleation, the bubble growth, and finally the detachment of the bubble from anode surface. Although the first two stages are affecting the convection scheme of the very near anode region slightly, the latter that is ignited by the momentum of turbulent flow in the cell is accelerated until the bubble release, and is an important local momentum source [9, 10]. Moreover, like other bubble generating reactions, the bubble nucleation on the lower anode surface has a limiting effect on the reaction source. In other words, the CO_2 bubbles or film (depending on the level of turbulence in the cell) is a resistive film for electric current flow and also for the ions heading to anode to participate in anodic reactions.

The closing ring of the chain of phenomena in the cell is mass transfer in the cell that takes place in the ionic form due to high temperature liquid electrolyte. The ion transfer in the cell is at the origin of bath conductivity [5]. The major charge carrying ion in the bath is Na^+ ions moving from anode to cathode. The other ions have minor role in carrying charges across the bath [11].

Based on the described coupled fields, solving mass transfer problem requires focusing on four other preliminary problems. These problems include:

1- thermodynamic, reactions and kinetics of the cell,
2- the current density profile in the electrolyte and on the electrodes,
3- temperature profile and heat transfer effects,
4- and the velocity of the bath.

The assumption of an isothermal cell will reduce the problem to three problems of mass transport of the cell, electric field, and velocity field. The simultaneous or segregated consideration of these aspects of the cell indicates the level of complexity and nonlinearity of the mass transfer analysis in the cell.

The thermodynamic, homogeneous and heterogeneous kinetics of the cell also need to be taken into account because they are closely linked to mass transfer in the cell. The homogenous reactions in the cell are the reactions that occur when alumina is dissolved in the bath. The alumina dissolution in the bath forms the different ions and complexes in the cell. However, there is still controversy over the reactions and the produced ions after these reactions [1]. The heterogeneous reactions are the electrochemical reactions at the cathode and at the anode. These reactions are the electrochemical reactions responsible to produce aluminium over the cathode surface and carbon dioxide on the anode surface. Nevertheless, the details of these electrode reactions are not clear and several models have been proposed for these reactions. One reason for the importance of mass transfer in this analysis is that electrode reactions are mostly mass transfer controlled, and the lack of mass transfer or the lack of one of the mechanism of mass transfer can lead to depletion of this species near the corresponding electrode [3]. Therefore, the favorable reaction of oxidation or reduction will be replaced by other side reactions which are undesirable or less favorable for current efficiency of the cell.

Such undesirable reactions in the cell are called back reactions which are responsible for the efficiency loss in the cell. As an example of this, take the aluminium already produced in the cathode that migrates to anode and that is oxidized to become alumina. It is believed that this reaction is caused by the migration of Al from cathode to anode [3]. The term migration indicates that Al dissolution in bath forms aluminium fluoride anions which are negatively charged. So, the electric field forces these negatively charged ions to move toward the anode where their oxidation produces alumina. This indicates another important aspect of mass transfer of ions on the functional parameters of the cell like current efficiency and the amount of produced aluminium.

1.3 Research project description

Briefly, the analysis of the mass transfer in high temperature aluminium electrolysis cell provides important information about the mutual interaction of different fields which can be used later on to predict, to control, and to optimize the functionality of aluminium electrolysis process. The harsh and corrosive ambience of the bath has been an important obstacle to study experimentally the bath mass transfer patterns to the extent that even our knowledge on the kinetics of reactions and of the ionic composition of the bath is limited. Based on this brief description, the basic question of the research project is: 'By using numerical simulation, is it possible to analyze the transient behavior of ionic mass transfer in the bath by considering the impacts of other coupled thermophysical problems like current density, reactions and kinetics, and flow? '.

As mentioned earlier, the focus of this study will be on the mass transfer in the bath. Consequently, the diffusion or penetration of bath in lower surfaces like cathode block or cast iron is not of the interests of this study. In fact, the domain of study will be limited by anode on the top, cathode on the bottom, sidewalls on sides of the cell and bath in the middle of these boundaries.

1.4 Research project objectives

1.4.1 Principal objectives

The principal objective of this study is to develop a numerical model representing the mass transfer patterns for different ions in the bath and to use it to study the transient behavior of ions in an aluminium electrolysis cell. This study will take into account the possible mechanisms of mass transfer and compares the importance of each mechanism for each ion in each stage of electrolysis process.

1.4.2 Specific objectives

To reach the principal objective of this study, it is necessary to fulfill certain specific objectives:

1. To provide the cell with an integrated ionic model, which can be applicable to the proposed electrode reactions and existing transport equations and parameters.
2. To study one dimensional mass transfer for different ions in between two electrodes. This model will take into account the migration and diffusion in the bath on the interelectrode line.
3. To study the electric current distribution in two dimensional cell considering the electrode reactions kinetics at both electrodes.
4. To study transient mass transfer of different ions in the bath for the 2D electrolysis cell. This objective is coupled with the third objective as the current density predicted at the previous objective will affect the ions movement in the cell.
5. To solve Maxwell-Stefan equation for mass transfer of the ions in the concentrated molten salt by implementing new libraries and solvers in open source software called OpenFOAM (Open source Field Operation And Manipulation). This code can be used for further studies on numerical simulation of coupled fields in electrochemical systems.

1.5 Contribution, originality of this study

As discussed earlier, the corrosiveness and high temperature functioning condition of the cell are major obstacles which make the analysis of the cell very difficult. These limitations are to the extent that even the chemical composition of the bath and also electrochemical reactions over electrodes are controversial subjects. Furthermore, the tight coupling between reaction kinetics, electromagnetic, hydrodynamic and chemical phenomena in the bath makes the numerical simulation of the mass a complex nonlinear,

highly coupled, time-consuming mathematical problem. Accordingly, there have been limited numbers of studies about the mass transfer analysis in the bath [12-14].

In spite of the complexity of the mass transfer problem in aluminium electrolysis cell, the importance and necessity of this study cannot be denied. The core of this important problem is based on the fact that most of reactions at electrodes are mass transfer controlled. In other words, mass transfer mechanisms are responsible to provide electrodes with the needed electroactive species. The lack of these species at the electrodes leads to other reactions, which are not desirable, and reduces the current efficiency of the cell. The other important aspect of the mass transfer analysis is its effects on the other fields like bubble evolution pattern under the anode surface, joule effect and temperature profile in the bath and finally hydrodynamic stability of the cell. Although considering all of these mutual effects of different fields demands a complicated numerical simulation, even the simplified decoupled models for mass transfer can provide us with valuable information that can be used to develop more complicated multi-field models.

Considering the importance, difficulties and limitations related to this subject, the contributions of this study are:

- Modeling one dimensional transient behavior of ions in the interelectrode space between anode and cathode considering the migration and diffusion as major mechanisms of mass transfer and turbulent diffusion to introduce the impact of turbulence in the system.
- Modeling the 2D current density distribution in the cell by considering the kinetics of electrode reactions at the anode and at the cathode and also the effect of bubble coverage under the anode area.
- Modeling the effect of turbulent diffusion through a mathematical model based on two dimensional geometry of the cell.

- Modeling the transient behavior of ions movement in the cell under the impact of electric and velocity fields.
- Development of an open source code which can be used and developed to model coupled phenomena in electrochemical systems.

The originality of this study can be summarized in these major aspects:

- I developed the first model to treat the mass transfer problem in the bath for NaF-AlF_3-Al_2O_3 system. This study includes the mass transfer analysis at both electrodes and inside the interelectrode space.
- The mass transfer model developed considers the migration of each species in the cell based on electric current density profile.
- The importance of each mechanism of mass transfer like diffusion and migration has been studied over the period during which the concentration profiles are evolving near the electrodes.
- The effect of turbulent diffusion has been added to the mass transfer equations through the wall distance mathematical model for 2D geometry of the cell.

1.6 Thesis plan

The thesis is to be presented in 6 chapters.

Firstly, the purpose of present chapter is to introduce the motivations, objectives, originalities and contributions of this study. In this chapter the general overview of research project and the problem to be face is described.

However, the details of the problem to be solved are given in the second chapter, state of art. The originality of the research objectives and its contributions in scientific and industrial fields are discussed in details in this chapter after having presented a review of other related studies in this field. The purpose of this chapter is to define the scientific frontier of known-unknown and done-undone around the subject of mass transfer in

aluminium electrolysis cell. As stated previously, the coupling between different fields makes the area of research a vast area including different subjects like:

- The electrochemical kinetic of reactions over the electrodes and current density distribution over the electrodes and in the electrolytic bath.
- The reaction and thermodynamic in the bath, the physicochemical properties of the ions in the bath and also the bath as the composition of these ions.
- The mechanisms of ion transfer in the bath and mass transfer problem in molten salt electrolytes.

The third chapter concentrates on the mass transfer in the interelectrode one dimensional distance. The purpose of this chapter is to analyze the concentration profiles formed at electrodes after the electrochemical reactions and also the diffusion and migration fluxes for each electroactive and electroinactive ions moving in the bath. The results and discussion of 1D modeling is also presented in this chapter. The model presented in Chapter 3 does not take into account the homogeneous reactions in the bath.

In one dimensional analysis of mass transfer in the cell, the current density is constant and the effect of current density distribution on migration flux is neglected. Therefore, there is a need for two dimensional analyses which can add the force of electric field on the ions. Chapter 4 presents a two-dimension model for electric current distribution in the bath. The mass transfer equations are solved by using the results obtained for current density distribution from the first model. This analysis generalizes the mass transfer pattern for two categories of electroactive and electroinactive ions in the cell and considers the evolution of diffusion and migration flux vectors, which are not necessarily in normal interelectrode direction. The simulation is done inside a finite element package, COMSOL Multiphysics and the results and discussion of the results are presented in the same chapter. However, homogenous reactions in the bath are considered only to calculate the initial concentration of species. Moreover, the model used to calculate the

concentration equations are mixture averaged Maxwell-Stefan equations, that are simplified form of Maxwell-Stefan equation.

In Chapter 5, a new C++ is developed to model transport phenomena in electrochemical systems. This code is built on OpenFOAM, an open source C++ platform that is capable of treating multiphysics structure of electrochemical cells. In chapter 5, the homogeneous reactions and also Maxwell-Stefan equations are implemented into codes and are solved for a parallel-plate electrolysis cell. The results and discussions are presented in the same chapter.

The final chapter concludes the final overview of this research project, the original findings of this study which can contribute to scientific and industrial purposes. Finally, the perspectives of this research project that can be proposed to continue this study in future works are illustrated.

2 STATE OF ART

This chapter draws a picture over the different studies on the mass transfer analysis in the cell. This literature review aims to distinguish the originalities of the present study compared to the previous studies in this field. As illustrated in previous chapter, the mass transfer analysis cannot be studied without considering different transport phenomena in the cell. Mass transfer in electrolytic solutions covers the description of ions movement and dynamics, material balances, electric current distribution, and fluid mechanics [15]. The general form of the problem is a nonlinear multiphysics problem. The consideration of the coupling between these different transport phenomena defines the complexity of mathematical model to be solved.

Most of the studies that have been done on the transport phenomena in the cell simplify the coupled nonlinear high-temperature turbulent physics of the electrolyte to a simpler decoupled or weakly coupled linear mathematical problem [12-14]. In this chapter, we try to illustrate the models related to various aspects of mass transfer in the cell with special focus on the studies over electric current density and mass transfer patterns in the cell.

2.1 Current density distribution and electric potential field

The current density distribution in aluminium electrolysis cell has been studied extensively through experimental and numerical methods [16-20]. There are three major mathematical models for simulation of electric current distribution in the electrochemical cell. These three models are known as primary, secondary, and tertiary current distributions in the cell. The source of difference between the different models lies on the consideration of the interaction between electrode reaction current and electrode kinetics and species concentration [15] .

The application of primary current distribution to the aluminium electrolysis cell sets the overpotential to be constant for any current density [21]. This makes the numerical calculation of the system easier by simplifying the Newman boundary conditions for electric potential to Dirichlet boundary condition. This model is suitable for the applications in which the effect of electrode kinetics can be neglected. The advantage of this assumption is that it is possible to solve it through many commercial codes [22].

Secondary current distribution considers the limiting impact of electrode overpotential on the current. This model is applied to aluminium electrolysis cell in different studies with different models for electrode reaction kinetics. Based on this model, overpotential varies with electrode current density and the correlation between current density and overpotential is typically exponentially nonlinear (Butler-Volmer general form) or linearized form of Butler-Volmer equation [20]. The linear or nonlinear form of Butler-Volmer correlation can be a limiting criterion for the use of software package tools capable of solving secondary current distribution in the cell.

Finally, tertiary current distribution assumption is used to treat transport phenomena by considering the effect of mass transfer on the current density profile. Generally, this model couples the charge transfer and mass transfer equations. Solving of the coupled equations demands highly robust programming methods and high computing capacity clusters. To the author's knowledge, there has not been any study using this method to model mass transfer and current density in aluminium electrolysis cell.

2.2 Mass transfer in aluminium electrolysis cell

As stated before, there is still controversy over the homogeneous (bath) and heterogeneous (electrode) reactions and consequently over the ionic composition of the electrolytic bath [1, 3]. Therefore, the studies that have been done on the mass transfer of these species are limited. The harsh and corrosive ambiance of bath is the reason of the lack of sufficient data on the kinetics of reactions, thermophysical properties of species,

and consequently the limited number of studies on the mass transfer of the cell. The studies on mass transfer include the studies over:

- Transport properties of the ions in the bath (dynamics of species in the bath)
- Studies over the non-ionic and ionic mass transfer in the bath

These two aspects of the mass transfer are related and will be discussed in details in the following sections.

2.2.1 Dynamic properties of the ions

The study of transport properties in high temperature salts is always a challenge because of the problem of high temperature and the corrosiveness that increases dramatically at high temperature. This difficult condition can be less important for the measurement of some thermophysical parameters like conductivity, density, and viscosity. However, the determination of dynamic properties of ions like diffusion and mobility in molten salts is more complicated compared to the above properties [23]. Nonetheless, there are some studies over the dynamics of species and ions in the electrolytic bath with special focus on the mobility of these ions in electrolytic bath. The percentage of the current that is transferred by each ion in the bath is called transference number [24]. The main charge carrier in the bath is the focus of many studies in the dynamics of ions in the bath. It has been found that Na^+ carries the largest fraction of charge through the bath [25]. In most of studies, the main charge carrier in the bath is Na^+ ions, to the extent that the transference number of Na^+ is proposed to be 0.99. The high transference number of Na^+ and F^- ions is justified by the fact that their size is smaller than fluoro-aluminate complexes in the bath and there is less friction against their movement [5, 11]. However, it should be noted that transference number is varying with the composition of the bath [24]. For example, the transference number of Na^+ reduces to 0.74 by adding AlF_3 to Na_3AlF_6 melt [6, 26].

2.2.2 Non-ionic and ionic mass transfer in aluminium electrolysis cell

The mass transfer in aluminium electrolysis cell can point out to several different phenomena in the cell. The microconvection near anode surface which points to nucleation, growth, and detachment of CO_2 bubbles that is followed by the diffusion of CO_2 in the bath [27-29]. Another important aspect of mass transfer concerns the alumina injection to the cell and its dissolution in molten bath. Alumina is added to the bath each 3 to 5 minutes. The rate of dissolution and diffusion of the resulting complexes is important to prevent the depletion of electroactive species over both electrodes.

While the diffusion of CO_2 and solid alumina in the bath are known as the two-phase diffusions or two-phase flow, the molecular mass transfer of ionic compounds can be classified as another type of phenomena that takes place in the cell. As stated previously, the number of studies that have been done on the latter are conducted to fulfill different objectives. These objectives includes different phenomena in the cell like degradation of cathodic block, diffusion of bath in cathodic block, crystallization of bath on the cathode surface, and current density distribution near the cathode[12-14]. The difficulties of measurement in the harsh condition prevailing in the bath make any of these studies a valuable work for better understanding of ions and complexes behaviour in the cell. However, the literature suffers from the lack of enough knowledge and data on thermophysical properties due to these limitations [1, 3]. Consequently, this makes the simulation of the cell more difficult than expected for conventional electrochemical systems.

By classifying the different aspects of mass transfer modelling of the cell, it can be said that there are three major steps to pass to model mass transfer inside electrochemical cell. These steps are:

- Reactions and chemical composition of the cell
- Mechanisms of mass transfer in aluminium electrolysis cell (migration and convection)

- Diffusion modelsfor dilute solution and concentrated solution theories

2.2.3 Reactions and chemical composition of the cell

The first step in the study of mass transfer in the cell is to define the reaction and the species participating in these reactions. The species and also the reaction mechanisms in the bath are still controversial subjects. Consequently, there are many models that have been proposed for the reactions and for the resulting ions in the cell. Furthermore, these different models are for different electrolyte systems with different additives and different cryolite ratio (CR) [3]. These models include $NaF\text{-}AlF_3$ and $NaF\text{-}AlF_3\text{-}Al_2O_3$ systems and also the systems that consider other minor additives like CaF_2, MgF_2 and LiF. These chemical models for the dissolution of alumina and other additives in the bath do not necessarily propose the electrochemical models for the reactions at electrodes. Therefore, one challenge is to find a chemical model that is consistent with existing electrochemical models. One way to overcome this problem is to consider simple models that have been proposed for the ionic composition of the cell, in order to be able to make it compatible to the electrochemical reactions. The $NaF\text{-}AlF_3$ system is one of those studies that is used in the few conducted studies on mass transfer of ions near the cathode [12-14]. This model is composed of ions of form AlF_x^{-y} like AlF_4^- and AlF_6^-. These two latter ions are known to be the species that react at the cathode to produce aluminium [1, 3, 30]. Therefore, $NaF\text{-}AlF_3$ presentation of the chemical composition of the cell makes it possible to take into account reduction of species at the cathode and to study mass transfer in the cathode diffusion boundary layer. Nonetheless, the weakness of this model is its incapability to consider alumina dissolution in bath and its effect on mass transfer. Moreover, the ions participating in anode reaction are found to be in form of $Al_xO_yF_z^{n-}$ that are products of alumina dissolution in the bath. Considering the reactions over anode are important since this can affect the concentration profiles in bulk and also in cathode diffusion layers. In other words, according to some studies, the species produced at the anode, AlF_4^-, will be reduced at cathode to produce aluminium. Consequently, considering the models that include anode and cathode reactions at the same time are

describing the real cell problem more realistically compared to those that consider only the reduction reaction at cathode. Therefore, for the simulation of mass transfer in the whole cell model, $NaF\text{-}AlF_3\text{-}Al_2O_3$ system is preferable compared to $NaF\text{-}AlF_3$ system.

Having defined the ionic composition of the system, the ions move from anode or cathode diffusion layer under the influence of electric field and bath flow. The major mechanisms of mass transfer in electrochemical cells are diffusion, migration, and convection [15]. However, not all of the mechanisms are necessarily included in the studies due to the physics of the cell, the region of study and the assumptions that are made. In the next sections, the importance and application of mass transfer mechanisms in previous studies for aluminium electrolysis cell will be discussed thoroughly.

2.2.4 Migration of ions in the electrolytic bath

Migration is the force exerted to charged species capable of moving in the sea of other ions. It is dependent on the ion charge and size [31]. Therefore, the studies that consider cell composition as a compound of uncharged complexes may neglect the migration flux[13]. Moreover, the migration might be neglected partially (for certain species) due to the transference number attributed to the ions [14]. For example, as illustrated in detail in section 2.2.1, the mobility of Na^+ ions is higher than that of the other ions in the cell. So, considering Na^+ as the only species with migration flux leads to neglect the migration flux for other ions [14] . In a more inclusive approach, Gagnon et al. has considered the 1-D migration flux of anions in cathode pores and in the cathode diffusion boundary layer for AlF_3-NaF system by using the Nernst-Einstein equation to calculate mobility of ions [12, 15]. It should be noted that the magnitude of migration flux vector is proportional to current density vector magnitude, and its direction is tangent to current density streamlines. Therefor, 1-D simulation of migration flux does not take into account the variation in direction and magnitude of current density vectors.

A more complete analysis can be done by finding the current density distribution and electric potential profile for a two-dimensional geometry of the cell. This electric model

can take into account the kinetics of reactions at both electrodes. Then, the migration flux for all charged species in the bath can be calculated in the mass transfer model based on the results obtained for electric field as it is already done for simpler dilute solutions [32-36]. Moreover, the electric conductivity is a function of ionic conductivities (function of concentration) of ions and can be calculated from the concentrations of mass transfer model. According to Gagnon et al, the electrical conductivity is almost constant in the aluminium cell bath, although it varies in the porous electrodes space [12].

2.2.5 Effect of convection on mass transfer in the electrolytic bath

Another important mechanism of mass transfer is the movement of the bulk of fluid by the momentum transfer. This mechanism establishes the impact of velocity field on the concentration field. There have been many studies on the modelling and controlling of velocity field in aluminium electrolysis cell. It is well-known that magnetohydrodynamic force and bubbly flow under the anode surface are the main two sources of momentum in the cell. In most of the mentioned studies that have been done on modeling the mass transfer in the bath, the bulk is considered as a well-mixed zero-gradient concentration solution whereas there is a diffusion boundary layer near the electrodes especially for electroactive ions[14]. This is explained by the fact that the flow is turbulent and the convection plays a very important role in the mass transfer of ions in the bulk far from the sidewalls and electrodes. To analyze the effect of convection on the concentration profile of the species in the bath, the systematic method would be to couple the Navier-Stokes equations with mass transfer equations and to resolve them simultaneously. Although this method is feasible for conventional electrochemical cells [34, 37, 38], its application on the aluminium electrolysis cell demands dealing with bubbly flow under the anode and MHD effect on the aluminium layer.Multiphase models are needed to be applied to take into account the momentum transfer between bath and aluminium and bubble layers [29, 39]. Also, the rigorous analysis of MHD calls for the inclusion of all geometrical aspects that is influencing the magnetic fields, like steel shells, busbar arrangements, etc. In the end, you have to solve a very large numerical problem,

involving the construction of a very complex mesh of the cell and its auxiliary equipments. It definitely becomes outside of the scope of an academic problem! Nevertheless, there have been many studies to simulate MHD and bubbly flow without considering mass transfer.

From one side, aluminium layer is the region where the electromagnetic force acts on the fluid. This force transfers from aluminium layer to the bath and influences the bath velocity field. The MHD force is a destabilizing factor in the cell, and there have been many concerns to control and to stabilize the flow in the cell [40-47].

From the other side, CO_2 is a product of anode reaction and starts to nucleate on the anode surface. The nucleation and growth of bubbles on the anode surface leads to microconvection over the anode surface that has been subject of some studies [9, 48]. However, the major interaction between bath and bubbles are the next step which is bubble detachment of anode surface and its acceleration and release out of the bath [9]. The bath momentum forces the ions to leave anode surface after reaching certain contact angle to the surface. In the next step, the flow of bubbles accelerates and exerts momentum on the bath flow. The modeling of bubbles nucleation, growth, detachment, collision, and release is done through Lagrangian approach for bubbles and Eulerian Navier-Stokes equation for bath [48]. The effect of MHD force also needs to be added as the momentum source or as the force exerted by third phase that is aluminium layer [29, 41].

Solving the momentum equations simultaneously with mass transfer and electric field that are already coupled through migration term demands a robust solving algorithm and high capacity computational systems. Moreover, the next question that could be asked is about the efficiency and necessity of treating the mass transfer problem in this way.It is reasonable to find a way to consider the effect of turbulent convection in the cell without solving the momentum equations. The concept of turbulent diffusion is helpful to have the effect of turbulent mixing near the walls. The turbulent diffusion coefficient which is

added to the molecular diffusion coefficient is proportional to the length of eddies of the turbulent flows and a function of the distance from the wall. This method is introduced by Levich and has been adapted to electrochemical turbulent cells by Newman [15, 49]. The turbulent diffusion was considered in the cathode diffusion boundary layer of aluminium electrolysis cell in previous studies [12, 14]. These studies use a 1-D geometry for the cathode zone, so turbulent diffusion coefficient is found easily as a function of distance from cathode surface. However, there has been no study for calculating the turbulent diffusion coefficient for 2-D geometries of electrochemical cell. In fact, there is a need for a geometrical model to calculate the wall distance as a field by taking into account the walls and boundaries of a 2-D geometry of the cell. This model has been developed in the present study. It should be noted that the wall distance field has been formulated and introduced by Fares, and to the author's knowledge, the present study is the first application of this concept to calculate turbulent diffusion coefficient [50].

2.2.6 Diffusion and dynamics of ions in the electrolytic bath

The electrode reactions of electroactive species, migration flux of charged ions, and convective flow of bulk of fluid affect the initial composition of the bath and form concentration gradients. The dynamics of mobile ions in solution tends to smooth the concentration gradient through diffusion of ions. The models to describe the dynamics of ions is different for different type of solutions.[15]. There are two major assumptions for the dynamics of the cell: dilute solution theory and concentrated solution theory.The dilute solution theory describes the flux of each ion to be a function of the same ion concentration gradient and independent of other ion concentration profiles. This theory is applicable to binary or dilute solutions. There have been many studies about modelling the mass transfer inside different electrolysis cell using dilute solution theory [32-34, 36, 51]. Generally, this method cannot be applied to multicomponent concentrated solutions since the flux of each ion is dependent on the friction force between these ions and the other ions [15]. In other words, the concentrated solution theory takes into account the interaction of each two ions and sum up the effects.

Molten salts are classified as concentrated solutions, and the theory of concentrated solution is valid for the molten salts. However, the difficulties in calculating the binary diffusion coefficient and other thermochemical properties of ions due to high temperature of molten salts make it a difficult task to apply the concentrated solution theory to the molten salts. Therefore, the other possible approach is to modify the dilute solution formulation for the multicomponent mixtures. This alternative approach uses the mixture average properties instead of binary properties of multicomponent mixtures for each species [52].

In case of aluminium electrolysis cell, there have been different approaches to model the mass transfer of ions and complexes in the cell. Gagnon et al. considers the dilute solution theory (Nernst-Planck equation) to model the dynamics of ions in the 1-D cathode pores and cathode diffusion layer [12]. Solheim applies the binary fluxes (simplified Maxwell-Stefan equations) for the dynamics of the species in the cell with simplifying the flux of each ion [14]. These two works are the main studies that have been done on modeling the mass transfer analysis for 1-D cathode diffusion boundary layer. To the author's knowledge, there has been no study on the mass transfer in whole cell that is cathode diffusion boundary, anode diffusion boundary layer and bulk of the bath. Moreover, mass transfer analyses that are limited to 1-D studies do not consider the current density streamlines in bath and its distribution over the electrodes.

Based on what is stated about the different studies on the mass transfer analysis of aluminium electrolysis cell, the originalities of the present study in each of the mentioned sections can be summarized as below:

Current density distribution and electric potential field:

- 2D whole cell model
- Bubble hyperpolarisation
- Butler-Volmer model

Reactions and chemical composition of the cell

- $NaF\text{-}AlF_3\text{-}Al_2O_3$ system
- Dissolution of alumina modeling
- Anode and cathode reactions

Migration of ions in the electrolytic bath

- 2D current density and migration vector field in the bath

Effect of convection on mass transfer in the electrolytic bath

- Applying 2D geometrical model to include the impact of turbulence in mass transfer

Mass transfer models

- Using mixture averaged mass transfer method
- Using Maxwell-Stefan's equation for 1D model

In next chapters, the mathematical models, the obtained results and required discussions will be done, and the conclusions will be presented in last chapter.

CHAPITRE 3 : AVANT-PROPOS

Auteurs et affiliation:

- Mohsen Ariana: étudiant au doctorat, Université de Sherbrooke, Faculté de génie, Département de génie mécanique.
- Martin Désilets : professeur, Université de Sherbrooke, Faculté de génie, Département de génie chimique et de génie biotechnologique.
- Pierre Proulx : professeur, Université de Sherbrooke, Faculté de génie, Département de génie chimique et de génie biotechnologique.

Date d'acceptation: 5 mars 2013

État de l'acceptation: version finale publiée

Revue: Proceedings of Light Metals 2013, 2013 TMS Annual Meeting & Exhibition

Référence: [53]

Titre français: Une étude numérique du transfert de masse des ions dans le bain électrolytique d'une cellule d'électrolyse d'aluminium

Contribution au document: Cet article contribue à la thèse en élaborant une simulation 1-D du transfert de mass des ions dans les couches limites de l'anode et de la cathode et dans le bain afin de pouvoir comparer les différents mécanismes de transfert de masse.

Résumé français : Le bain électrolytique est la solution fondue à haute température de la cryolite et de l'alumine. Comme tous les bains de sel fondus, il est composé des ions se déplaçant sous l'effet de la migration et de la convection. Le mouvement et la concentration des ions ont un impact considérable sur les paramètres fonctionnels du procède, tel que l'efficacité du courant. Cette étude modélise le transport des ions du système $NaF\text{-}AlF_3\text{-}Al_2O_3$ sous l'effet de la turbulence, du champ électrique et des

réactions hétérogènes aux électrodes en utilisant la simulation par éléments finis. Pour les ions électroactifs, les résultats montrent que la migration est le mécanisme de transport le plus important au début de la simulation. Toutefois, le régime permanent atteint, c'est la diffusion qui devient prépondérante pour le transport des ions proche des électrodes. Pour les ions non-électroactifs, la migration reste majoritaire et le rapport des flux de diffusion et de migration s'approche au maximum de l'unité en régime permanent.

3 NUMERICAL ANALYSIS OF IONIC MASS TRANSFER IN THE ELECTROLYTIC BATH OF AN ALUMINIUM REDUCTION CELL

3.1 Abstract

In the Hall-Héroult process, the electrolytic bath is a molten solution of cryolite and alumina. Like all other molten salts, it ends up in different moving ions driven by mechanisms such as convection, diffusion and migration. The motion of these ions and their concentration distribution are important because they determine many functional macroscopic parameters of the electrolytic cell like current density distribution, heat generation, back reactions, current efficiency, and mass-transfer controlled reactions at the electrodes. In this study, a numerical model for the fluxes of most important ions in a NaF-AlF_3-Al_2O_3 system has been proposed. The reactions in the bath and the resulted ions have been added to the reactions that take place at the cathode and anode, and a finite element model has been presented for the electrolyte portion of the aluminium reduction cell. The transient motion of the different ions under the migration and diffusion mechanisms have been modelled based on the classical mass transfer equations. The results illustrate the significant role of the migration in the early stages of electrochemical process. This mechanism is also the dominating effect in the motion of electroinactive species. For larger time scales, because of the depletion of the consumed species and accumulation of the produced species near the electrodes, the mass transfer is dominated by the diffusion.

3.2 Introduction

In the Hall-Héroult production process, alumina is dissolved in molten cryolite at high temperature. This molten solution, called the bath, is composed of different charged ions

moving in an electric field, a few of them being involved in the reactions at electrodes. Most of them can be considered as rapid reactions due to the high temperature prevailing inside the cells. However, the flux of ions has an important impact on the electrochemical reactions since the motion of these ions is at the origin of the mass transfer controlled reactions. Also, another important functional parameter of the cell, the current efficiency, is greatly influenced by the species mass transfer. It is well known that current efficiency is inversely proportional to the rate of back reaction [3] . The source of the back reaction is the chemical dissolution of aluminium in the bath, its mass transfer toward the anode and finally its oxidation by CO_2 [3] . From this point of view, defining the mass transfer mechanisms can be viewed as the fundamental analysis of the loss of current efficiency in the bath.

Despite the importance of the current density and the mass transfer controlled reaction at the anode and cathode, the experimental measurement of the flux or concentration of these ions is very difficult due to high temperature and harsh conditions inside the electrolysis cell [1, 3] . The driving forces for the different mechanisms of ionic mass transfer are either the electric field or the concentration gradient of each ion in the bath. The convection also plays an important role in the mixing of these ions.

Modeling of the mass transfer in the cell thus couples four different fields: electric, concentration, velocity and temperature fields. There have been many modeling studies dedicated to the analysis of several of these fields. Zoric et al. [20, 54, 55] modeled the electric potential and current densities in the cell by applying the secondary current distribution assumption for a two dimensional cell. More recently, Solheim [13]predicted the mass fractions of NaF, AlF_3, Al_2O_3, and CaF_2 in order to analyze the rate of cryolite crystallization. His model is based on the resolution of the Maxwell-Stefan diffusion equation for different ions in the bath near the cathode [14] . Gagnon et al. solved the coupled Nernst-Planck and Poisson's equations to simulate the ions concentration near the cathode for a NaF-AlF_3 electrolyte [12] . These two latter studies are the most recent works on mass transfer modeling in an aluminium reduction cell. There have been other

studies focusing on the convection and mass transfer in the cell, however, these studies are not considering ions in the cell nor the motion of these ions based on migration or diffusion mechanisms [27-29] .

For the first time in this study, the mass transfer of charged ions in a NaF-AlF_3-Al_2O_3 mixture is predicted by considering diffusion, migration, and electrochemical reactions at both electrodes in a full cell model.

3.3 Model

The ionic composition of bath is a controversial subject. In fact, the ions and complexes in the bath are not completely defined yet and different ionic equilibriums have been proposed. In addition, the reactions that take place at the electrodes are not well defined [1, 3] . This situation certainly explains some of the difficulties inherent to the development of a whole-cell mass transfer model.

3.3.1 Homogeneous reactions

The initial composition of bath is based on the dissolution of alumina in cryolite, as modeled by Zhang and Rapp (9). These authors consider five simultaneous reactions and five products, as it is shown below:

$$\frac{1}{3}Al_2O_3(s) + 2NaF(l) + \frac{4}{3}AlF_3(s) \rightarrow Na_2Al_2OF_6(l)$$

$$\frac{2}{3}Al_2O_3(s) + 2NaF(l) + \frac{2}{3}AlF_3(s) \rightarrow Na_2Al_2O_2F_4(l)$$

$$\frac{2}{3}Al_2O_3(s) + 4NaF(l) + \frac{2}{3}AlF_3(s) \rightarrow Na_4Al_2O_2F_6(l) \qquad 3.1$$

$$3NaF(l) + AlF_3(s) \rightarrow Na_3AlF_6(l)$$

$$NaF(l) + AlF_3(s) \rightarrow NaAlF_4(l)$$

The molar fractions of the above species are calculated by considering the activities of Al_2O_3, AlF_3, and NaF given by the following relations:

$$\begin{aligned}
[Na_2Al_2OF_6] &= K_1 {a_{NaF}}^2 {a_{AlF_3}}^{\frac{4}{3}} {a_{Al_2O_3}}^{\frac{1}{3}} \\
[Na_2Al_2O_2F_4] &= K_2 {a_{NaF}}^2 {a_{AlF_3}}^{2/3} {a_{Al_2O_3}}^{2/3} \\
[Na_4Al_2O_2F_6] &= K_3 {a_{NaF}}^4 {a_{AlF_3}}^{2/3} {a_{Al_2O_3}}^{2/3} \\
[Na_3AlF_6] &= K_4 {a_{NaF}}^3 a_{AlF_3} \\
[NaAlF_4] &= K_5 a_{NaF} a_{AlF_3}
\end{aligned} \qquad 3.2$$

Where K_i are the equilibrium constants, and a_{NaF}, a_{AlF3}, and a_{Al2O3} are the activities of NaF, AlF_3, and Al_2O_3, respectively. Moreover, the value of activities and equilibrium constants are functions of temperature and cryolite ratio, as given by Zhang and Rapp [56] . It should be noted that bath is assumed to be saturated in alumina. In consequence, the activity of alumina is equal to unity [57] .

It is well known that the only cation in the system is Na^+, in such amount that it surrounds all other anions [3] . Therefore, in this study, it is assumed that the complexes on the right hand side of above reactions directly dissociate into Na+ ions and its corresponding anion.

3.3.2 Heterogeneous reactions

There have been several mechanisms proposed for reactions that take place at the electrodes [1, 3] . In this study, a single one step global reaction is assumed at both electrodes.The global anodic reaction is given as:

$$2{Al_2OF_6}^{-2} + 4F^- + C \rightarrow 4{AlF_4}^- + CO_2 + 4e \qquad 3.3$$

For the cathode, the global reaction can be expressed as:

$$AlF_4^- + 3e \rightarrow Al + 4F^- \quad (3.4)$$

In other words, $Al_2OF_6^{-2}$ is consumed at the anode, where AlF_4^- is produced. This last species will then move to the cathode by diffusion, where it will react to produce aluminium. The F^- ions produced as a result of electrochemical reactions diffuse and migrate to the anode. Globally, there will be two products, CO_2 and Al. It is assumed in this study that they leave the system immediately without affecting the mass transfer of all other components.

3.3.3 Reaction kinetics

As stated before, electric forces and concentration gradients are the two mechanisms of the ionic mass transfer considered. To evaluate the electric field and consequently the current density, Poisson's equation should be solved in the electrolyte:

$$\nabla^2 \varphi = -\frac{\rho_E}{\varepsilon \varepsilon_0} \quad (3.5)$$

Where φ is the electric potential, ρ_E the electric charge density ($C.m^{-3}$), ε_0 is the electric permittivity of vacuum, and ε is the static dielectric constant (or relative electric permittivity).

The boundary condition on each electrode is defined with the electric potential as a function of the current density, based on the corresponding reaction kinetics.

For the anodic reaction, a Tafel equation, which is a logarithmic approximation of the Butler-Volmer equation, is proposed [22] :

$$\varphi_A = U_{cell} - E_{rev,A} - a_A - b_A log(j) \quad (3.6)$$

Where $E_{rev,A}$ is equal to 1.23 V; a_A and b_A are the Tafel parameters, taken as 0.5 V and 0.25 V.decade^{-1} respectively. j finally represents the current density.

For the cathode reaction, a linearized Butler-Volmer equation is applicable:

$$\varphi_C = -E_{rev,C} - b_C|j| \tag{3.7}$$

Where $E_{rev,C}$ is equal to zero for cathodic reaction and b_C is taken as 0.008 Ω.cm^2.

3.4 Mass transfer model

The prediction of the mass transfer of different ions is based on classical mass conservation equation for each species, as given below:

$$\frac{\partial(\rho w_i)}{\partial t} + \nabla N_i + R_i = 0 \tag{3.8}$$

Where w_i, N_i and R_i represent mass fraction, mass flux, and the reaction rate for species i, respectively. The flux of species for a concentrated solution is driven by the electric forces acting on charged species and also by the concentration gradients, as given by the following equation:

$$N_i = -(\rho D_i \nabla w_i + \rho w_i D_i \frac{\nabla M_n}{M_n} + \rho w_i z_i u_i \nabla \varphi) \tag{3.9}$$

Where ρ_i, D_i, M_n, z_i, and u_i are the density, mass diffusivity, mean molar mass fraction, charge number, and mobility, respectively.

The boundary conditions for this equation can be given for two categories of ions at each electrode:

For electroinactive ions:

$$N_i = 0 = -(\rho D_i \nabla w_i + \rho w_i D_i \frac{\nabla M_n}{M_n} + \rho w_i z_i u_i \nabla \phi) \quad 3.10$$

And for electroactive ions:

$$N_i = \frac{\nu_i}{nF} j(\eta) = -\left(\rho D_i \nabla w_i + \rho w_i D_i \frac{\nabla M_n}{M_n} + \rho w_i z_i u_i \nabla \phi\right) \quad 3.11$$

Where n is the number of electron transferred in the reaction, ν_i is the stoichiometric coefficients of species i in the corresponding reaction, and F the Faraday's constant. Additional mass transfer due to turbulence is considered through the use of a total diffusion coefficient, which is the sum of the molecular and turbulent contributions:

$$D_i = D_{Mi} + D_t \quad 3.12$$

Where D_{Mi} and D_t are molecular and turbulent diffusion coefficients, respectively. The value for the turbulent diffusion is proportional to the distance from the electrodes [13] and is given by the following relation:

$$D_t = Cx^3 \quad 3.13$$

The mobility of the ions is given by the Nernst-Einstein equation.

$$u_i = \frac{D_{Mi}}{RT} \quad 3.14$$

3.5 Properties of the system and solver

A 1-D domain has been assumed, representing the space between the two electrodes, considered as 0.05 m in this study. In the presented results, the cathode and anode are at a

location of x=0[m] and x=0.05[m], respectively. The other properties of the system are given in the table below:

Table 3.1 Properties of the cell

Properties	value
Temperature, T	1240 K
Cryolite ratio, CR	1.5
Bath electric conductivity, Ω [58]	2.4 $\Omega^{-1}.cm^{-1}$
Bath density, ρ [3]	2.059 $g.cm^{-3}$
Current density, j	7500 A/m^2

The sets of equations and boundary conditions are discretized and solved by the finite element method software, COMSOL Multiphysics. The maximum mesh size is 0.01 mm and the number of degrees of freedom solved is 35008.

3.6 Results and discussion

The results are presented for the behavior of different ions during the first 1000 seconds after the startup of the electrolysis process. The initial condition that prevails in the bath is such that the equilibrium condition can be considered. The concentration and flux of ions will be presented in order to illustrate the motion of these ions and the progression of their concentration with time.

Figure 3.1 illustrates the mass fraction of F^- ions near the cathode and the anode, respectively. As shown, the mass fraction of this ion near the cathode is increasing with time because of the production of F^- in the cathodic reaction. Once produced, this negatively charged ion is migrated and diffused away to the anode. Based on the concentration increase with time, it can be concluded that the production rate exceed the migration and diffusion fluxes. However, this tendency levels off as the concentration gradient of F^- ions becomes larger.

As expected, the concentration of F^- near the anode is lower than the bulk value because of its participation in the anodic reaction. It also shows that the consumption rate is dominant compared to migration and diffusion mass fluxes of this ion. As a result of the cathodic reaction and migration, the bulk value of the F^- becomes larger with time, creating larger concentration gradients near the anode and explaining the increase in the mass fraction of this ion between 500 s and 1000 s.

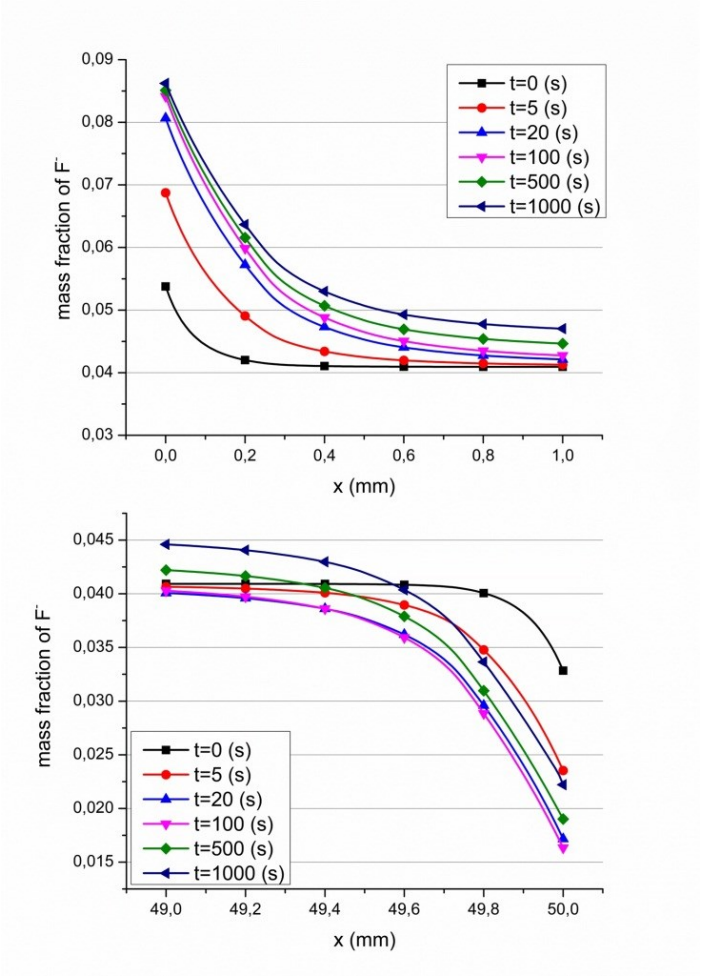

Figure 3.1: Mass fraction profile of F^- near the cathode (above) and the anode (below) for the first 1000 s.

While $Al_2OF_6^{2-}$ is participating in the anodic reaction, it is considered as an electroinactive ion at the cathode where only diffusion and migration takes place. The variation of concentration of this ion close to the cathode and anode is shown in Figure 3.2. As it is negatively charged, the electric field forces this ion away from cathode while diffusion acts in the opposite direction. This is why $Al_2OF_6^{2-}$ is found at such a low concentration near the cathode. On the other side of the cell, two mechanisms are opposed. Migration and diffusion brings this ion toward the anode but it is consumed through the anode reaction. The consumption rate being higher than the migration and diffusion flux, there is depletion of this ion near the anode with time.

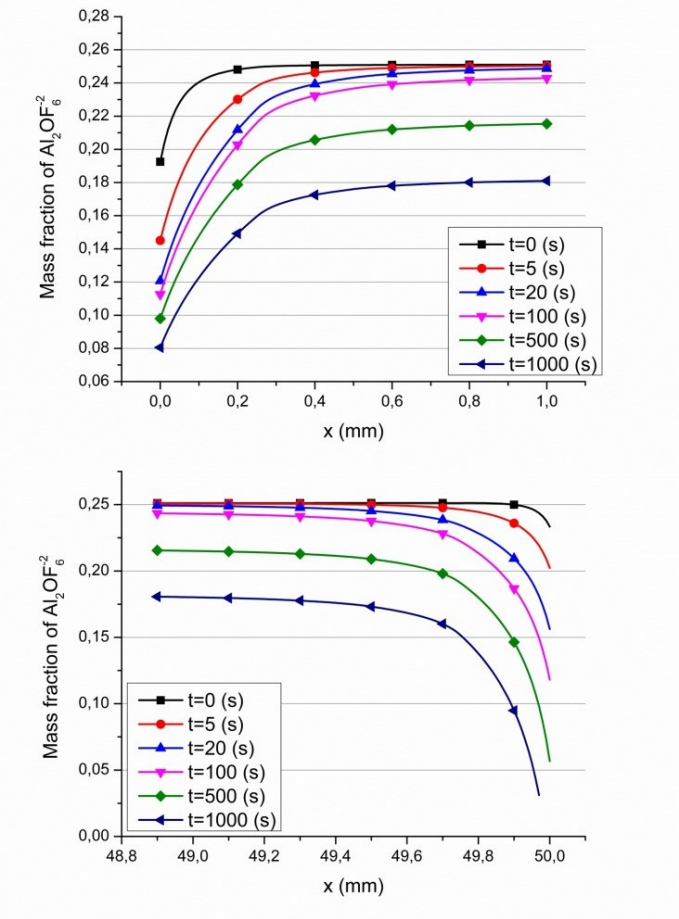

Figure 3.2: Mass fraction profile of $Al_2OF_6^{2-}$ near the cathode (above) and the anode (below) for the first 1000 s.

It should be noted that the effects of moving CO_2 bubbles and micro-convection below the anode has been neglected in this study. In reality, these phenomena will add additional movement of bulk, which would most probably prevent the depletion of $Al_2OF_6^{2-}$ near the anode, when the alumina concentration in the bulk is sufficient enough to sustain the production of aluminium.

AlF_4^- is participating in both anodic and cathodic reactions. At the cathode, the consumption and also the migration of this ion decrease its mass fraction. Near the anode, both the reaction and migration increase its concentration while diffusion acts in the

opposite direction. It is clear from Figure 3.3 that bulk value of AlF_4^- mass fraction increases with time. This is because of the stoichiometry of the reactions. In other words, its production rate is higher at the anode that its consumption rate at the cathode.

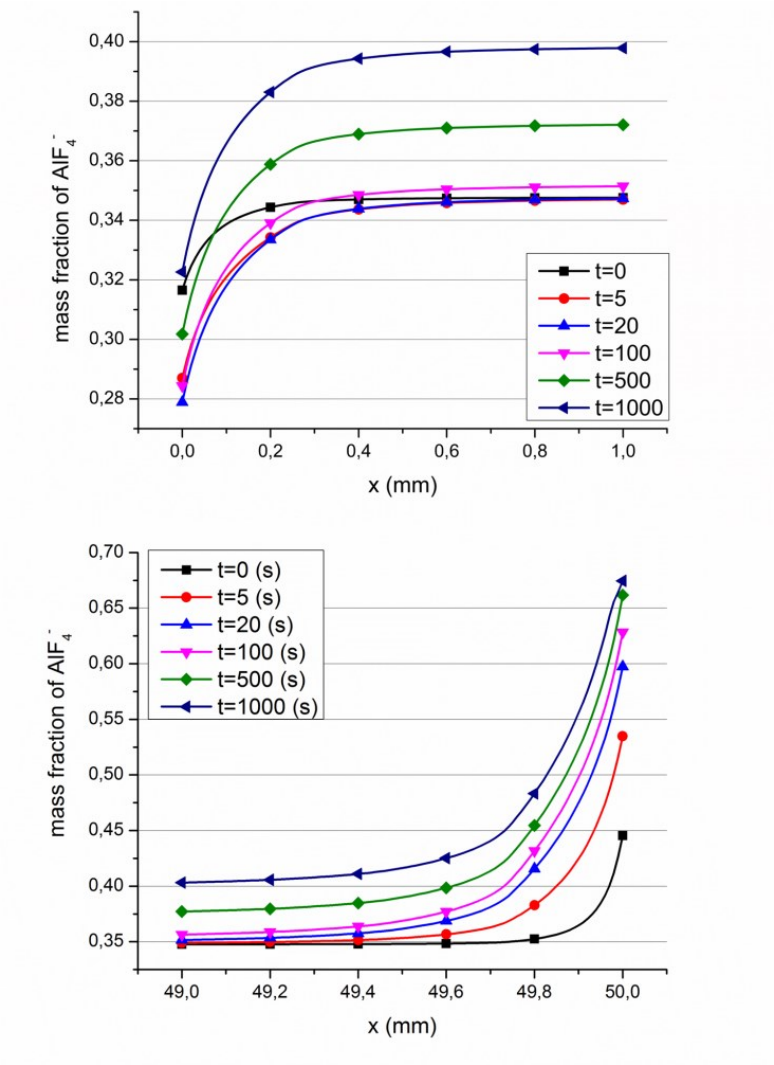

Figure 3.3: Mass fraction profile of AlF_4^- near the cathode (above) and the anode (below) for the first 1000 s.

The ratio of diffusion to migration fluxes provides valuable information about their relative contributions. Such a ratio is shown in Figure 3.4 for electroactive species like AlF4-. For such species, in the early stages of electrolysis, the migration flux is

dominantin comparison to diffusion, especially in the bulk. Shortly after the startup, the concentration gradients near the electrodes are growing, responsible for the increasing role of diffusion mass transfer with time. For AlF4-, the ratio of diffusion to migration is higher in the anode region because of higher concentration gradients at this location

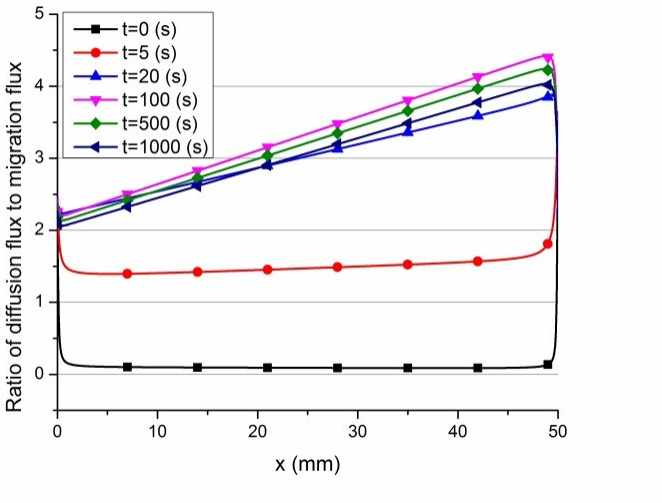

Figure 3.4: Ratio of diffusion flux to migration flux along the cell for AlF_4^-

The diffusion to migration ratio of the $Al_2OF_6^{2-}$ is shown in Figure 3.5. Near the cathode, this ratio takes values below or near unity, meaning that the migration plays a major role for this electroinactive ion. In fact, diffusion is sort of compensating the mass transfer initiated by the migration in reaction to the presence of an electric field. On the other side of the cell, consumption of $Al_2OF_6^{2-}$ is at such a level that there is a depletion of this species near the anode. This creates a very high concentration gradient and causes the ratio of diffusion over migration to be very high in this region. In fact, this ratio is around 30 near anode for 1000 s which cannot be seen in the Figure 3.5 because of the range of the y axis.

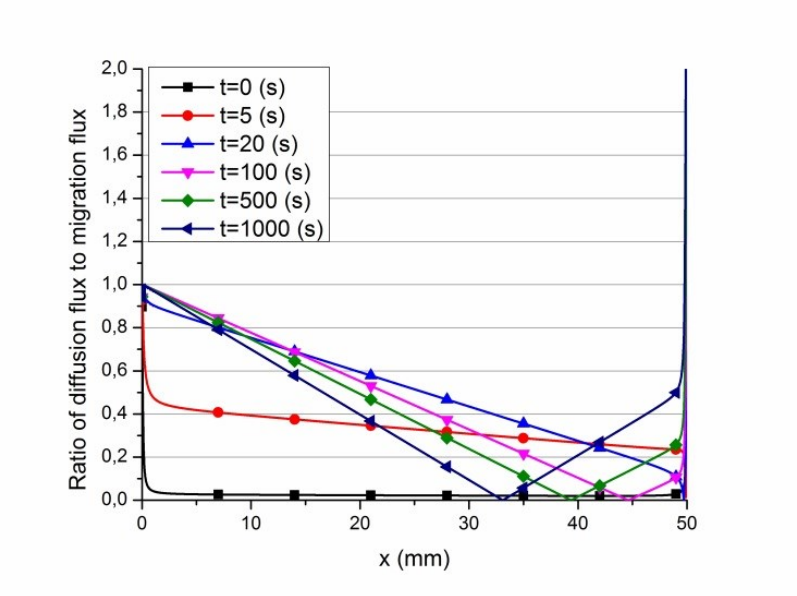

Figure 3.5: Ratio of diffusion flux to migration flux along the cell for $Al_2OF_6^{2-}$

For electroinactive ions, the diffusion to migration ratio is always below one, as shown in Figure 3.6 for $Al_2O_2F_4^{2-}$. The mass transfer for these species is essentially driven by migration. It then creates a concentration gradient and a diffusion flux, in relation to migration.

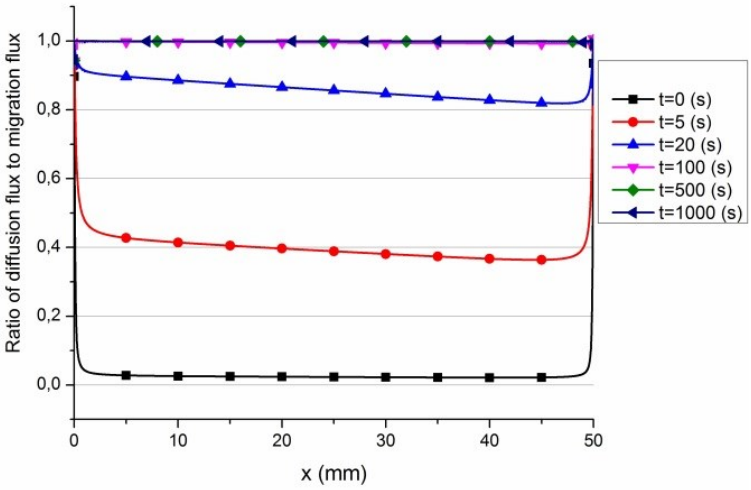

Figure 3.6: Ratio of diffusion flux to migration flux along the cell for $Al_2O_2F_4^{2-}$

3.7 Conclusion

The mass transfer of different ions in the $NaF\text{-}AlF_3\text{-}Al_2O_3$ molten salt has been analyzed considering electrochemical reactions, diffusion and migration as the main mechanisms of transport. The results indicate that migration plays an important role for all anions, especially for F^- and $Al_2OF_6^{2-}$ that move toward anode to participate in anodic reaction. For $Al_2OF_6^{2-}$, produced by the decomposition of the alumina fed to the cell, diffusion becomes the dominant mass transfer mechanism in the region near the anode because of the presence of high concentration gradients caused by the reaction. At the cathode, the migration of $Al_2OF_6^{2-}$ is the dominant mechanism of transport. The story is similar for other electroactive ions like AlF_4^-. Diffusion has a considerable effect on mass transport since electrochemical reactions are responsible for large concentration gradients at both electrodes. However, the mass fluxes for nonelectroctive anions are essentially driven by the electric field force and diffusion flux is consequently always less or equal to the migration flux. This new knowledge of the dominant mechanism of mass transfer for

different ions opens up new possibilities as to control the flux of specific ions or to prevent the undesirable reactions.

NOMENCLATURE

A anode surface$[m^2]$

A_h available anode area for the current passage$[m^2]$

D_i mixture-averaged diffusion coefficient of species i, $\left[\frac{m}{s^2}\right]$

$D_{i,j}$ multicomponent diffusion coefficient of species i , $\left[\frac{m}{s^2}\right]$

D_t turbulent diffusion coefficient, $\left[\frac{m}{s^2}\right]$

D_w wall distance, [m]

E_{rev} electrode reaction equilibrium voltage$[V]$

F faraday constant $\left[\frac{C}{mol}\right]$

M_i molar mass of species i, [kg]

M_n mean molar mass, $[kg]$

N number of species

R_i mass rate of production of species I by homogeneous reaction$\left[\frac{kg}{m^3.s}\right]$

U_{cell} cell voltage$[V]$

a_i activity of species i

g inverse distance function $\left[\frac{1}{m}\right]$

i current density magnitude $\left[\frac{A}{m^2}\right]$

$\boldsymbol{i}$ current density vector $\left[\frac{A}{m^2}\right]$

$\boldsymbol{j}_i$ mass flux of species *i*, $\left[\frac{kg}{m^2.s}\right]$

$\boldsymbol{j}_t$ turbulent mass flux of species *i*, $\left[\frac{kg}{m^2.s}\right]$

n number of electron transfered in electrode reaction

u_i mobility of species *i*

x_i molar fraction of species *i*

z_i charge number of species *i*

Greek letters

α factor of convection $\left[\frac{1}{m.s}\right]$

CHAPITRE 4 : AVANT-PROPOS

Auteurs et affiliation:

- Mohsen Ariana: étudiant au doctorat, Université de Sherbrooke, Faculté de génie, Département de génie mécanique.
- Martin Désilets : professeur, Université de Sherbrooke, Faculté de génie, Département de génie chimique et de génie biotechnologique.
- Pierre Proulx : professeur, Université de Sherbrooke, Faculté de génie, Département de génie chimique et de génie biotechnologique.

Date d'acceptation: 10 mars 2014

État de l'acceptation: version finale publiée

Revue: Canadian journal of chemical engineering

Référence: [59]

Titre français: À propos du transfert de masse des ions dans le bain électrolytique utilisé au sein des cellules d'électrolyse d'aluminium

Contribution au document: Cet article contribue à la thèse en élaborant une simulation 2-D du transfert de mass des ions dans les couches limites de l'anode et de la cathode et dans le bain afin de pouvoir analyser l'effet de la distribution du courant électrique sur comparer les différents mécanismes de transfert de masse dans les différent région.

Résumé français : Le bain électrolytique de la cellule d'électrolyse d'aluminium est composé de différents ions qui se déplacent dans le champ électromagnétique généré par le courant électrique intense utilisé pour l'application industrielle. Le mouvement des ions a des effets importants sur les paramètres fonctionnels du procédé comme l'efficacité du courant. Cette étude numérique modélise le mouvement des ions dans le

mélange de $NaF\text{-}AlF_3\text{-}Al_2O_3$ en utilisant la méthode des éléments finis. L'équation de conservation de la charge électrique dans le bain électrolytique est limitée aux électrodes par la cinétique des réactions hétérogènes. Elle est résolue pour obtenir le potentiel électrique, la densité de courant et la chaleur générée. Par ailleurs, les équations de la conservation de la masse sont résolues pour obtenir la concentration et le flux des ions. Les résultats obtenus pour la simulation de 3 minutes de l'électrolyse montrent les gradients abrupts de concentrations sur les électrodes pour les ions électroactifs, comme AlF_4^- et $Al_2OF_6^{2-}$. Ainsi, la portion de la migration qui est le mécanisme dominant de transfert de masse dans les premières phases est diminuée par rapport à la diffusion pour les ions électroactifs. Néanmoins, les vecteurs de flux de migration et de diffusion sont du même ordre de grandeur pour les ions non-électroactifs. En outre, les résultats montrent un transfert de masse entre l'espace inter-électrodes et la région proche de la couche de gelée pour éviter l'épuisement ou la surconcentration des ions aux électrodes.

4 ON THE ANALYSIS OF IONIC MASS TRANSFER IN THE ELECTROLYTIC BATH OF AN ALUMINUM REDUCTION CELL

4.1 Abstract

An electrolyte typically used in an aluminum electrolysis cell is composed of different ions moving in the electromagnetic field generated by the high intensity current needed for the industrial application. The flux of these ions has an important impact on the functional parameters of the cell, like current efficiency. In this study, the transient behaviour of these ions in the NaF-AlF_3-Al_2O_3 mixture is modelled using a numerical finite element method. The electric potential field equation governed by electrochemical reaction kinetics at electrodes is solved to obtain the electric potential field, current density, and consequently heat generation in the cell. Subsequently, the concentration field is solved for ionic species in the bath. The results indicate formation of a high concentration gradient of electroactive ions like $Al_2OF_6^{2-}$ and AlF_4^- at the corresponding reacting electrodes with time and diffusion as the main mechanism for these ions transfer. It is found that from the early stages of the 3 minute simulation of the electrochemical process, the difference between bulk concentration and surface concentration of electroactive ions remains constant. Moreover, the results indicate that although the flux of electroactive species is dominated by diffusion, especially for larger times, migration is the controlling mechanism of transport for the electroinactive ions.

Keywords: modelling, aluminum reduction cell, mass transfer, migration, diffusion

4.2 Introduction

Aluminum is produced through the famous Hall-Héroult process in which the alumina dissolved in a molten salt is reduced in order to produce aluminum [1, 14]. Like all molten salts, the solution of cryolite, alumina, and other additives, which is called a bath, is composed of different species and ionic complexes. The motion of these ionic species is at the origin of the current that passes through the bath from the anode to the cathode. In other words, an important aspect of ionic flux is its effect on the current transfer mechanism and conductivity of the bath. The other aspect that makes the mass transfer in the cell so important is its role in providing the electrodes with reactants since, most of the time, the reactions of the cell are mass transfer controlled. In addition to these reactions, one of the causes of back reactions is said to be the anodic oxidation of the migrated dissolved aluminum, probably in the form of AlF^{2-} ions [3]. Back reaction has detrimental effects on the current efficiency of the cell [1].

Mass transfer analysis of an electrolytic bath includes the study of parameters like bath ionic conductivity, transference number, mobility, and diffusivity of different ions. In addition to these parameters, this analysis also involves the mutual interaction of four different fields: concentration, velocity, electric potential, and temperature fields and their gradients, all of which can be considered as the source of the mass transfer in the cell. The corrosive and high temperature environment of the bath makes it a harsh reacting media in which it is nearly impossible to observe the ionic behaviour or to measure the properties of the system at the extent that even the existing ions in the cell are not well defined yet [3]. In spite of these restrictions, some experimental and modelling studies have been conducted on the transport phenomena parameters in the Hall-Héroult cell.

There have been some studies to estimate the ionic conductivity and transference number of each ion in the bath [5-7, 11]. Transference number is defined as the fraction of current that each ion is carrying in multicomponent electrolytic solutions. In these studies, the

mobility of the ions in the cell is also calculated in the absence of concentration gradient in the cell. One of the benefits of the analysis of the flux of ions in the cells and in boundary layers is that it defines the importance of the mass transfer mechanisms for each ion in the electrode regions (diffusion boundary layers) and in the bulk of the system where convection plays an important role.

The analysis of the importance of different mechanisms of mass transfer in the cell needs to consider the mutual impact of mentioned fields. For the potential electric field in an aluminum electrolysis cell, Zoric et al. solved the secondary current distribution for a two-dimensional cell [16, 22, 54, 55]. In addition, they tried to model the effects of current density on the shape of the anode [20]. They also studied the role of the side ledge on the current density distribution [22]. Later on, Sterten discussed the mechanism of the cathodic reaction and migration of the Na^+ ions to carry the current along with a qualitative analysis of the concentration of species like NaF and AlF_3 in the AlF_3-NaF-Al system [30]. In their analysis, the proposed electrode reactions couple the concentration and potential fields. Solheim developed a non-ionic mass transfer model based on Maxwell-Stefan equations in order to calculate the concentration of species like NaF, AlF_3, Al_2O_3, and CaF_2 and to define the rate of cryolite crystallization [13]. Other studies focussed on the solution of the coupled fields of velocity, electromagnetics, and concentration by considering certain assumptions. Addressing the momentum transport, Li et al. established an inhomogeneous three-phase model for the calculation of the current efficiency of the cell [29]. This finite volume model took into account the flow of aluminum, bath, and bubble layers under the anode and their interaction with each other, considering the MHD forces as the main momentum source term. In this study, the concentration of dissolved Na^+ is calculated assuming that it has a large effect on the current loss. In order to reduce the complexity of the multiphase model to a single-phase model, Kuzmin et al. assumed the different regions of the bath as the mixture of electrolyte and aluminum with different concentration compositions, and then proposed a numerical model for the mass and momentum transfer due to these concentration patterns [28].

Three recent studies presented new modelling approaches for the ionic diffusion in the cell. First, Gagnon et al. modelled a $NaF\text{-}AlF_3$ ionic system considering diffusion and migration near a porous cathode [12]. Therefore, the model takes into account the cathodic reactions and the motion of species near the cathode. Secondly, Solheim developed his previous model for the analysis of anion concentration near the cathode by solving one-dimensional Maxwell-Stefan diffusion equations [14]. In other words, these two studies can be regarded as the numerical models for the concentration and flux of the ions in the cathode boundary region. Finally, Ariana et al. modelled one-dimensional mass transfer in the anode and the cathode mass transfer boundary layer for a one-dimensional interelectrode distance [53]. Considering the bath as a concentrated solution alongside with the electrode reactions, this study was done for two categories of electroactive and electroinactive ions in the bath to obtain the transient movement of these ions in the cell [53].

In the present study, after having calculated the electric current density and electric potential field for a two-dimensional model of whole cell, see Figure 4.1, the concentration and flux of the main ions of the $NaF\text{-}AlF_3\text{-}Al_2O_3$ system are calculated. It should be noted that the kinetics of anode and cathode reactions have been taken into account in the calculation. The present study also considers diffusion and migration as the two mechanisms of mass transfer in the cell and analyzes the transient behaviour and importance of each mechanism for different ions in the bath.

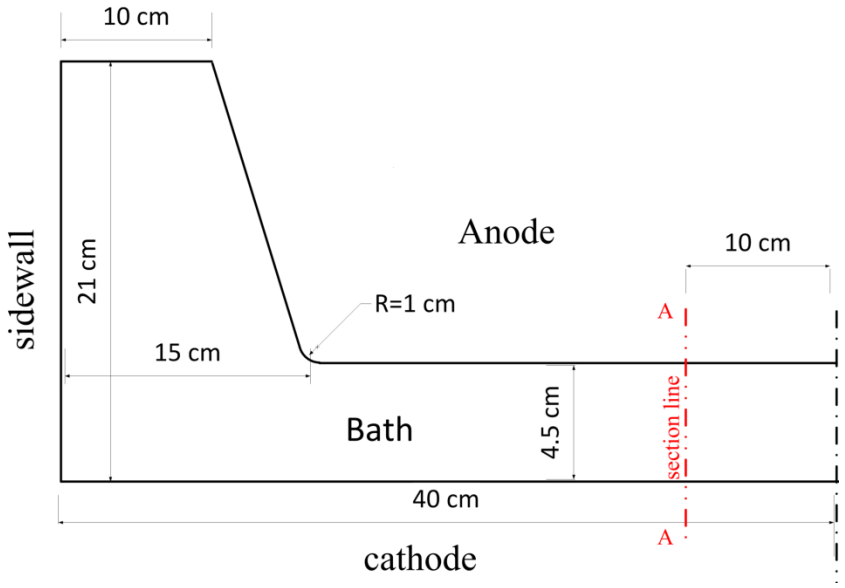

Figure 4.1. Two dimensional geometry of an aluminum electrolysis cell.

4.3 Material and methods

4.3.1 Homogenous reactions, activities, and initial mass fractions

It is well known that the bath is a mixture of different ions and ionic complexes. However, there is still controversy over the ionic composition of a typical industrial bath, and the equilibriums and the electrochemical reactions in the bath and at electrodes [1]. Several models are proposed to predict the ionic equilibrium and the electrochemical reactions at the electrodes [60-62]. Since the aim of this study is to analyze the mass transfer of species in the bath, it is necessary to define an ionic model that is compatible with the kinetics of the reactions available in the literature.

Based on the ionic model proposed by Zhang et al. [57] and Zhang and Rapp [56] for dissolution of alumina, the existing complexes in the bath come from the following homogeneous reactions:

$$\frac{1}{3}Al_2O_3(s) + 2NaF(l) + \frac{4}{3}AlF_3(s) \rightarrow Na_2Al_2OF_6(l)$$

$$\frac{2}{3}Al_2O_3(s) + 2NaF(l) + \frac{2}{3}AlF_3(s) \rightarrow Na_2Al_2O_2F_4(l)$$

$$\frac{2}{3}Al_2O_3(s) + 4NaF(l) + \frac{2}{3}AlF_3(s) \rightarrow Na_4Al_2O_2F_6(l) \qquad 4.1$$

$$3NaF(l) + AlF_3(s) \rightarrow Na_3AlF_6(l)$$

$$NaF(l) + AlF_3(s) \rightarrow NaAlF_4(l)$$

Based on the above alumina dissolution reactions, the molar fraction of the complexes are calculated by the following correlations [56] :

$$[Na_2Al_2OF_6] = K_1 {a_{NaF}}^2 {a_{AlF_3}}^{\frac{4}{3}} {a_{Al_2O_3}}^{\frac{1}{3}}$$

$$[Na_2Al_2O_2F_4] = K_2 {a_{NaF}}^2 {a_{AlF_3}}^{2/3} {a_{Al_2O_3}}^{2/3}$$

$$[Na_4Al_2O_2F_6] = K_3 {a_{NaF}}^4 {a_{AlF_3}}^{2/3} {a_{Al_2O_3}}^{2/3} \qquad 4.2$$

$$[Na_3AlF_6] = K_4 {a_{NaF}}^3 a_{AlF_3}$$

$$[NaAlF_4] = K_5 a_{NaF} a_{AlF_3}$$

where K_i, a_{NaF}, and a_{AlF_3} are the equilibrium constant of the *i*th reaction, the activity of NaF, and the activity of AlF_3, respectively, which are functions of cryolite ratio and temperature. Moreover, $a_{Al_2O_3}$ is the activity of alumina and is equal to 1 by assuming alumina saturation [56]. The values for the equilibrium constants and activities for different cryolite ratios and temperatures are tabulated by Zhang and Rapp [56].

It is assumed that the produced species are already ionized in the molten salt where an instantaneous ionic equilibrium between Na^+ ions and other anions is established. This assumption is supported by the idea that the only cation present in the bath is Na^+, and all other anions are moving in an ocean of Na^+ [14]. Based on this assumption, the ionic composition of cell is composed of F^-, $Al_2OF_6^{2-}$, $Al_2O_2F_4^{2-}$, $Al_2O_2F_6^{4-}$, AlF_6^{3-}, AlF_4^-, and Na^+ ions. Molar fractions obtained by the above relationships are converted to mass fraction and are considered as initial concentrations of the ions in the bath.

4.3.2 Heterogeneous reactions and chemical kinetics

In addition to alumina dissolution reactions, there are heterogeneous reactions that take place at the surface of electrodes.

At the anode, the following reaction is proposed [58]:

$$2Al_2OF_6^{-2} + 4F^- + C \rightarrow 4AlF_4^- + CO_2 + 4e \qquad 4.3$$

$Al_2OF_6^{-2}$ is the dissolved form of alumina in the bath and reacts at the anode to produce AlF_4^-. The AlF_4^- produced at the anode then diffuses to the cathode and feeds cathodic reaction (see Equation 4.4). It is assumed that the produced aluminum and CO_2 leave the bath immediately after being produced, so the analysis of these two products of reactions are neglected. However, the effect of CO_2 on the anode overvoltage is considered and will be discussed later in this study.

At the cathode, the following reaction takes place, which leads to the production of aluminum [3]:

$$AlF_4^- + 3e \rightarrow Al + 4F^- \qquad 4.4$$

It should be noted that some studies considered this reaction as a two-step reaction [58]. The two-step model can be important for the analysis of the diffusion and migration of the intermediate product, AlF_2^-, to the anode which is said to be the reason of back reactions in the cell [3]. However, since the main concern of this study to analyze the movement of main electroactive and electroinactive ions, the overall reaction is assumed.

4.4 Mathematical model

4.4.1 Electric potential field

The electric potential and concentration fields are strongly coupled. Indeed, the concentration of charged ions is influenced by the electric potential gradient in the migration component of the flux of species. On the other side, the flux of ions as the charge carriers is at the origin of the bath conductivity. The electric field can be solved by using primary, secondary, or tertiary current distribution models [15]. In this study, a secondary current distribution is assumed in order to calculate the electrical potential field. The secondary current distribution considers the kinetics of reaction occurring at electrodes. The potential field is governed by the Poisson's equation [15],

$$\nabla^2 \varphi = -\frac{\rho_E}{\varepsilon \varepsilon_0} \tag{4.5}$$

where φ is electric potential, ρ_E is the electric charge density, ε_0 is the electric permittivity of vacuum, and ε is relative electric permittivity of bath. The assumption of electroneutrality sets the RHS of the above equation to zero.

4.4.2 Boundary conditions for electric field

As stated before, based on the existing secondary current distribution models for electrode reactions, the boundary conditions for the anode is the electric overpotential at the anode, which is given by the following relation[22]:

$$\varphi_A = U_{cell} - E_{rev,A} - \eta_A \quad (4.6)$$

where φ_A, U_{cell}, and $E_{rev,A}$ are anode electric potential, cell voltage, and electrode reaction equilibrium voltage, respectively. The corresponding values are given in Table 4.1.

Based on what is proposed in the literature for anodic reaction in an aluminum cell [22], the Tafel equation, which is the logarithmic form of the Butler-Volmer equation, is valid for the anode reaction:

$$\eta_a = a_A + b_A log(i) \quad (4.7)$$

where a_A and b_A are the Tafel parameters. Their values are given in Table 4.1.

The effect of CO_2 bubbles on the electric potential profile at the interface of the anode surface and electrolyte can be considered by applying the bubble hyperpolarization overvoltage, which is a function of bubble surface coverage over the anode surface [63].

$$\eta_h = b_A log\left(\frac{A}{A_h}\right) \quad (4.8)$$

where A is the anode nominal area, and A_h is the available anode area for the current passage. The bubble coverage ratio is a function of local current density. In this study, hyperpolarization voltage has been calculated for 35 % of bubble surface coverage (A/A_h). The following expression is obtained from the combination of the previous expressions for the anode overpotential:

$$\varphi_A = U_{cell} - E_{rev,A} - a_A - b_A log(i\frac{A}{A_h}) \quad (4.9)$$

For the cathode overpotential, a linearized form of Butler-Volmer is proposed [22]:

$$\varphi_C = -E_{rev,C} - b_C|i| \tag{4.10}$$

where $E_{rev,C}$ is the cathode reaction equilibrium voltage. The values for $E_{rev,C}$ and b_C are given in Table 4.1.

The boundary condition for other boundaries of the system is zero current condition.

4.4.3 Concentration field

For the concentration field, the conservation of mass for each species is given by

$$\frac{\partial(\rho\omega_i)}{\partial t} + \boldsymbol{\nabla}.\boldsymbol{j}_i - R_i = 0 \tag{4.11}$$

with

$$\sum_{i}^{N} \omega_i = 1 \tag{4.12}$$

where ω_i, $\mathbf{j}_i$, and R_i represent mass fraction, mass flux, and the mass rate of production for species *i*, respectively.

The mixture-average multicomponent diffusion model for concentrated solution is giving the mass flux for each ion:

$$\boldsymbol{j}_i = -\left(\rho D_i \boldsymbol{\nabla}\omega_i + \rho\omega_i D_i \frac{\boldsymbol{\nabla}M_n}{M_n} + \rho\omega_i z_i u_i F \boldsymbol{\nabla}\varphi\right) \quad 4.13$$

where z_i and u_i are the charge number and the mobility of species i in the bath, respectively.

The mixture average diffusion coefficient D_i is given by the Wilke correlation [52]:

$$D_i = \frac{1-\omega_i}{\sum_{\substack{i=1 \\ i\neq j}} \frac{x_i}{D_{ij}}} \quad 4.14$$

where x_i is molar fraction of species i and D_{ij} is the multicomponent diffusion coefficient of species i in species j.

M_n is the mean molar mass and is calculated by the following relation:

$$M_n = \left(\sum \frac{\omega_i}{M_i}\right)^{-1} \quad 4.15$$

The electric potential and current density obtained by solving Poisson's equation is used to calculate explicitly the electric potential gradient in the migration term of the mass transfer equations. In the mixture of N species, the mass conservation equation is solved for $N-1$ species, and the concentration of last species is calculated as excess species by Equation 4.12 to respect the sum of mass fractions equals to unity.

4.4.4 Physical properties

4.4.4.1 Transference number and mobility of the ions

It have been widely discussed in the literature that the transference number of Na^+ ions is almost 1 in the bath melt due to the small size of these ions[24]. The anions have larger sizes and thus the friction with other ions is larger for them in comparison to cations like Na^+ and Li^+. In other words, we can consider that the Na^+ ions are the main charge carriers in the bath and the transference number of Na^+ ions is about 1. Moreover, Rolin states that this value is near 1 for larger cryolite ratios [5]. However, it is lower for lower cryolite ratios or for more acidic melts. Generally, mobility of the ions in bath melt is a function of their size. The mobility of smaller ions in the bath, like Na^+ and F^-, is higher than larger ions like alumina-fluoride anions. Considering Na^+ and F^- as the main charge carriers in the cell, Rolin has proposed 0.88×10^{-3} cm/s and 0.098×10^{-3} cm/s for the velocity of Na^+ and F^- ions in the cell, respectively [5]. The mobility of aluminum oxyfluoride anions is given by their molecular diffusion coefficients through the Nernst-Einstein equation:

$$u_i = \frac{D_i}{RT} \qquad 4.16$$

4.4.4.2 Molecular diffusion coefficients

The binary molecular diffusion coefficient for Na^+ and F^- ions is given by the study of Rollet et al. [23]. However, there is still a controversy over the diffusion coefficients of aluminum fluoride and aluminum oxyfluoride anions. As long as the identity of the species in the bath is still a subject of scientific research, their diffusion coefficients and also their mobility are also disputed. However, one can find values that are widely used in some studies [14], which are essentially based on the work of Thonstad[64].

Accordingly, the binary diffusion coefficients for aluminum fluoride anion pairs are $1 \times 10^{-8}\left[\frac{\mathrm{m}^2}{\mathrm{s}}\right]$ while a value of $1.5 \times 10^{-9}[\mathrm{m}^2/\mathrm{s}]$is considered for others.

4.4.4.3 Turbulent diffusion coefficients

Although the turbulent flow has not been considered in this study, turbulent diffusion coefficient is added to the molecular diffusion in order to consider the effect of turbulent mixing in the cell. The turbulent mass flux near the electrodes that is caused by the fluctuation of concentration and velocity can be modelled as [15]:

$$J^t = -\rho D_t \nabla \omega_i \tag{4.17}$$

where D_t is called turbulent diffusion coefficient or eddy diffusivity. Based on the study by Levich, this effect is smaller near the electrodes and walls, and larger far away from the electrodes [49]. Based on this study, to find the effect of turbulent stirring of solution on the rate of ion supply to the electrodes, the turbulent diffusion coefficient is calculated as a function of the distance from the wall as given by the following formula [15, 49]:

$$D_t = \alpha (D_w)^3 \tag{4.18}$$

where D_w is the distance from electrodes for one-dimensional models, and α is the factor of convection that indicates the degree of turbulence in the system. This factor is calculated from average mass transfer rate at the wall, and its value is given in Table 4.1.[14, 60]

However, for the two dimensional model in this study, the wall distance model is adapted based on the approach proposed by Fares[50]. The equation to be solved in order to find a distance function for all points in the field is given by

$$(\frac{\partial g}{\partial x})^2 + (\frac{\partial g}{\partial y})^2 = g^4 \qquad 4.19$$

where g is equal to the inverse of distance function, $1/D_w$. The initial condition for g is zero. In order to avoid infinite values for g at walls, the distance function, D_w, is fixed at a small no zero value.

Having solved the above equations, the distance function obtained represents the effect of the walls on the flow in the cell. The wall boundary condition is applied to all boundaries except at the symmetry line on the left.

The results for the distance function (and for the turbulent diffusion term) are shown in Figure 4.2.

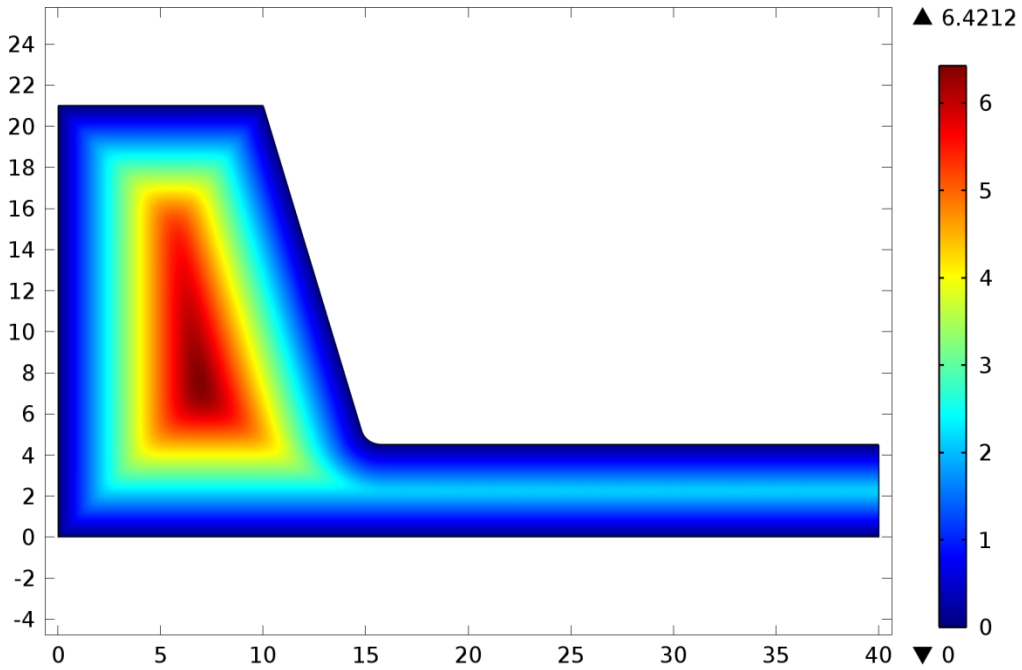

Figure 4.2. Wall distance function, $\mathbf{1/g}$, in the cell [cm].

The obtained wall distance field presents the effective distance for the assumed geometry in order to apply the mixing effect of turbulent flow in the cell.

4.4.5 Boundary conditions for concentration field

At the cathode, zero mass fluxes are considered for electroinactive species, whereas the mass fluxes for electroactive species are proportional to the current density.

Thus, for electroactive species,

$$-\left(\rho D_i \nabla \omega_i + \rho \omega_i D_i \frac{\nabla M_n}{M_n} + \rho \omega_i z_i u_i F \nabla \phi\right) = \frac{M_i \nu_i}{nF} \boldsymbol{i}(\eta) \tag{4.20}$$

for electroinactive species,

$$-(\rho D_i \nabla \omega_i + \rho \omega_i D_i \frac{\nabla M_n}{M_n} + \rho \omega_i z_i u_i F \nabla \phi) = 0 \tag{4.21}$$

where ν_i is the stoichiometric coefficient of species *i* in the corresponding electrode reaction, and *n* is the number of electrons transferred in the corresponding reaction, and *F* is Faraday constant. The values of parameters in mathematical model are gathered in Table 4.1.

Table 4.1 Properties of the cell

Properties	**Value**
Temperature, *T*	1240 [K]
Cryolite ratio, *CR*	1.5
Bath electric conductivity[58]	2.4 [$\Omega^{-1}.cm^{-1}$]
Bath density, ρ[3]	2.059 [$g.cm^{-3}$]
Cell voltage, U_{cell}	3 [V]
$\boldsymbol{E_{rev,A}}$	1.23 [V]
$\boldsymbol{a_A}$	0.43 [V]
$\boldsymbol{b_A}$	0.31 [$V.decade^{-1}$]
$\boldsymbol{E_{rev,C}}$	0 [V]
$\boldsymbol{b_C}$	0.08 [$\Omega.cm^2$]
$\boldsymbol{\alpha}$	12000 [$m^{-1}.s^{-1}$]

4.5 Solver

The steady state electric potential equation with corresponding Butler-Volmer boundary conditions are solved in order to find the electric potential and current density vector in the electrolyte. The transient mass conservation equations are solved by taking into account the results for electric field. As the species fluxes and concentration gradient are larger near electrodes, a thin layer of 0.05 cm thickness is considered normal to the electrode surfaces with 15 quadrilateral elements and stretching factor of 1.2, see Figure 4.3. Totally, there are 21 300 quadrilateral elements in addition to 45 381 triangular elements. The number of degrees of freedom to be solved is 358 456. The simulation is done by using finite element package, COMSOL Multiphysics.

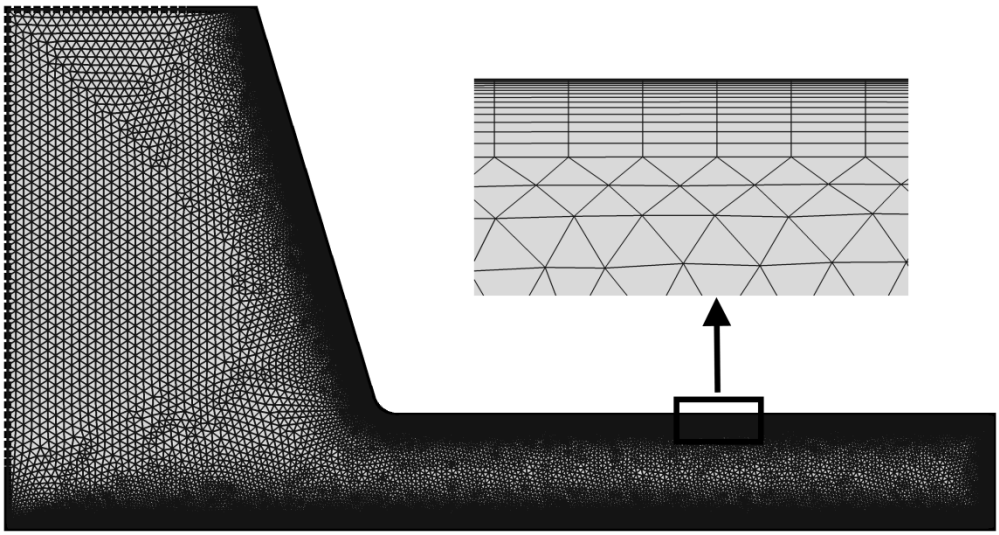

Figure 4.3. Triangular meshing in the bulk and quadrilateral meshing near the electrode surfaces.

4.6 Results and discussion

4.6.1 Electric potential field and current density

The current density magnitude and normalized vectors are shown in Figure 4.4a and b, respectively. The current density between the electrodes is higher in the narrow part of the cell (interelectrode space) comparing to the other regions in the cell, with a current peak near the edge of the anode. The results are obtained by applying 3 [V] as the cell voltage. Considering the cell voltage, the different overvoltages and the bath conductivity mentioned above, the average current density is found to be 6225 [$A.m^{-2}$] on the cathode and 5495 [$A.m^{-2}$] over the anode surface. The difference comes from the larger area of the anode, and the overall current in and out of the cell is equal to zero. It should be noted that the anode surface includes the anode lower surface in addition to the side surface.

The electric potential field for the electrolyte is given in the Figure 4.4c. The values shown in this figure are the electric potential values in the bath and do not include the electrode voltages.

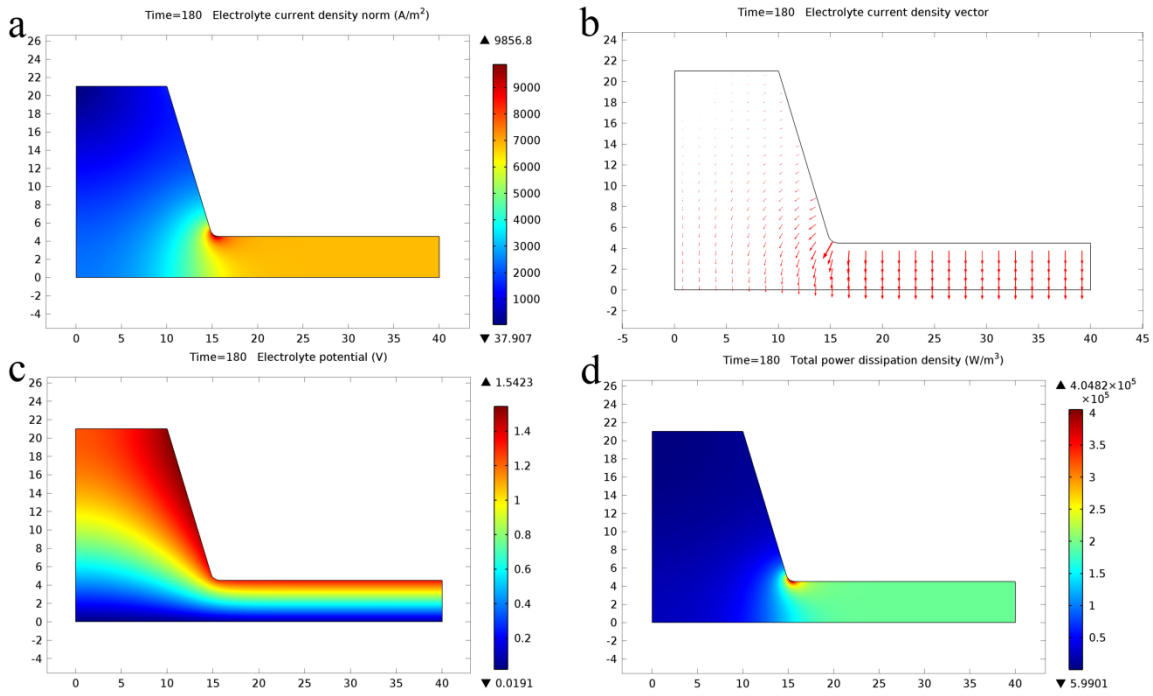

Figure 4.4. a) Current density magnitude [A.cm^{-2}]; b) Normalized vector in electrolyte; c) Electric potential of the electrolyte [V]; d) Heat generation in the cell [W.m^{-3}].

The heat generation by joule effect in the electrolyte is shown in Figure 4.4d. Because of the assumed constant conductivity of the electrolyte, the heat generation follows the pattern of current density. Although the temperature field has not been included in the present study, the heat generation could be used as a source term in the energy equation models of the bath in further studies.

The dimensions of the cell in Figure 4.4and all figures in the following sections are given in centimeters.

4.6.2 Mass transfer in the cell

The mass transfer results in the bath are presented by comparing the transient behaviour of migration and diffusion fluxes for three categories of ions: $Al_2OF_6^{2-}$ and AlF_4^- as the

main electroactive ions, Na^+ as the only cation in the system, and $Al_2O_2F_6^{4-}$ as one of the electroinactive ions.

4.6.2.1 Migration and diffusion fluxes of $Al_2OF_6^{2-}$

Based on the assumptions made in material and methods section, $Al_2OF_6^{2-}$ can be considered as the ionic form of alumina in the bath and is the main electroactive species participating in anode reaction. This negatively charged ion is oxidized and consumed in the anodic reaction. The flux of this ion to the anode includes the migration and diffusion fluxes. The migration flux magnitude and direction after 180 seconds are shown in Figure 4.5a. As is clear in this figure, the migration flux is a function of the electric potential gradient, which is higher in the interelectrode space and especially near the anode edge. As shown in Figure 4.5b, the direction of the migration flux is in the opposite direction relative to the current density vectors. It should be noted that the migration flux is not a strong function of time.

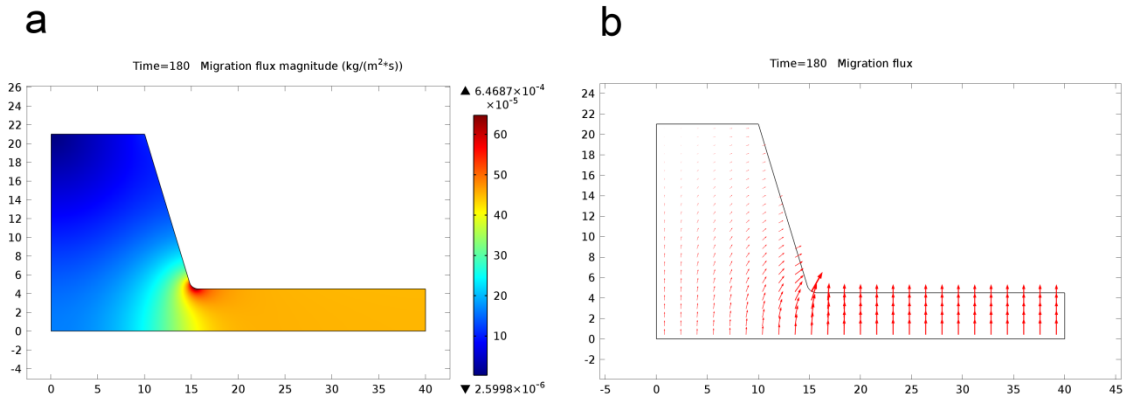

Figure 4.5 Migration flux magnitude [$kg.m^{-2}.s^{-1}$] and migration flux normalized vector for $Al_2OF_6^{2-}$.

However, according to Figure 4.6, the diffusion flux of $Al_2OF_6^{2-}$ shows a strong time dependence due to the fact that diffusion is proportional to the concentration gradient caused by two sources. First, the electrochemical reaction that takes place at the anode leads to the depletion of $Al_2OF_6^{2-}$ ions near the anode surface. Second, the migration of negatively charged $Al_2OF_6^{2-}$ towards the anode as the dominant mass transfer mechanism

in the early stages of electrochemical process is not as high as the anode reaction rate of this ion. This can be explained by the fact that the mobility of large $Al_2OF_6^{2-}$ ions is not high enough to provide the cell with the flux needed to avoid depletion. Therefore, although diffusion and migration are of the same order of magnitude in the early stages of the electrochemical processes, diffusion becomes more important and even becomes the dominant mechanism of mass transfer near the anode as the concentration gradient of this species near the anode surface becomes higher, as is shown for 30 [s], 60 [s], 120 [s], and 180 [s] in Figure 4.6.

Participation of $Al_2OF_6^{2-}$ in anodic reaction and the diffusion and migration of this ion towards the anode decrease the concentration of the ion between the two electrodes. Therefore, the reduction in the concentration of $Al_2OF_6^{2-}$ in the interelectrode region leads to the diffusion from the left part of the cell to the interelectrode region. In other words, the left-hand side of the cell acts as a reservoir of reactants that feeds the cell through diffusion.

On the other side, at the cathode, the flux pattern is completely different since $Al_2OF_6^{2-}$ is an electroinactive species. In this zone, only the electric field forces this species away from the cathode. The diffusion flux then gets in equilibrium with the migration along the cathode where it is far enough from the anode edge high concentration gradient region.

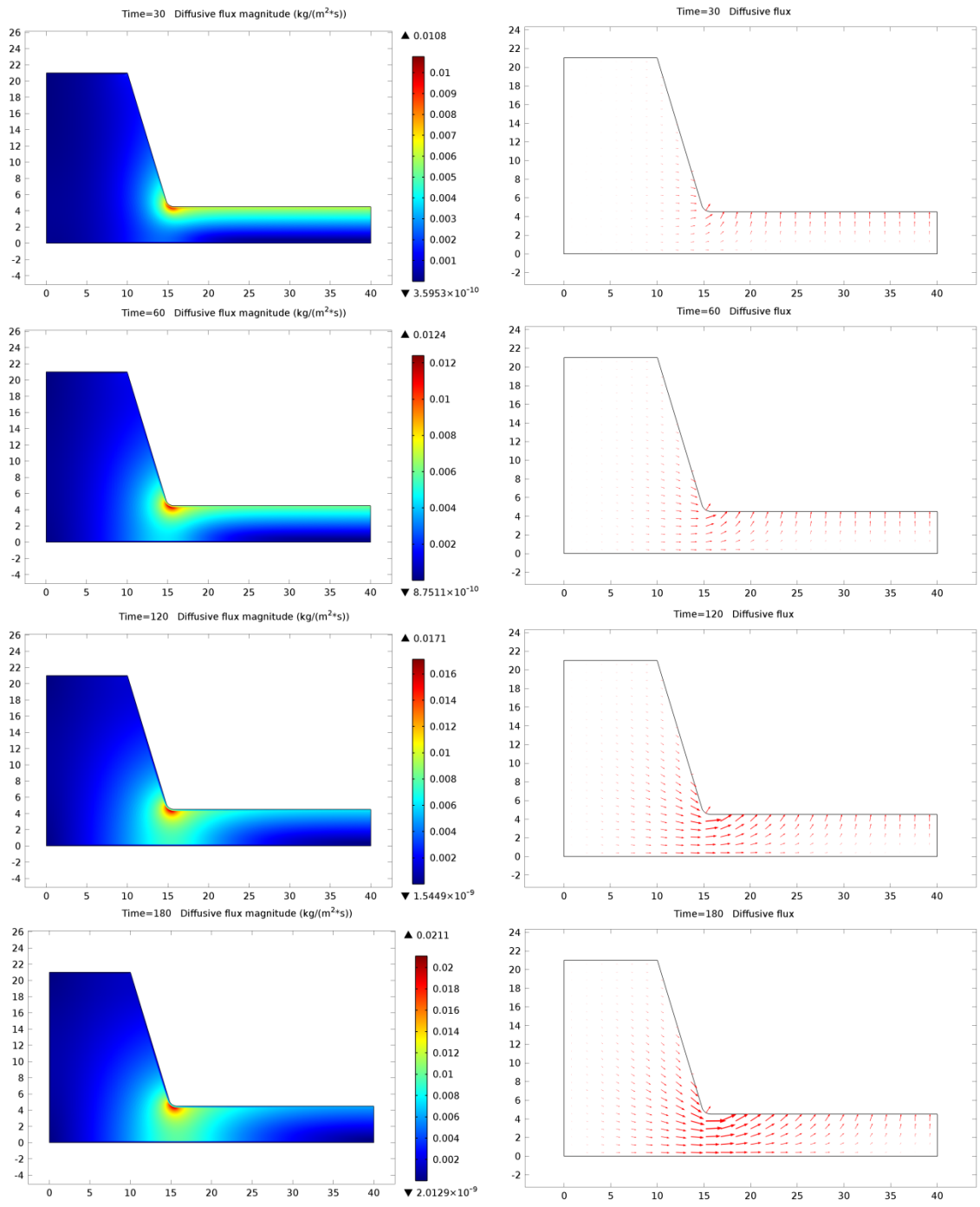

Figure 4.6. Diffusion flux magnitude [$kg.m^{-2}.s^{-1}$] and normalized diffusion flux vector for $Al_2OF_6^{2-}$ after 30[s], 60[s], 120[s], and 180[s].

The flux patterns mentioned in previous figures are at the origin of the concentration profiles near the electrodes, which leads to mass transfer boundary layer near the electrodes, as shown in Figure 4.7a. Although the concentration shows a transient behaviour in the anode diffusion boundary layer, the difference between the bulk concentration and the anode surface concentration becomes quickly constant, as shown in Figure 4.7b. Considering this concentration difference between the anode surface and bulk value, the mass transfer coefficient over the anode can be found using the following equation:

$$j_i = k_i \rho (\omega_i{}^{bulk} - \omega_i{}^{anode}) \qquad 4.22$$

Therefore, the mass transfer coefficient of $Al_2OF_6^{2-}$ at the anode is 5.5×10^{-5} [m/s].

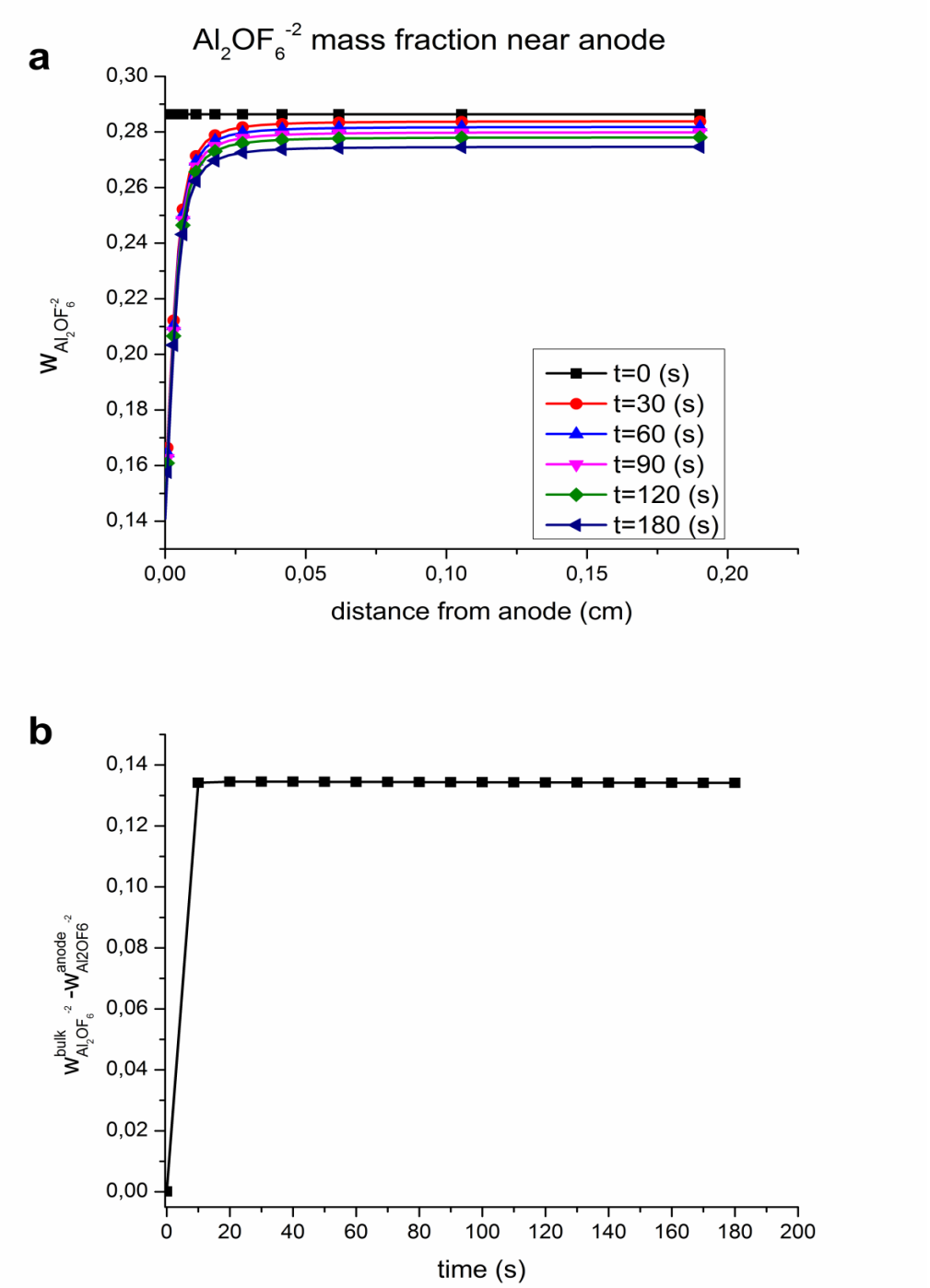

Figure 4.7. a) Concentration boundary condition of $Al_2OF_6^{2-}$ near the anode on the section line AA; b) Difference of bulk concentration and the anode surface concentration for different time steps near the anode on the section line AA.

4.6.2.2 Migration and diffusion fluxes of AlF_4^-

AlF_4^- is a species that is electroactive at both electrodes. Indeed, it is produced in the anodic reaction, and then reduced at the cathode, thereby producing aluminum.

The migration flux magnitude and the normalized migration flux vector are shown in Figure 4.8a and b, respectively. The migration flux for this negatively charged ion is towards the anode surface and is in the same direction as electric potential gradient along the electric current streamline. The migration flux changes very slightly with time due to its concentration change, but it can be considered in steady state when compared to transient behaviour of diffusion flux (see Figure 4.9).

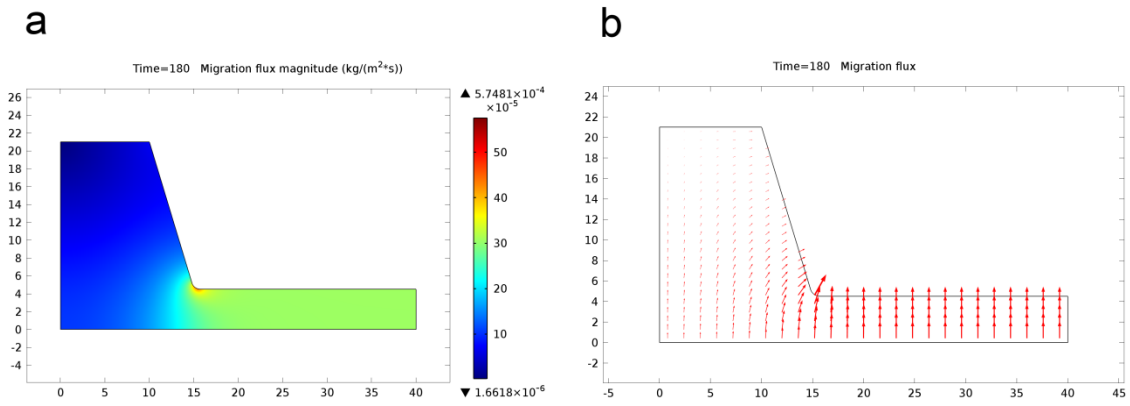

Figure 4.8. a) Migration flux magnitude [$kg.m^{-2}.s^{-1}$]; b) migration flux normalized vector for AlF_4^-.

As mentioned earlier, diffusion is driven by the concentration gradient caused by the migration of charged ions in the bulk of bath and also by the production or consumption of these ions by electrode reactions.

In the anode concentration boundary layer, the production of AlF_4^- ions at the anode in addition to the migration of these ions towards the anode initially increases the concentration of this ion. On the other side of the cell, AlF_4^- reacts at the cathode, and its

concentration becomes smaller than the bulk value. This concentration difference between the anode and cathode is the source of the diffusion flux of AlF_4^- ions across the cell. Indeed, in spite of the migration of AlF_4^- negatively charged ions away from the cathode, the high concentration difference between the anode and the bulk and, consequently, between bulk and the cathode makes the diffusion the most significant mechanism of mass transfer in the system, thereby preventing AlF_4^- depletion near the cathode surface.

As shown in Figure 4.9, the diffusion flux increases with time as the concentration gradients at both electrodes becomes larger. However, after 30 [s], this increase is much smaller for AlF_4^- when compared to the diffusion flux increase of $Al_2OF_6^{2-}$ already shown in Figure 4.6. The difference between the diffusion behaviour of these two species comes from the fact that migration of AlF_4^- ions is in the inverse direction of the needed diffusion flux, whereas for the case of $Al_2OF_6^{2-}$, both migration and diffusion help the ion to reach the reaction site. So the diffusion pattern formed from the early stages against migration flux is in the same direction as the diffusion flux which will be developed later on against depletion or accumulation of ions due to electrode reactions.

Moreover, by comparing the migration and diffusion fluxes, it is clear that the diffusion flux of AlF_4^- is the dominant mass transfer mechanism from the early stages of the electrochemical process in both the anode and cathode boundary layer.

Considering the development of diffusion flux vectors in Figure 4.9, it can be seen that AlF_4^- diffuses also from the interelectrode space to the left part of the cell. This can be explained by the fact that the rate of production of AlF_4^- at the anode is higher than its rate of consumption at the cathode for a specific reaction current, so its concentration becomes higher in the interelectrode space, and the left part of the cell works as a depository of AlF_4^- ions.

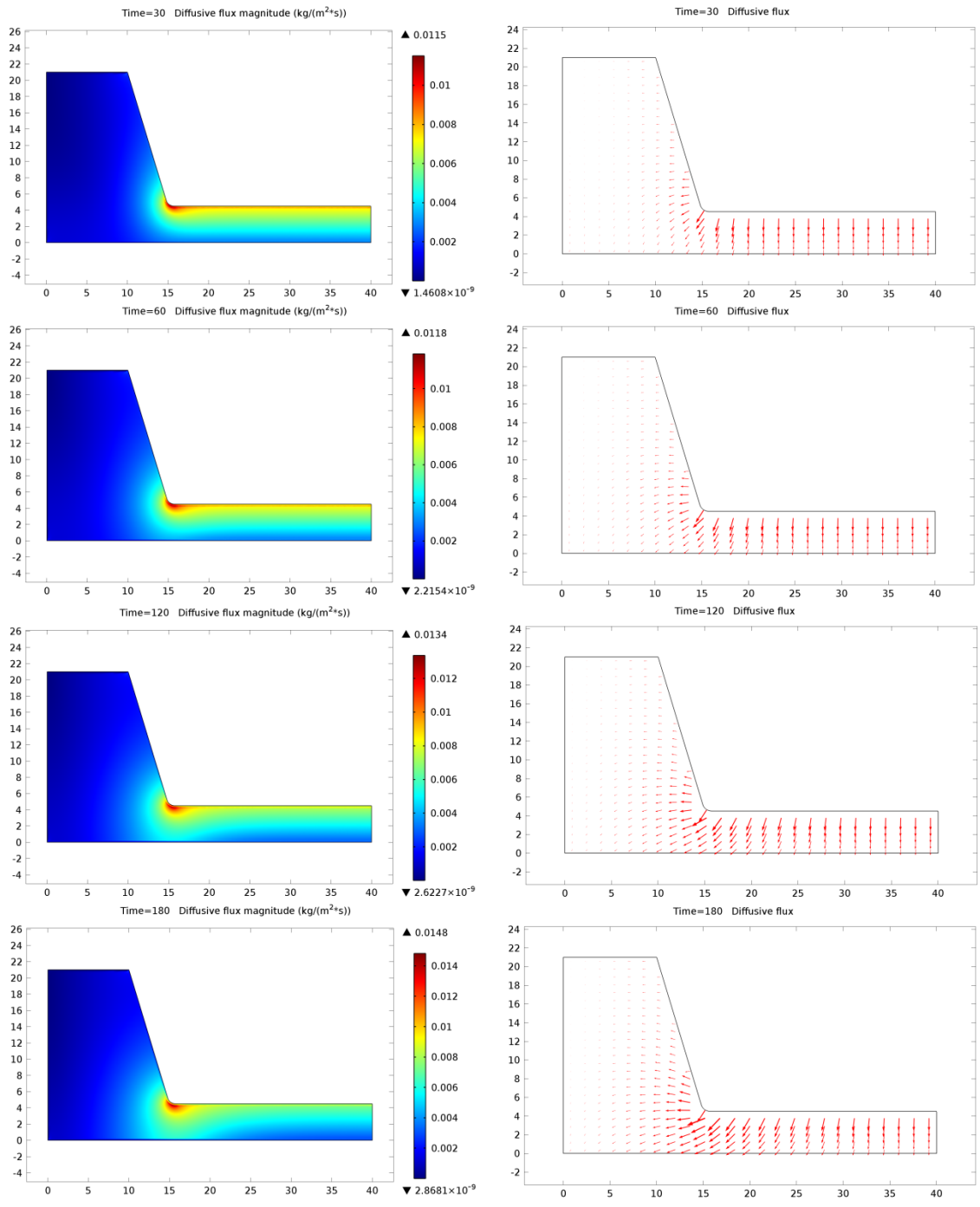

Figure 4.9. Diffusion flux magnitude [$kg.m^{-2}.s^{-1}$] and normalized diffusion flux vector for AlF_4^- after 30 [s], 60 [s], 120 [s], and 180 [s].

Figure 4.10a and b present the transient concentration of AlF_4^- on the section line AA (see Figure 4.1), near the cathode and anode region, respectively. The concentration of this ion in the anode boundary layer increases constantly with time as a result of the anode reaction in the first place and of the migration of AlF_4^- in the second place. However, in the cathode boundary layer, the concentration decreases in the early stages of cathode reaction, and, after passing through a minimum, an increase in the concentration of this ion is seen. The concentration is lower than the bulk value is for all times since AlF_4^- is an electroactive reactant at the cathode, which is reduced to produce aluminum. But the concentration out of the near the cathode layer increases with time due to:

- the production of this ion by the anode reaction; it should be noted that there are more AlF_4^- ions produced at the anode than consumed at the cathode;
- its diffusion towards the lower concentration regions near the cathode.

Although the concentration shows a transient behaviour, the difference between the bulk concentration and cathode surface concentration becomes quickly constant, as shown in Figure 4.10c. In the same manner as illustrated for $Al_2OF_6^{2-}$, the mass transfer coefficient of AlF_4^- near the cathode is found to be 1.18×10^{-4}. As already mentioned, it assumed to be a good representation of the steady state behaviour of the diffusion flux in the cell for larger times if we assume that regular alumina feeding re-establishes the initial mass condition in the electrolyte.

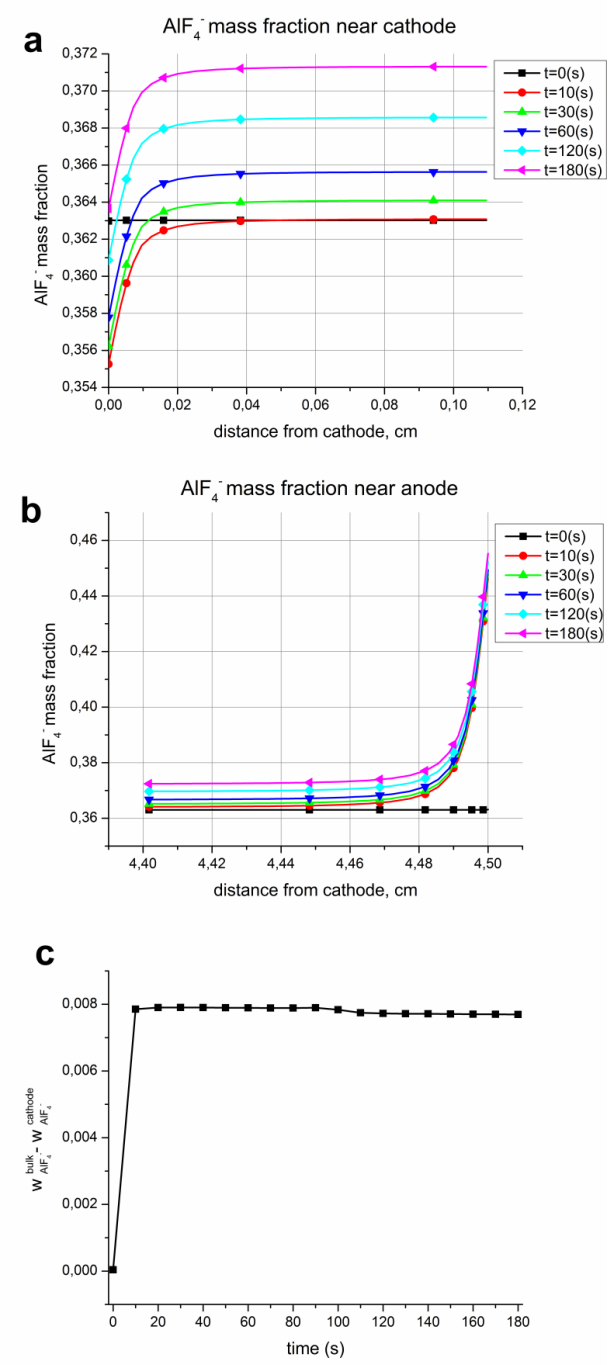

Figure 4.10. Mass fraction of AlF_4^- in a) cathode boundary layer, b) anode boundary layer, c) difference of bulk mass fraction and surface mass fraction for AlF_4^- with time.

4.6.2.3 Migration and diffusion fluxes of Na^+

It was shown for electroactive ions that high reaction rates produce a high concentration gradient for these ions near the electrodes, so that diffusion increases with time due to this concentration gradient. Nonetheless, the flow pattern of electroinactive ions, which do not participate in any reaction, is the result of equilibrium between migration and diffusion fluxes of these ions. As it is shown in Figure 4.11, the migration flux of Na^+, the only cation present in the cell, is in the same direction as current density vectors that pass through the bath.

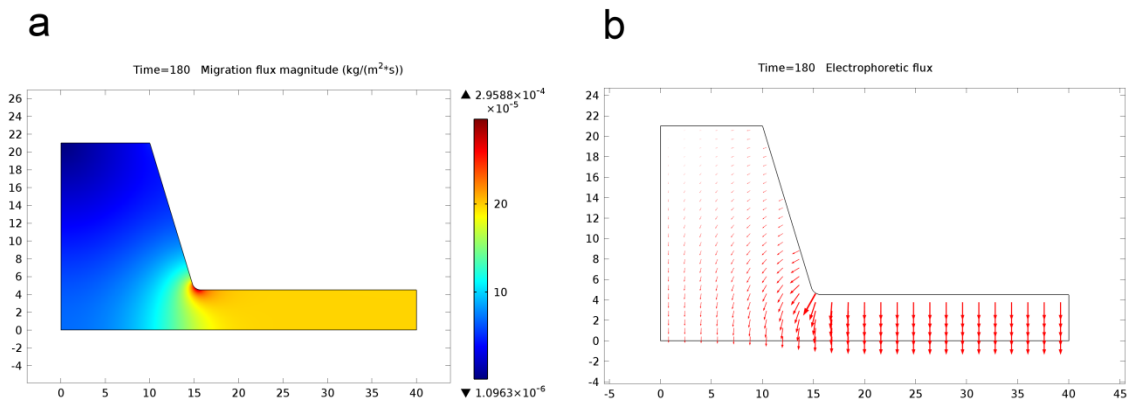

Figure 4.11. Migration flux magnitude [$kg.m^{-2}.s^{-1}$] and migration flux normalized vector of Na^+.

One of the main differences between Na^+ and previously discussed anions is that diffusion is not the dominant transfer mechanism and ultimately becomes of the same order of magnitude as migration for larger times, as shown in Figure 4.12. In other words, considering the hypothesis made in this study that this ion is absent in the electrode reactions, diffusion can be considered as the resistance of the concentration field against the migration caused by the electric field. The second point is that the migration of Na^+ ions towards the cathode makes the concentration in the interelectrode space near the anode lower than the left part of the cell. This creates a flow of the cations into the interelectrode space near the anode.

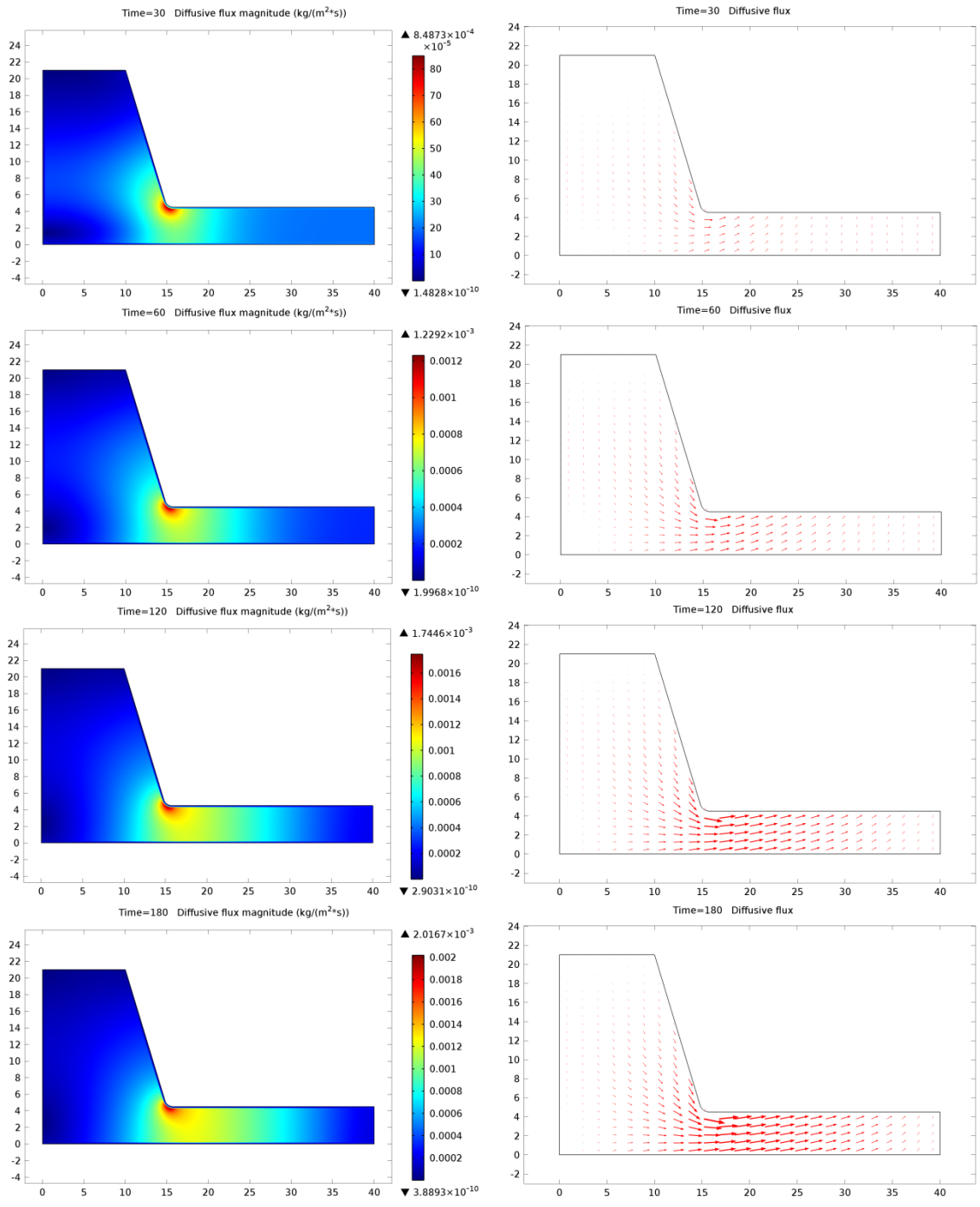

Figure 4.12. Diffusion flux magnitude [$kg.m^{-2}.s^{-1}$] and normalized migration flux vector for Na^+ after 30 [s], 60 [s], 120 [s], and 180 [s].

Migration and diffusion fluxes of electro-inactive anions

For other electroinactive anions, similar mass transfer pattern can be observed as for the case of Na^+. The difference is in the inverse direction of migration flux of negatively charged ions, as shown in Figure 4.13. Since negative anions are attracted to the anode, the direction of diffusion flux of the ions is in the opposite direction compared to the flux of Na^+. As it was shown in a previous (one-dimensional) work by the authors [53] the diffusion magnitude flux starts from zero and becomes equal to the migration flux for larger times, so there is equilibrium between migration and diffusion fluxes for these electroinactive ions, as seen in Figure 4.14. For the present two-dimensional study, the same phenomenon is observed; however, the diffusion flux from left part of the cell to interelectrode surface near the cathode is also added to this surface.

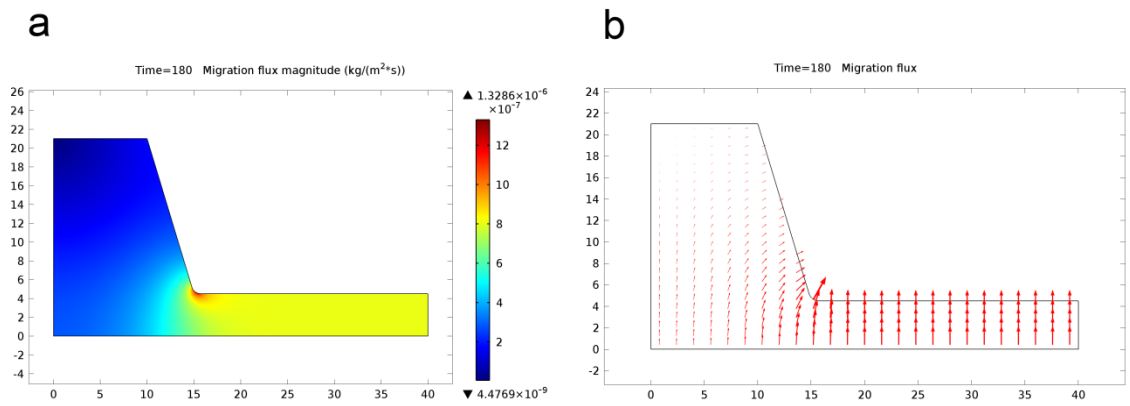

Figure 4.13. Migration flux magnitude [$kg.m^{-2}.s^{-1}$] and migration flux normalized vector for electroinactive anions.

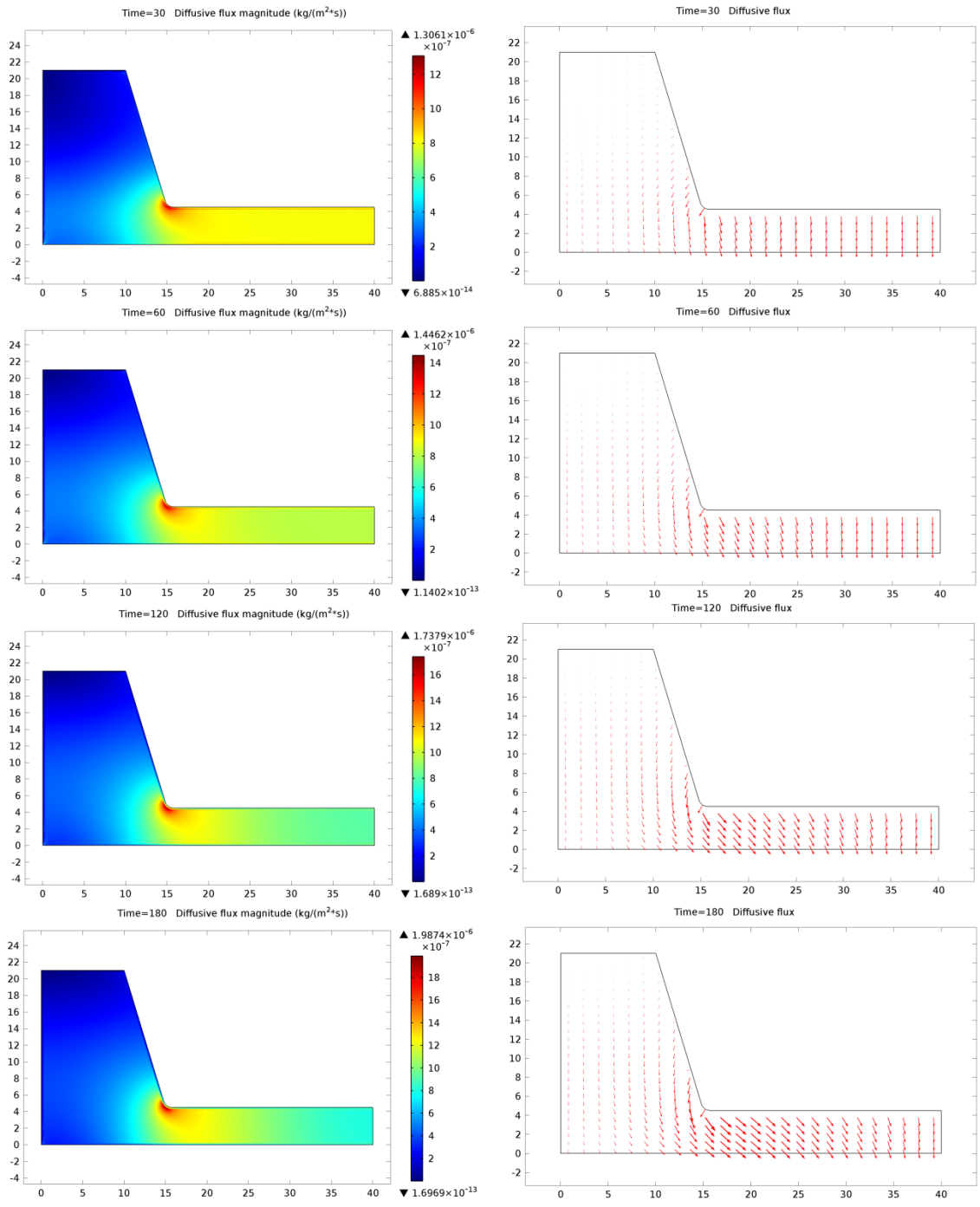

Figure 4.14. Diffusion flux magnitude [$kg.m^{-2}.s^{-1}$] and normalized diffusion flux vector for electroinactive anions after 30 [s], 60 [s], 120 [s], and 180 [s].

4.7 Conclusion

The electric and concentration fields in the electrolytic bath of an aluminum production cell have been modelled considering the kinetics of reactions at both electrodes, and the solution of the equations is made using COMSOL. The mass transfer model includes the coupled movement of three categories of ions: electroactive anions, electroinactive anions, and finally Na^+ as the only cation. The important contribution of convection has been modelled by adding a turbulent diffusion term to the system. The transient migration and diffusion as the main mechanisms of mass transfer has been studied at 180 seconds. This period is characteristic of the industrial operation of aluminum cells where alumina is added to the cell typically every 3 or 4 minutes.

Among the electroactive ions, $Al_2OF_6^{2-}$ and AlF_4^-, migration is the dominant mechanism of transport for the very early stages of the electrochemical processes. However, a high rate of consumption or production of these ions at the corresponding electrodes forms high concentration gradients near the surfaces of these electrodes, which at later times leads to high diffusion rates of the species into or out of the corresponding boundary layer. This makes diffusion the governing mechanism of ion transfer near the electroactive electrodes. For the case of $Al_2OF_6^{2-}$, which is the ionic form of dissolved alumina, the region out of the interelectrode space (at the left of the anode) is depleted very slowly, thus acting as an alumina "reservoir". This causes a diffusion flux from the reservoir into the interelectrode space at later stages, when the concentration between the two electrodes decreases. On the other hand, since the rate of production of AlF_4^- at the anode is higher than its rate of consumption at the cathode because of stoichiometry, its concentration becomes higher in the interelectrode space and a diffusion flux is observed from this region to the left part of the cell. For this species, the left part of the cell works as a depository.

For electroinactive ions and Na^+, the concentration profiles near the electrode are formed by migration of these charged ions towards the opposite electrode, so the rate of diffusion

flux is much smaller when compared to electroactive anions. Moreover, the migration flux of Na^+ in the bath is the larger than all other anions due to higher mobility of this ion as compared to the other larger anions in the cell.

In further studies, the temperature field will be solved for the electrolytic bath using heat generation source terms. Since it has been noted that the turbulent flow of the bath has such an important impact on the concentration and temperature fields, the flow fields should be included. This is a very important modification to the model since it implies a full three-dimensional description of the cell and inclusion of the electromagnetic effects on convective fluxes.

Acknowledgement

The authors are very grateful to the Natural Sciences and Engineering Council of Canada (NSERC) for its financial support.

Nomenclature

A anode surface$[m^2]$

A_h available anode area for the current passage$[m^2]$

D_i mixture-averaged diffusion coefficient of species i, $\left[\frac{m}{s^2}\right]$

$D_{i,j}$ multicomponent diffusion coefficient of species i , $\left[\frac{m}{s^2}\right]$

D_t turbulent diffusion coefficient, $\left[\frac{m}{s^2}\right]$

D_w wall distance, [m]

E_{rev} electrode reaction equilibrium voltage$[V]$

F faraday constant $\left[\frac{C}{mol}\right]$

M_i molar mass of species i, [kg]

M_n mean molar mass, $[kg]$

N number of species

R_i mass rate of production of species I by homogeneous reaction$\left[\frac{kg}{m^3.s}\right]$

U_{cell} cell voltage$[V]$

a_i activity of species i

g inverse distance function$\left[\frac{1}{m}\right]$

i current density magnitude $\left[\frac{A}{m^2}\right]$

$\boldsymbol{i}$ current density vector $\left[\frac{A}{m^2}\right]$

$\boldsymbol{j}_i$ mass flux of species *i*, $\left[\frac{kg}{m^2.s}\right]$

$\boldsymbol{j}_t$ turbulent mass flux of species *i*, $\left[\frac{kg}{m^2.s}\right]$

n number of electron transfered in electrode reaction

u_i mobility of species *i*

x_i molar fraction of species *i*

z_i charge number of species *i*

Greek letters

α factor of convection $\left[\frac{1}{m.s}\right]$

ε relative permittivity of bath

ε_0 electric permittivity of vacuum $\left[\frac{F}{m}\right]$

η overpotential [V]

ν_i stoichiometric coefficient of species *i*

ρ mass density of solution $\left[\frac{kg}{m^3}\right]$

ρ_E electric charge density $\left[\frac{C}{m^3}\right]$

φ electric potential $[V]$

ω_i mass fraction of species i

Subscripts

A anode

C cathode

5 MASS TRANSFER MODELING FOR ELECTROCHEMICAL CELLS USING OPENFOAM

5.1 Abstract

In this chapter, an open source code is exploited and developed for the purpose of numerical simulation of electrochemical cells. This code is built and installed on existing open source toolbox, OpenFOAM (Open source Field Operation and Manipulation). The developed toolbox has the capacity to solve secondary current distribution for electric field, velocity field, and Maxwell-Stefan equations for mass transfer in concentrated solutions. In this chapter, the mathematical presentation of mass transfer problem and also the numerical algorithm used to develop the code are explained. As an example, the case of parallel plate electrodes applied to the electrolysis of aluminum is considered. The chemical equilibrium representing the dissolution of alumina in electrolytic bath (homogeneous reactions) is also modeled. The flow of electrolytic bath between the electrodes (velocity field) and also the transport of chemicals in the cell (concentration field) are also solved using transient solvers. The model is also applied to the case without considering the homogenous reaction. The results indicate that both systems reach the steady state if enough time is let to the system. However, it takes more time for the model with chemical equilibrium reactions to reach steady state. The depletion of $Na_2Al_2OF_6$ occurs at the surface of the anode. The chemical equilibrium affects and limits $NaAlF_4$ concentration in high concentration region near anode.

5.2 Introduction

As stated in previous chapters, mathematical modeling of the mass transfer inside electrochemical cells involves taking into consideration the three mechanisms of mass

transport: diffusion, migration and convection. The total mass of each species should be conserved when also considering the reactions that take place at the electrodes and in the electrolyte. The previous models presented in this study carry three different assumptions that were dictated by the limitations of the solving toolbox (COMSOL). Firstly, convection was simplified through the use of a turbulent diffusivity and the corresponding turbulent diffusive flux. Although the simplified turbulent diffusion model was a good way to take into account the effect of eddies on the mass transport, it did not consider all effects of convection on mass transport, especially for more complicated geometries. Secondly, the chemical equilibrium between cryolite and alumina in the solution was only considered at the beginning of the simulation: representing the time after cell feeding. The calculation of this equilibrium in each control volume and for each time step would give a more realistic description of mass transport in the cell, particularly for the electroactive ions showing high concentration gradients. Thirdly, the model presented in previous chapters for diffusion was based on modified Fick's law for concentrated solution. This model is based on the use of an effective diffusion coefficient for each ion, which is locally dependent on the concentration of different ions. However, a more rigorous approach to model diffusive fluxes in multicomponent mixtures is described by Maxwell-Stefan equations [52]. In contrast to Fick's law, the Maxwell-Stefan equations describe the binary interfluxes of each pair of species. In other words, the application of concentrated solution theory implies that diffusive flux of each species relative to the other species can be different and may not be reduced to only one diffusion coefficient [15]. The Maxwell-Stefan formulation and solution is discussed in details in the coming sections.

The implementation of convection and chemical reactions demands a robust numerical structure, especially for turbulent high temperature flows. Moreover, the application of Maxwell-Stefan implies that fluxes are the functions of the binary diffusion coefficients and demands that intensive implicit calculation of fluxes from concentrations. Moreover, these equations are either not implemented in existing multiphysics codes or their numerical solution convergence is difficult because of the high number of species system

due to nonlinear coupled nature of the differential equations. These limitations lead us to implement the model in a more sophisticated and flexible platform with the capability of multiphysics formulation for multi-region geometries. The capabilities to handle the hydrodynamic and thermal aspect of the problem are also very important. Moreover, the capability to solve partial differential equations for other fields like electric or magnetic fields can be also valuable and helpful, see Appendix A. OpenFOAM (Open source Field Operation and Manipulation) is a C++ toolbox for the development of customized numerical solvers of continuum mechanics problems including Computational Fluid Dynamics (CFD). This software has the capability to integrate new solvers and boundary conditions designed and developed by the new users into the existing solvers and libraries.

In OpenFOAM, there is no specific solver dedicated to the electrochemical reaction kinetic aspects or more generally to the transport phenomena inside electrochemical cells. Moreover, the mass transfer solvers already implemented in OpenFOAM are designed for combustion cases, with Fick's diffusive fluxes, which are not applicable to concentrated solutions and more generally to electrolytic solutions. However, this toolbox provides valuable solvers and libraries and also the advanced geometry and meshing tools which can be helpful in the simulation of electrochemical processes, all of which representing strong benefits.

This chapter of thesis tries to describe the developments that have been made into OpenFOAM to simulate the mass transfer of electrochemical cells. It includes the mathematical formulation, the numerical modeling, and an example of its application to the simulation of aluminium electrolysis cell. Finally, the results obtained by simulating aluminium electrolysis process for parallel plate geometry are to be discussed and analyzed.

5.3 Transport phenomena modeling and conservation laws

Transport phenomena in electrochemical cells deal with four major fields: electric potential, concentration, velocity, and temperature. Moreover, it should be noted that there may be other fields like electromagnetic field, which have very important impact on the transport pattern of other fields, especially in large scale cells. The mathematical models that describe these fields are conservation laws as applied to momentum, mass and electrical charges, each of which being based on continuum mechanics formulation.

One conservation law is not necessarily decoupled from the other conservation laws. Typically, all conservation laws are coupled and their solutions involve a coupled system of partial differential equations. All assumptions that can uncouple or limit the strength of the coupling without major loss of generality or precision of the study can be helpful in the solution of the coupled partial differential equations. For example, the constant temperature assumption reduces the mass transfer problem to interaction of concentration field with the two other fields left: velocity and electric potential. In fact, coupling between these three fields are related to convection and migration flux in species mass conservation equations. Poisson's equation should be solved to satisfy the electric charge continuity, see Appendix A. Navier-Stokes equations are to conserve the mass and momentum in the system. The solution of the equations will be explained in the coming sections by their application on a simplified aluminium electrolysis cell.

5.4 Case for mass transfer in aluminium electrolysis cell

The purpose of this study is to study the effect of convection and bath equilibrium on the species concentration using OpenFOAM. This study will take into account the following missing parts in previous studies:

- The effect of chemical equilibrium of the bath is added.
- The convection flux is added to the diffusive flux.

- The multicomponent diffusion flux is calculated based on Maxwell-Stefan formulation.

In order to reduce the complexity of velocity field, the simpler geometry of two parallel electrodes is considered, see Figure 5.1.

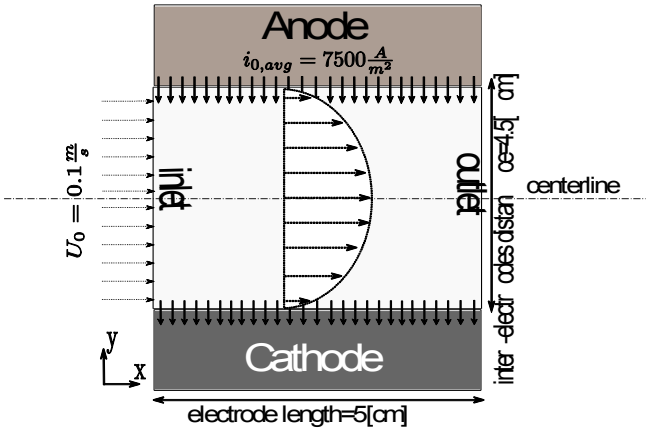

Figure 5.1 Parallel-plate electrode model for aluminium cell

5.4.1 Chemical equilibrium

The solution of alumina (Al_2O_3) and cryolite (Na_3AlF_6) is considered as an ideal solution with saturated alumina dissolved in the bath. This will set the activity of alumina to be unity in this solution. The species are considered to be the species proposed by Zhang et al. with anions surrounded by Na^+ ions [56, 57]. Consequently, the migration is only devoted to Na^+ ions as it has been already considered in other studies. The electrolytic bath is initially at NaF-AlF_3-Al_2O_3 equilibrium. The bath equilibrium is calculated based on the chemical model proposed by Zhang et al.:

$$\frac{1}{3}Al_2O_3(s) + 2NaF(l) + \frac{4}{3}AlF_3(s) \rightarrow Na_2Al_2OF_6(l)$$

$$\frac{2}{3}Al_2O_3(s) + 2NaF(l) + \frac{2}{3}AlF_3(s) \rightarrow Na_2Al_2O_2F_4(l)$$

$$\frac{2}{3}Al_2O_3(s) + 4NaF(l) + \frac{2}{3}AlF_3(s) \rightarrow Na_4Al_2O_2F_6(l) \qquad 5.1$$

$$3NaF(l) + AlF_3(s) \rightarrow Na_3AlF_6(l)$$

$$NaF(l) + AlF_3(s) \rightarrow NaAlF_4(l)$$

Moreover, the flow entering interelectrode distance at the inlet boundary is also at equilibrium.

Two cases are considered for this analysis: one without homogenous reaction and the other one with homogenous reaction (bath chemical equilibrium). Homogenous reactions are modeled through two forward and back reactions, with the ratio of specific reaction rates equal to equilibrium constants, as proposed in previous studies [13, 14].

5.4.2 Velocity field

To obtain the velocity field, Navier-Stokes equations are to be solved for the reactor domain for a case of duct transient flow. The solution entering the reactor is assumed to have a uniform inlet velocity of $0.1\ \frac{m}{s}$, a value typically found in aluminum electrolysis cells[29]. The system is considered to be isothermal at 1240 K, a condition that is closely encountered in aluminum electrolysis cells [12-14, 29]. The simulation is done using transient PISO solver, as mathematical model and its numerical algorithm is presented in following sections.

5.4.2.1 Momentum-conservation equations

The momentum conservation equation for fluids is given by Navier-Stokes equations:

$$\frac{\partial(\rho \boldsymbol{v})}{\partial t} + \nabla.(\rho \boldsymbol{v}\boldsymbol{v}) - \nabla.\tau = -\nabla p \tag{5.2}$$

Where ρ is the fluid density, $\boldsymbol{v}$ is the fluid velocity, τ is the viscous stress tensor and, p is the pressure. This equation is solved with another conservation equation that is mass conservation equation or mass continuity equation:

$$\frac{\partial(\rho)}{\partial t} + \nabla.(\rho \boldsymbol{v}) = S_y \tag{5.3}$$

Where $\boldsymbol{v}$ is given by the momentum-conservation equations and S_y stands for the volumetric mass sources. These equations give the velocity as a vector field in the computational domain. The algorithm used for solving these equations is explained in next section.

5.4.2.2 Numerical model

OpenFOAM is basically developed to treat the momentum and heat transfer in fluid mechanics. The momentum conservation equations, Equation 5.3, are solved through PISO (Pressure Implicit with Splitting of Operators) algorithm. The PISO algorithm was originally proposed by Issa[65] and is implemented as a standard solver into OpenFOAM by Jasak[66].The algorithm of the solver is shown in Figure 5.2.

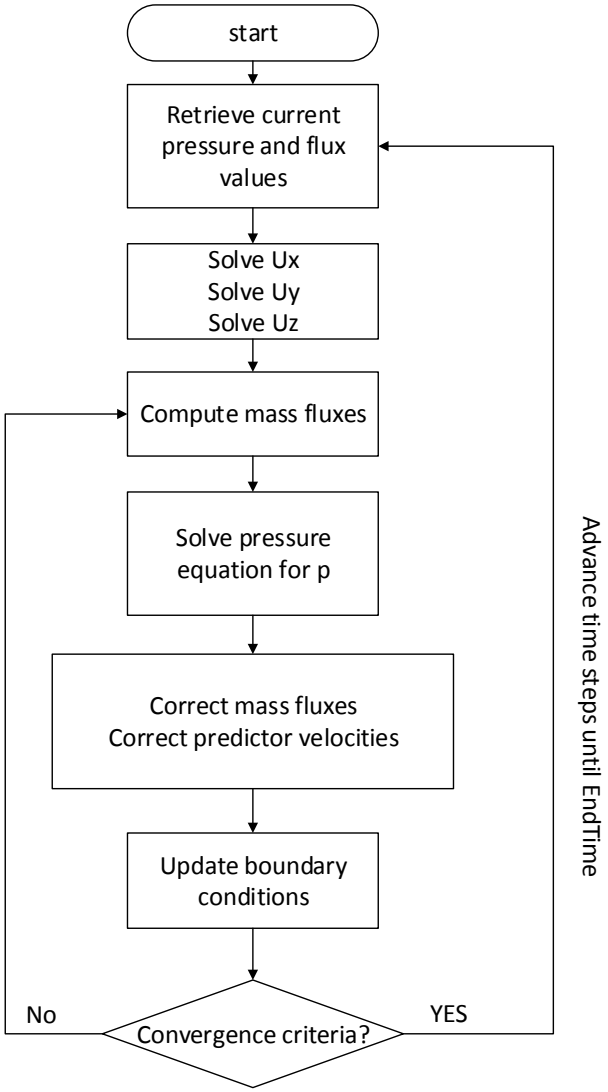

Figure 5.2 PISO algorithm flowcharts

5.4.3 Species mass-conservation equation

The mass conservation for each species is given by the following equation:

$$\frac{\partial(\rho w_i)}{\partial t} + \boldsymbol{\nabla}.(\rho w_i \boldsymbol{v}) + \boldsymbol{\nabla}.(\boldsymbol{j_i}) = S_{y_i} \qquad 5.4$$

Where ρ is the fluid density, $\boldsymbol{v}$ is the fluid velocity, w_i is the mass fraction of species i, j_i is the mass diffusion-flux of species i relative to the mass-average velocity, and S_{y_i} stands for the volumetric sources or sinks of the species i.

The modeling of the diffusion flux j_i is depending on the solution of species and the medium in which the diffusion takes place. For dilute solutions, Fick's diffusion law is applicable. For concentrated solutions, the Fick's law is modified to be applicable to concentrated solutions as it was the case for the diffusion models in the two previous chapters. However, a more accurate analysis of the mass transport can be given by Maxwell-Stefan (M.S.) equation.

5.4.3.1 Maxwell-Stefan model

The Maxwell-Stefan, that relates diffusion mass fluxes to molar fractions, is written below:

$$\nabla x_i = \sum_{\substack{j=1 \\ j\neq i}}^{j=N} \frac{x_i x_j}{\mathcal{D}_{ij}} \left(\frac{\boldsymbol{j_j}}{\rho} - \frac{\boldsymbol{j_i}}{\rho}\right) \qquad 5.5$$

Where x_i is the mole fraction of species i, and $\mathcal{D}_{ij}$ is the binary diffusion coefficient of species i in medium j. As it can be seen in Equation 5.5, the relation between diffusion coefficients and fluxes is an implicit relation. However, in order to calculate the diffusive mass fluxes j_i explicitly from concentration matrix, it is possible to sum up all the binary diffusion fluxes of a species in other species, see Equation 5.6.

$$\boldsymbol{j_i} = -\sum_{j=1}^{j=N} \rho D_{ij} \nabla w_i \tag{5.6}$$

Where D_{ij} is different from multicomponent diffusion coefficient $\mathcal{D}_{ij}$, and is equivalent to Fick's binary diffusion coefficient in multicomponent mixtures. D_{ij} is calculated by the following correlation which converts the matrix of Maxwell-Stefan diffusion coefficients to Fick's multicomponent diffusion coefficient matrix.

$$[D] = [A]^{-1}[B] \tag{5.7}$$

Where the matrixes A and B are given below.

$$A_{ii} = -\left(\frac{x_i}{\mathcal{D}_{iN}} \frac{1}{W_N} + \sum_{\substack{j=1 \\ j \neq i}}^{N} \frac{x_j}{\mathcal{D}_{ij}} \frac{1}{W_i} \right)$$

$$A_{ij} = x_i \left(\frac{1}{\mathcal{D}_{ij}} \frac{1}{W_j} - \frac{1}{\mathcal{D}_{iN}} \frac{1}{W_N} \right) \tag{5.8}$$

$$B_{ii} = -\left(x_i \frac{1}{W_N} - (1 - x_i) \frac{1}{W_i} \right)$$

$$B_{ij} = -x_i \left(\frac{1}{W_j} - \frac{1}{W_N} \right)$$

Equation 5.7 gives the diffusion flux; the convection and migration fluxed must be added to this flux, through calculation of velocity and current density fields. Finally, having calculated the fluxes, the mass conservation equation for each species can be solved.

The boundary conditions for mass transfer are in form of Newman-type boundary conditions.

$$\boldsymbol{j_i} = \rho D_{im} \nabla w_i$$

Therefore, such conditions are derived from generic Newman-type boundary condition in OpenFOAM called fixedGradientFvPatchfield. This boundary condition imposes the normal gradient on the surface based on the flux which is given from electrode kinetic current density (for coupled case with electric field) or from electrode surface reaction rate (for uncoupled case or for uniform current density assumption over the electrodes), as it is shown below:

$$snGrad(w_i) = \frac{-\boldsymbol{j_{avg,i}} \cdot \boldsymbol{n}}{\rho D_{im}} \qquad 5.9$$

The algorithm, which calculates the diffusivity matrix, the M.S. fluxes, and solves the concentration field is shown in Figure 5.3. The code of mass conservation with M.S. fluxes is implemented in a library named multiSpeciesTransportModels that is located in the OpenFOAM user directory.

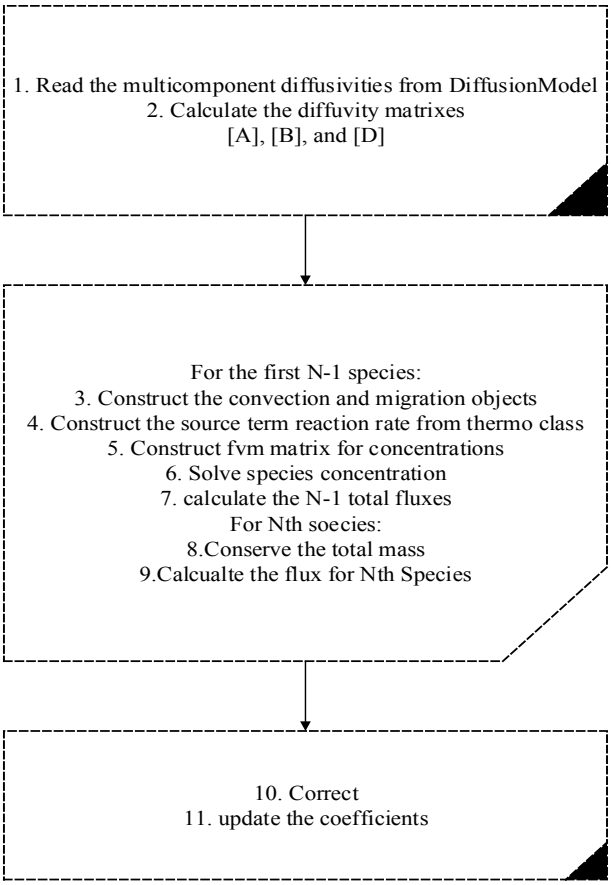

Figure 5.3 Mass transfer library: Maxwell-Stefan equation solver

5.5 Meshing and solution

The officially implemented tool in OpenFOAM, *blockMesh,* is used to create geometry and to create a structural mesh. The meshes are cubic meshes and include about 5000 finite volumes for this geometry.

The system is considered to be isothermal, a condition that is closely encountered in aluminum electrolysis cells[13, 14]. The simulation is done using transient PISO solver. The system reaches steady state before 120 seconds for the case with homogeneous reactions and after 45 seconds for the case without homogeneous reaction. In the next section, the results will be discussed.

5.6 Results and discussion

As stated in the previous sections, the initial composition of electrolytic bath between the electrodes is at chemical equilibrium. In the same manner, the electrolytic that enters the reactor is also in chemical equilibrium. The heterogeneous electrode reactions starts at t=0 and forms diffusion boundary layers for electroactive species near the electrodes.

Among the species present in the cell, $Na_2Al_2OF_6$ and $NaAlF_4$ are of great importance. In fact, the first species ($Na_2Al_2OF_6$) has the highest concentration at equilibrium in electrolytic bath with lower cryolithe ratio (CR). It is represents the concentration of alumina dissolved in the bath. The second one ($NaAlF_4$) is the species that is reduced at the cathode thereby producing aluminum. $NaAlF_4$ is also a product of the anode reaction. In fact, along with NaF, these ions are the main electroactive species in the cell. Being electroactive at electrodes, these species form concentration gradients near the active electrodes and consequently a diffusion boundary layer is formed near the electrodes.

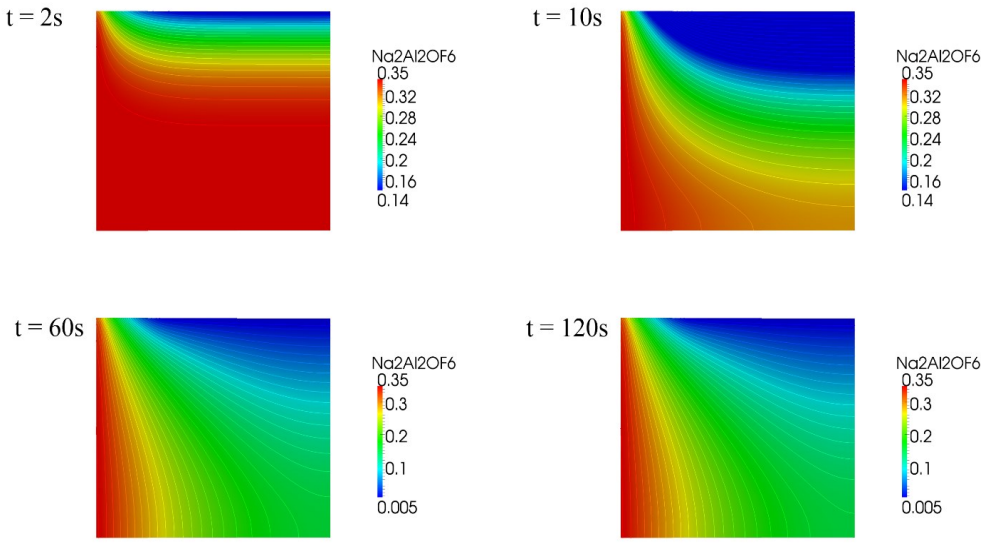

Figure 5.4 Transient mass fraction of $Na_2Al_2OF_6$ for different time steps between parallel electrodes

Figure 5.4 shows the development of concentration profiles and contours of concentration for $Na_2Al_2OF_6$ after 2, 10, 60, and 120 seconds. The system converges to steady sate response after 120[s]. As it can be seen in Figure 5.4 , the area near the anode is depleted of $Na_2Al_2OF_6$ species due to high anode reaction rate. Figure 5.5 illustrates the decrease of $Na_2Al_2OF_6$ mass fraction in the centerline of the reactor from 0.35 in the reactor inlet to 0.11 for the outlet of the reactor at steady state conditions.

The difference between the mass fraction of $Na_2Al_2OF_6$ of entering and leaving fluid can be viewed along the outlet boundary, as it is shown in Figure 5.5 B). $Na_2Al_2OF_6$ is depleted over the anode. As it is clear, the concentration of $Na_2Al_2OF_6$ in the cathode region is higher than in the anode region. However, it is still much lower than the inlet mass fraction. The decrease in mass fraction of $Na_2Al_2OF_6$ is the result of fast anode reaction that produces $NaAlF_4$ and CO_2 at the anode. In this study, it is assumed that all CO_2 produced leaves the bath and reactor immediately after production and does not accumulate in the cell.

Although the decrease in concentration of $Na_2Al_2OF_6$ in the cell is observed, the concentration of $NaAlF_4$ is increasing in the anode diffusion boundary layer. This will create a high concentration difference for this species in the interelectrode direction (normal to electrode), as it is shown in Figure 5.6.

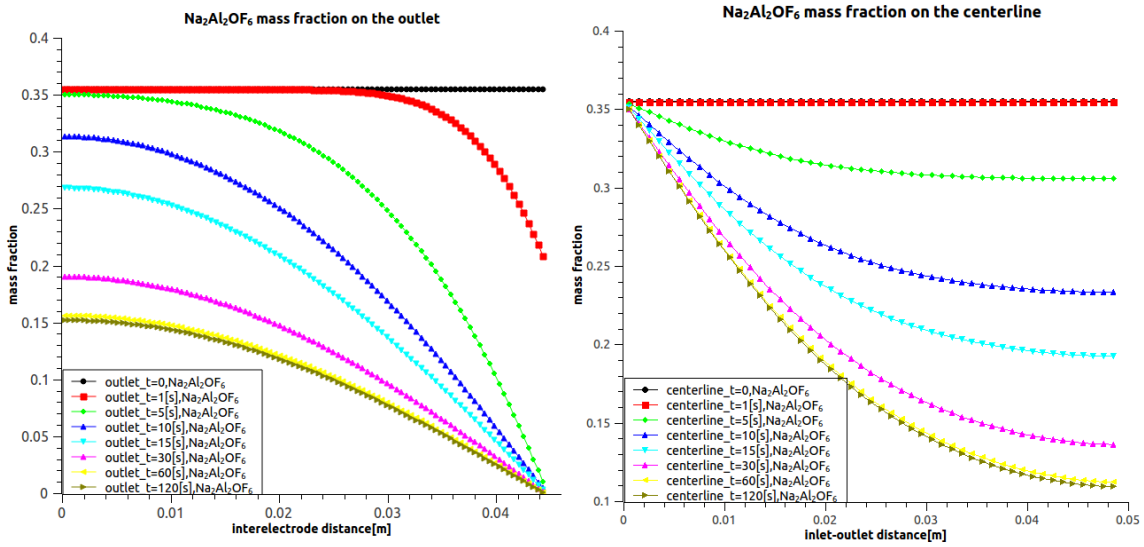

Figure 5.5 Mass fraction of $Na_2Al_2OF_6$ in the outlet (left) and in the centerline of the reactor (right)

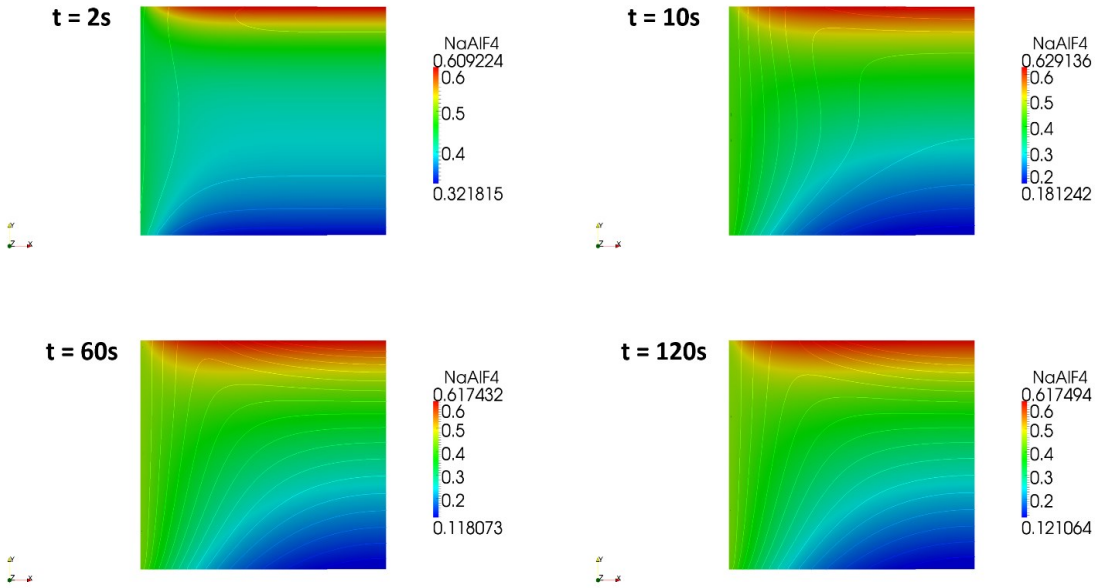

Figure 5.6 Transient mass fraction of $NaAlF_4$ for different time steps between parallel electrodes

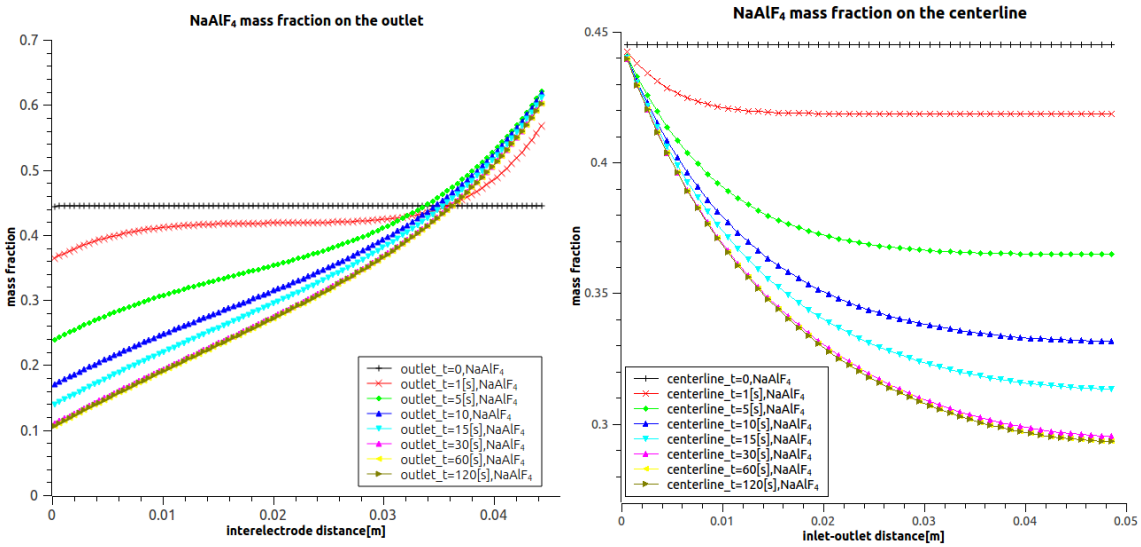

Figure 5.7 Mass fraction of $NaAlF_4$ in the outlet (left) and in the centerline of the reactor (right)

This normal concentration gradient between anode and cathode leads to important $NaAlF_4$ molecular diffusion toward cathode region. Although $NaAlF_4$ concentration gradient is only in the boundaries diffusion layer in early stages of the electrolysis process, this gradient is developed to the bulk region for later times, far from the inlet of the cell, as it is shown in Figure 5.6. This will lower the concentration gradient between bulk and the electrode region for this ion, as it is clear in Figure 5.7. It should be noted that $NaAlF_4$ concentration decreases near cathode and increases near the anode as the flow move to outlet region. However, the rate of production is higher than the rate of consumption, due to stoichiometric coefficient of two reactions for a constant number of electron transfer. This high concentrated area of $NaAlF_4$ in the anode region affects the chemical equilibrium of the bath. This will reinforce the reverse effect of chemical equilibrium to lower $NaAlF_4$ mass fractions, as it can be understood from Figure 5.8. By comparing the two simulations, the first without considering equilibrium and the second with equilibrium calculations, it is clear that this will result in considerably lower mass fraction of $NaAlF_4$ near the anode ($\omega_{NaAlF_4} = 0.62$) comparing to the case without considering chemical equilibrium ($\omega_{NaAlF_4} = 0.9$).

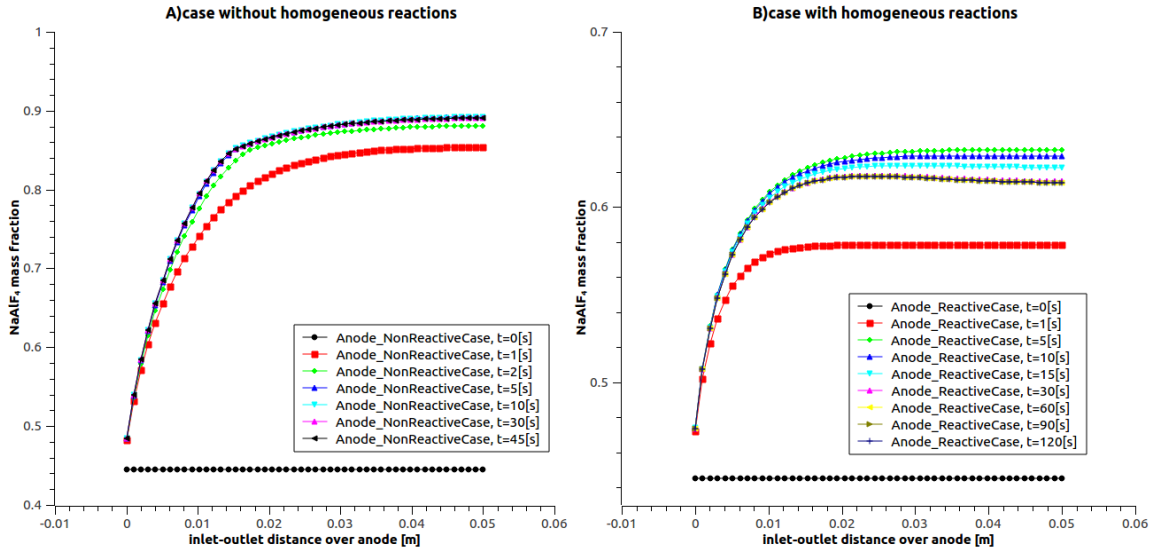

Figure 5.8 Concentration of $NaAlF_4$ over the anode for the cases neglecting the chemical equilibrium of electrolytic bath (left) and considering the chemical equilibrium of electrolytic bath (right)

5.7 Conclusion

There have been few studies dedicated to mass transfer analysis in aluminum electrolysis cell. High temperature and high corrosiveness of the bath have been major obstacles for experimental researches in this field. Numerical modeling of the cell also suffers from the lack of data, high nonlinear coupling between different fields. However, the studies done in the previous two chapters of the thesis analyze 1-D and 2-D mass transfer in the cell by considering the impact of diffusion and migration and turbulent diffusion. These studies consider certain assumptions, which are imposed by the limits of the numerical toolbox that was used. These assumptions can be described as below:

- Neglecting the chemical equilibrium in the bath
- Reducing the impact of convection on mass transfer to turbulent diffusion
- Using simplified concentrated solution theories for mass transfer instead of employing Maxwell-Stefan equations

In the study presented in this chapter, an open source code built on an open source platform (OpenFOAM) is exploited and developed to be capable of handling transport phenomena in the electrochemical reactors. Since OpenFOAM is a code specifically developed for computation fluid dynamic (CFD) applications, the developed code uses the powerful tools already implemented in OpenFOAM to treat complicated flow patterns like turbulence and multi-phase flow and even homogeneous reactions. Moreover, the developed code is capable of modeling mass transfer models like Fick's and Maxwell-Stefan equations. Other developments in OpenFOAM include the new boundary condition treatments and manipulations for Butler-Volmer kinetics at electrodes. This will allow the users to model "Robin type" boundary conditions in the software.

In addition to the numerical contributions of this study, a convective-diffusive model of aluminum electrolysis process between parallel plate electrodes is modeled in OpenFOAM. The application of the code to two cases, one with and the other without chemical equilibrium in the bath, indicates that the latter reaches steady state faster. The reaction has limiting effect on the concentration of ions in diffusion boundary layer, like for the $NaAlF_4$ species in the anode diffusion boundary layer.

For further studies based on the developed code, it is important to analyze the effect of velocity on the mass transfer in the cell, since velocity has large impacts on the turbulence of the system. Other factors also need to be modified, like the parameters defining the geometry of the cell. Considering the capacities of OpenFOAM in magnetohydrodynamic modeling, the inlet-outlet flow pattern may be developed to a more realistic form of flow, including MHD as one of the main source of momentum. The effect of temperature can also become important in special operational conditions. To summarize, there are many aspects of transport phenomena in electrochemical systems that can be modeled by the developed codes within OpenFOAM toolbox platform, all of which can bring new scientific and numerical contributions to this field.

6 CONCLUSION

The research project presented in this thesis is a study that is covering the analysis of mass transfer of ions in electrolytic bath of aluminium electrolysis cell. This study analyzes mass transfer analysis in both cathode and anode diffusion layer and the bulk of the bath. The study should also consider that this field mutually influences and is influences by bath velocity field, creation of bubble below anode, current density distribution, and electrode reactions.

The experimental studies on the mass transfer are limited because of the harsh condition like high temperature and corrosiveness of the bath to the extent that even determination of ions is a controversial subject, and there are many models proposed for electrochemical reactions mechanisms at the electrodes. The uncertainties over the basic problems in addition to the coupled nonlinear nature of the mass transfer problem are the main obstacles that impose the limitations on the progress in this field.

However, there have been recent studies on the mass transfer of ions in the cathode diffusion boundary layers for $NaF\text{-}AlF_3$ mixtures by neglecting anode or bath effects on the concentration of ions in this region. Furthermore, the preliminary studies are all done for 1-D geometry in the cell without considering the current distribution over the electrodes and in the bath. In the study presented in this thesis, we try to widen the boundaries of mass transfer problem in order to overcome some defects and limitation of these studies.

Firstly, the mass transfer problem in $NaF\text{-}AlF_3\text{-}Al_2O_3$ is modelled for 1-D interelectrode geometry. Two mechanisms of migration and diffusion are considered as main flux terms in mass conservation equation. The effect of convection is added as turbulent diffusion. The results indicate major role of diffusion flux for electroactive ions at corresponding electrodes when the concentration profiles are fully developed. In the early stages before formation of concentration profiles, migration is of greater importance comparing to

diffusion. For electroinactive ions, diffusion is of the same magnitude as migration and opposes the concentration gradient created by migration in the early stages.

The 1-D model does not account for the distribution of current over the electrodes in the bath. Moreover, the mass transfer in interelectrode 1-D geometry cannot explain the mass transfer between interelectrode space and the regions between sidewall and crust. In the second step of this study, the electric current distribution is modelled for typical 2-D geometry of the cell. Moreover, mass conservation equations are solved in 2-D cell by considering the impact of migration and turbulent diffusion. A geometrical method is applied to calculate the wall distance field and turbulent diffusion coefficient. In this study, the transient behaviour of ion fluxes is given in different part of the cell.

The 2-D cell simulation shows other different diffusion fluxes that are resulted from concentration gradient between the interelectrode space and the region beside sidewalls and farther from electrodes. For example, $Al_2OF_6^{-2}$ is depleted near the anode so there is firstly the diffusion in interelectrode space from cathode to anode. Secondly, the lower concentration of $Al_2OF_6^{-2}$ in interelectrode region compared to region near sidewall creates diffusion fluxes from this region into the interelectrode region.

Although applying a geometrical 2-D model to include turbulent diffusion as the impact of convection on mass transfer is a new contribution in this work compared to the previous works, it does not take into account the real convective flux in the cell. A more rigorous approach is to solve Navier-Stokes equations, Poisson's equation of electric field, and mass transfer equations simultaneously to obtain the ideally realistic picture of the cell. A solver is developed in OpenFOAM, a C++ coding open source CFD platform, to include convection and chemical reactions in electrochemical cells. The solver is applied to a parallel-plate-electrode aluminium cell. The model solves Maxwell-Stefan equations and Navier-Stokes equation simultaneously by considering the bath chemical equilibrium at each time step.

The results obtained for a parallel-plate-electrode cell illustrates concentration profile for $NaAlF_4$ and $Na_2Al_2OF_6$ as major electroactive species under convection and by considering bath chemical equilibrium. The comparison between two cases of with and without bath chemical equilibrium shows that it takes more time for the case with bath equilibrium to reach steady state compared to the case without bath chemical equilibrium.

The main contributions obtained in this study can be summarized as below:

- Development of mass transfer model for the complete cell including cathode and anode diffusion layers in addition to the bulk of the bath.
- Considering NaF-AlF_3-Al_2O_3 system and alumina-cryolite dissolution equilibrium.
- Development of 2-D model for the ionic fluxes in the cell considering migration and turbulent diffusion. This development gives broader view over transient 2-D fluxes between different cell regions for two categories of electroactive and electroinactive ions.
- Application of a 2-D geometrical model to calculate the turbulent diffusion for 2-D geometries. This model can be applied to any 2-D geometry to estimate the turbulent diffusion in electrochemical systems.
- Development of an open source C++ library on OpenFOAM platform to model current distribution for nonlinear electrode kinetics. Moreover, there is another library that is developed to model mass transfer in dilute and concentrated solutions.

6.1 Future works

Although this research project brings out mentioned scientific contributions compared to limited previous studies in the field of mass transfer in high temperature electrolysis cell, it comes with several limitations and defects that can be surpassed or improved in future

work. The perspective of future works to improve or to develop the presented study can be outlined as:

- The role of convection is of great importance in the mass transfer of the cell. Convective mass transfer, especially near electrodes, is influenced by other phenomena. Over the anode, the evolution of bubbles creates a convective movement which influences the entire cell. This has a very important role in the mass transfer in the anode diffusion layer. On the other side of the cell, MHD momentum is transferred to the bath through the movement of the aluminium layer. This effect is of great importance in the instability of the cell. On one side, adding these two phenomena to the model demands a tightly coupled field solution and also a robust numerical toolbox. On the other side, the results bring a lot of information of the mass transfer in boundary layers of the cell.
- The assumption of an isothermal cell is a common assumption in the studies about mass transfer in this type of cell. However, this field can have an important impact on the geometry of the cell and on convection, the side ledge being essentially driven by the heat flux through the side of the cell. The source of heat is the Joule effect created by the passage of the electric current through the electrolytic bath. Therefore, this coupling can be the closure point for the analysis of transport phenomena in the cell.
- OpenFOAM gives many capabilities to the user to solve multi-physics, multi-region transport problems. The library that was developed for the mass transfer and electrode kinetics is just a starting point. It can be developed further to add more flexible convective schemes. MHD and muti-phase solvers of OpenFOAM can be very helpful toolboxes if they are coupled to the existing code.
- There has been several boundary condition treatments developed in this study, for linear Robin boundary conditions and also nonlinear Newman boundary conditions. However, there is still a need to implement the coupled migration-diffusion boundary condition of type Robin in OpenFOAM to be able to model

the electrochemical fluxes at electrodes and fully model the tertiary current distribution situations.

For conclusion, the analysis of the ion movement is a multiphysic nonlinear problem that needs to be treated by multiphysic robust numerical tools. Fulfillment of all aspects related to the movements of ions is difficult to be done in one step; however, this study can be used as one of the preliminary steps for more robust simulation of this aspect of aluminium electrolysis cell and other similar electrochemical systems.

APPENDIX A ELECTRIC FIELD MODELING AND ELECTRIC CURRENT CONSERVATION

As discussed in chapter 2, the governing equation for the electric field is Poisson's equation, which can be simplified to Laplacian of electric field when considering the electroneutrality assumption and constant conductivity in the bath as it is shown in below:

$$\nabla.(\sigma\nabla\varphi) = 0 \qquad \text{A.1}$$

The application of this equation would make the electric current that passes each node or each cell in the domain conserved. As for boundaries of the system, there are other mathematical models that illustrate the transport phenomena and fluxes like electric potential or current on the electrodes and insulated walls.

A.1 Boundary conditions for the electric field

The boundary conditions of an electrochemical system can be either a specified electric current or a specified electric potential, as it is shown in Figure A.1. However, it is essential to impose at least one Dirichlet boundary condition for the electric potential to have a reference point for electric potential in the cell, so all cases in Figure A.1 are valid except the last pair of boundary conditions that is not acceptable.

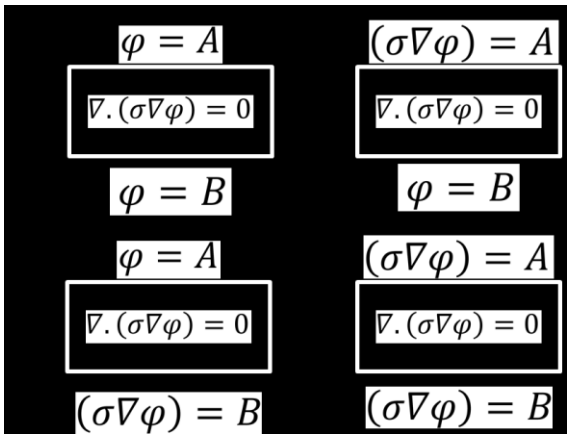

Figure A.1 Boundary conditions combinations for the electric field

Generally speaking, the parameters A and B in Figure A.1 depend upon the kinetics of electrochemical reactions and the assumptions made to get them. As it was discussed in chapter 2, there are three major assumptions to treat electrochemical reactions in the boundaries of the system. The first assumption is called the primary current distribution (PCD), which considers constant overpotential along the electrodes, so the boundary conditions are simply Dirichlet boundary conditions of electric potential, see Figure A.1A).

The secondary current distribution (SCD) assumption takes into account the kinetics at the electrode. The kinetics of the reactions correlates the electrode current to the surface overpotential through the Butler-Volmer (B.V.) equation. The linear and Tafel equation are two especial forms of the B.V. equation, for small and large electrode overpotential, respectively.

The third model is tertiary current distribution (TCD), which adds the effect of mass transfer over the electrodes. In addition to the kinetics of reactions, this will again limit the electric current over the electrodes.

Several models have been proposed for the electrode reactions in aluminum electrolysis cell. These models present different forms of B.V. equation for anode and cathode reactions. The model considered in this study takes into account the Tafel form

(exponential) for the anode reaction and the linear form of B.V. for the cathode. For the linear B.V. case, electrode current (or gradient of potential) is equal to a linear function of overpotential. For Tafel or more general forms of B.V., the function is exponential and nonlinear.

The existing boundary conditions in OpenFOAM are usually explicitly field-dependent either for the field (fixedValue) or for the gradient of the field (fixedGradient). For example, these boundary conditions can be used for the insolated walls when there is no current that passes through the wall (zeroGradient). It is also possible to use fixedValue boundary condition for primary current distribution. The fixedGradient boundary condition is capable of applying uniform current flow over the boundary cell faces(patches), as it is imposed for infinitely long parallel-plate-electrodes cell. However, modeling secondary boundary condition is more difficult because the field and the gradient are implicitly combined.

MixedFvPatchField is the generic form of boundary condition developed in OpenFOAM. It can be used to model the linearized combination of a field and its gradient. This boundary condition is simplifying to fixedValue and to fixedGradient boundary conditions when the fraction factor, α, is equal to one and zero, respectively.

$$\varphi_{face} = \alpha.valueExpression + (1-\alpha)(\varphi_{center} + gradExpression.\delta) \quad \text{A.2}$$

Where the subscripts $face$ and $center$ show the values at face (patch) and cell center, respectively; δ is the distance between cell center and face center in each cell. The linear form of Butler-Volmer is derived as LinearBVFvPatchField, in which $valueExpression$ and $gradExpression$ are calculated as a function of conductivity, exchange current density, temperature and other Butler-Volmer kinetic parameters.

However, this approach cannot take into account other nonlinear forms of Butler-Volmer like Tafel equation, since the field and the gradient of the field are not linearly coupled. Therefore, there is a need for the manipulation of the electric field matrix in order to apply the nonlinear boundary conditions on the electrodes. This is done through the manipulation of the finite volume method (*fvm*) matrixes. The flow chart of the iterative algorithm used in the electric field solution and patch (boundary) *fvm* matrix member manipulation is given below, in Figure A.2.

The algorithm starts by imposing primary current distribution over both electrodes. Then, the boundary faces (patches) are selected and the gradient of electric field is calculated over the patches. This gradient is the used to modify the values that are assigned as fixedValue boundary conditions for the next round of primary current distribution calculation iteration. The loop is stopped when the convergence criteria obtained for the electric potential field are met.

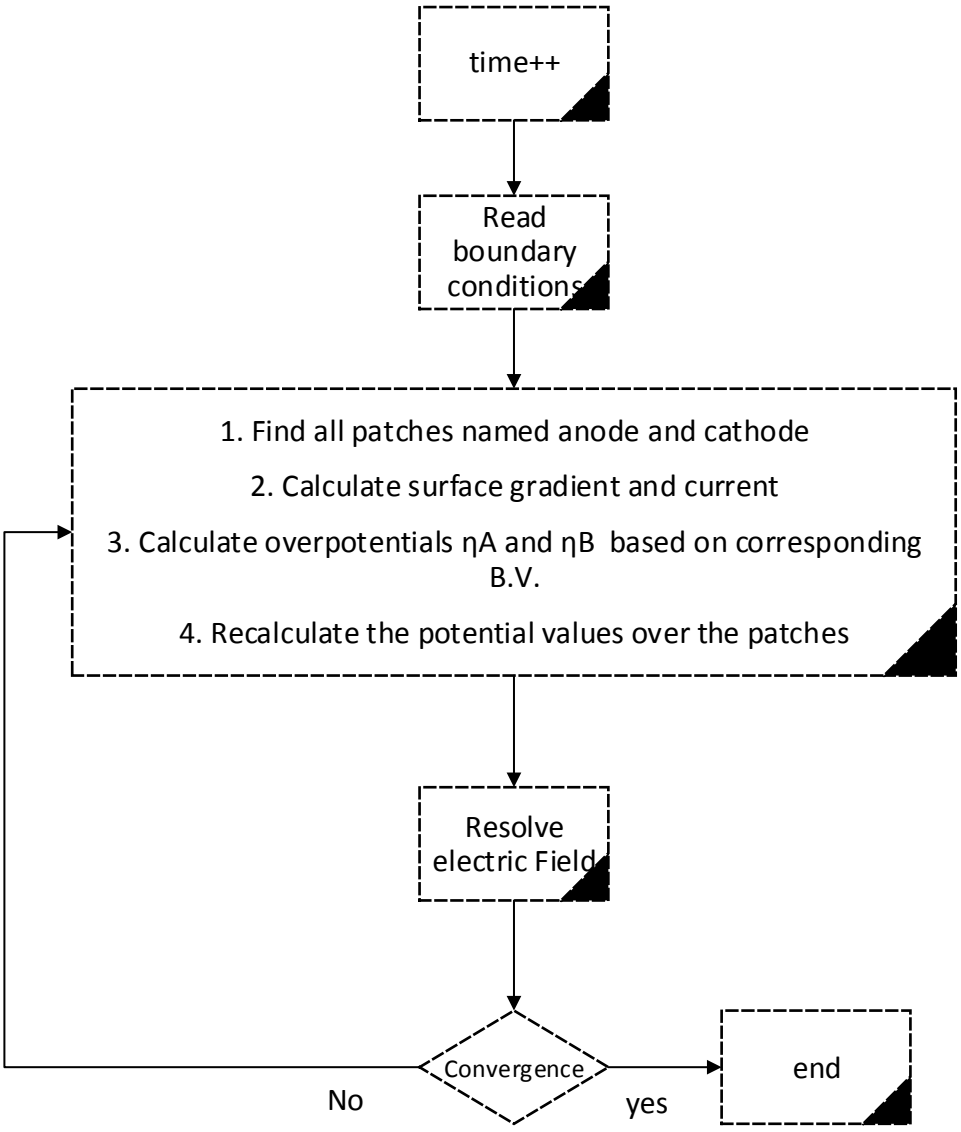

Figure A.2 Solution algorithm in OpenFOAM for secondary current distribution assumption

A.2 The numerical simulation and software structure

As it was discussed in the introduction section of this chapter, open source codes have this advantage to provide users with a collaborative platform for developing new ideas and applications based on the features of the source code. The work presented in this chapter is conducted on the OpenFOAM® platform. The code is developed to solve the current, momentum and mass conservation equations. The structure of the libraries developed to solve these field equations is given in Figure A.3.

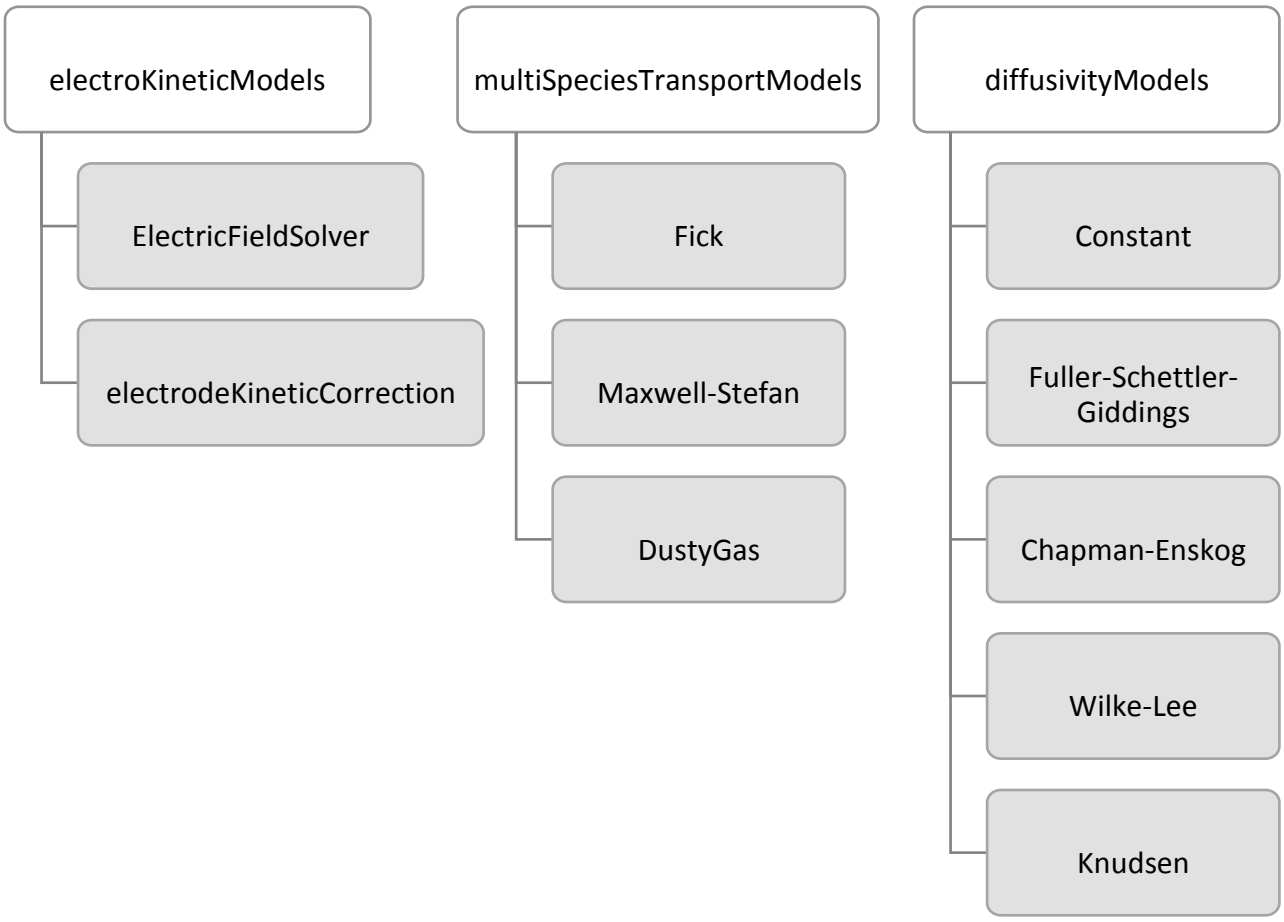

Figure A.3 Structure of mass transfer library in OpenFOAM

There are three subsections in the mass transfer library to treat different aspects of mass transfer. However, the mass transfer code has also access to other libraries implemented

in OpenFOAM, through the objects that are created from classes like turbulenceModels and thermoClass, in order to treat the velocity, eddy diffusion and reactions, respectively.

Looking back at mass transfer library, the first part of the library is designed to solve the electric field. For constant electric conductivity, the electric field is decoupled from the concentration field (primary and secondary current distributions). In such cases, the Poisson's equation can be easily solved. The third block calculates diffusivities based on different models for gases and liquids. The mass conservation equation based on different flux models is implemented in the central library of multiSpeciesTransportModels.

A.2.1 File structure of solver cases in OpenFOAM

The libraries and solvers form the main part of the computational code in OpenFOAM. However, the geometry, meshing, initial values for the fields to be solved and the selection of the methods for discretization or solution are gathered in the *case* directory.

The structure of the *case* directory in OpenFOAM is shown in Figure A.4. Generally speaking, the runtime control parameters like *startTime*, *endTime*, and *timeSteps* are set in the *controlDict* file. Discretization schemes are located in *fvSchemes* file. The equation solvers, tolerances and other algorithm controls are set for the run in *fvSolution* file.

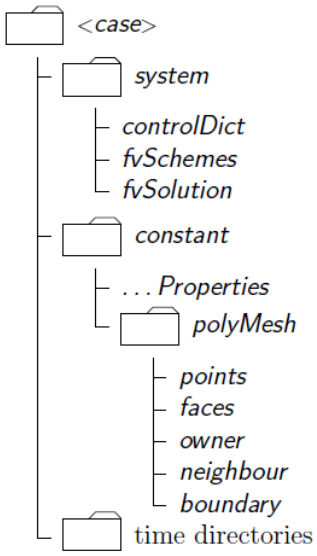

Figure A.4 File structure of OpenFOAM cases

The reactions, constants and transport properties, thermodynamic and thermophysical parameters are all given in constant directory. Geometry and meshing tool are also located in *polymesh/blockMesh* files, which is located in constant properties.

Finally, the last directory in *case* is the *0* directory, which is for initial values of the fields. The other time directories are added and save in *case* directory when each run time is completed.

REFERENCES

[1] K. Grjotheim et H. Kvande (1993). *Introduction to Aluminium Electrolysis: Understanding the Hall-Héroult Process*, 2nd edition édition. Aluminium-Verlag, Dusseldorf, 260 p.

[2] Blais, M., Désilets, M. et Lacroix, M. (2013). Optimization of the cathode block shape of an aluminum electrolysis cell. *Applied Thermal Engineering,* volume 58, numéro 1-2, p. 439-446.

[3] Thonstad, J., Fellner, P., Haarberg, G. M., Híveš, J., Kvande, H. et and Sterten, A. (2001). *Aluminium Electrolysis. Fundamentals of the Hall_Héroult Process*. Aluminium-Verlag, Dusseldorf,

[4] Tual, A. et Rolin, M. (1972). Etude des nombres de transport ioniques dans les mélanges cryolithe-alumine selon le principe de la methode de Hittorf-I. mise en oeuvre de la methode. *Electrochimica Acta,* volume 17, numéro 11, p. 1945-1954.

[5] Rolin, M. (1972). Conductivite electrique des melanges a base de cryolithe fondue: Systemes NaFAlF3, AlF6Na3Al2O3 et AlF6Na3CaF2. *Electrochimica Acta,* volume 17, numéro 12, p. 2293-2307.

[6] Híveš, J., Fellner, P. et Thonstad, J. (2013). Transport numbers in the molten system NaF-KF-AlF3-Al2O3. *Ionics,* volume 19, numéro 2, p. 315-319.

[7] Sokhanvaran, S., Thomas, S. et Barati, M. (2012). Charge transport properties of cryolite-silica melts. *Electrochimica Acta,* volume 66, p. 239-244.

[8] Boissonneau, P. et Byrne, P. (2000). Experimental investigation of bubble-induced free convection in a small electrochemical cell. *Journal of Applied Electrochemistry,* volume 30, numéro 7, p. 767-775.

[9] Kiss, L. I., Poncsák, S., Toulouse, D., Perron, A., Liedtke, A. et Mackowiak, V. (2004). Detachment of bubbles from their nucleation sites. Dans *Multiphase Phenomena and CFD Modeling and Simulationin Materials Processes*p. 159-168.

[10] Perron, A., Kiss, L. I. et Poncsák, S. (2006). An experimental investigation of the motion of single bubbles under a slightly inclined surface. *International Journal of Multiphase Flow,* volume 32, numéro 5, p. 606-622.

[11] Tual, A. et Rolin, M. (1972). Etude des nombres de transport ioniques dans les melanges cryolithe-alumine fondus selon le principe de la methode de hittorf-II. Resultats. *Electrochimica Acta,* volume 17, numéro 12, p. 2277-2291.

[12] Gagnon, F., Ziegler, D. et Fafard, M. (2011). A preliminary finite element electrochemical model for modelling ionic species transport in the cathode block of a Hall-Héroult cell. Dans *TMS Light Metals*p. 537-542.

[13] Solheim, A. (2002). Crystallization of cryolite and alumina at the metal-bath interface in aluminium reduction cells. Dans *Light Metals: Proceedings of Sessions, TMS Annual Meeting (Warrendale, Pennsylvania)*p. 225-230.

[14] Solheim, A. (2012). Concentration gradients of individual anion species in the cathode boundary layer of aluminium reduction cells. Dans *TMS Light Metals*p. 665-670.

[15] Newman, J. S. (1991). *Electrochemical systems*, second edition édition. Prentice-Hall, New Jersey, 560 p.

[16] Zoric, J., Rousar, I., Kuang, Z. et Thonstad, J. (1996). Current distribution in aluminium electrolysis cells with Søderberg anodes part II: Mathematical modelling. *Journal of Applied Electrochemistry,* volume 26, numéro 8, p. 795-802.

[17] Hyland, W. W. (1984). *Light Metals 1984,* p. 711-720.

[18] Ziegler, D. (1991). Current distribution modeling for novel alumina electrolysis. Dans *Light Metals 1991*p. 363-374.

[19] Solli, P. A., Haarberg, T., Eggen, T., Skybakmoen, E. et Sterten, A. (1994). *Light Metals 1994,* p. 195-203.

[20] Zoric, J., Roušar, I. et Thonstad, J. (1997). Mathematical modelling of industrial aluminium cells with prebaked anodes Part I: Current distribution and anode shape. *Journal of Applied Electrochemistry,* volume 27, numéro 8, p. 916-927.

[21] Fraser, K. J., Billinghurst, D., Chen, K. L. et Keniry, J. T. (1989). Some applications of mathematical modelling of electric current distributions in Hall Heroult cells. Dans *Light Metals: Proceedings of Sessions, AIME Annual Meeting (Warrendale, Pennsylvania)*p. 219-226.

[22] Zoric, J., Roušar, I., Thonstad, J. et Haarberg, T. (1997). Mathematical modelling of aluminium cells with prebaked anodes Part II: Current distribution and influence of sideledge. *Journal of Applied Electrochemistry,* volume 27, numéro 8, p. 928-938.

[23] Rollet, A., Sarou-Kanian, V. et Bessada, C. (2010). Self-diffusion coefficient measurements at high temperature by PFG NMR. *Comptes Rendus Chimie,* volume 13, numéro 4, p. 399-404.

[24] Ratkje, S. K., Rajabu, H. et Førland, T. (1993). Transference coefficients and transference numbers in salt mixtures relevant for the aluminium electrolysis. *Electrochimica Acta,* volume 38, numéro 2-3, p. 415-423.

[25] Frank, W. B. et Foster, L. M. (1957). Investigation of transport phenomena in the cryolite-alumina system by means of radioactive tracers. *Journal of Physical Chemistry,* volume 61, numéro 11, p. 1531-1536.

[26] Fellner, P., Híveš, J. et Thonstad, J. (2011). Transport numbers in the molten system NaF-KF-AlF 3-Al 2O 3. Dans *TMS Light Metals*p. 513-516.

[27] Kuzmin, R. N., Savenkova, N. P. et Shobukhov, A. V. (2009). Mathematical modeling of aluminum electrolysis over a long interval of time. *Moscow University Physics Bulletin,* volume 64, numéro 3, p. 294-298.

[28] Kuzmin, R. N., Provorova, O. G., Savenkova, N. P. et Shobukhov, A. V. (2009). Mathematical modelling of electrochemical reactions in aluminium reduction cells. Dans *WIT Transactions on Engineering Sciences*, volume 65p. 141-149.

[29] Li, J., Xu, Y., Zhang, H. et Lai, Y. (2010). An inhomogeneous three-phase model for the flow in aluminium reduction cells. *International Journal of Multiphase Flow,*

[30] Sterten, Å (1988). Current efficiency in aluminium reduction cells. *Journal of Applied Electrochemistry,* volume 18, numéro 3, p. 473-483.

[31] J.A. Wesselingh, R. K. (2000). *Mass transfer in multicomponent mixtures*, 1st. ed. éditionDelft, Netherland,

[32] Bortels, L., Deconinck, J. et Van Den Bossche, B. (1996). The multi-dimensional upwinding method as a new simulation tool for the analysis of multi-ion electrolytes controlled by diffusion, convection and migration. Part 1. Steady state analysis of a parallel plane flow channel. *Journal of Electroanalytical Chemistry,* volume 404, numéro 1, p. 15-26.

[33] Byrne, P., Fontes, E., Parhammar, O. et Lindbergh, G. (2001). A Simulation of the Tertiary Current Density Distribution from a Chlorate Cell: I. Mathematical Model. *Journal of the Electrochemical Society,* volume 148, numéro 10, p. D125-D132.

[34] Dahlkild, A. A. (2001). Modelling the two-phase flow and current distribution along a vertical gas-evolving electrode. *Journal of Fluid Mechanics,* volume 428, p. 249-272.

[35] Vogt, H. (1980). On the supersaturation of gas in the concentration boundary layer of gas evolving electrodes. *Electrochimica Acta,* volume 25, numéro 5, p. 527-531.

[36] Wallgren, C. F., Bark, F. H. et Andersson, B. -. (1996). Electrolysis of a binary electrolyte in two-dimensional channel flow. *Electrochimica Acta,* volume 41, numéro 18, p. 2909-2916.

[37] Aldas, K. (2004). Application of a two-phase flow model for hydrogen evolution in an electrochemical cell. *Applied Mathematics and Computation,* volume 154, numéro 2, p. 507-519.

[38] Pillay, B. et Newman, J. (1993). Modeling diffusion and migration in dilute electrochemical systems using the quasi-potential transformation. *Journal of the Electrochemical Society,* volume 140, numéro 2, p. 414-420.

[39] Gerbeau, J., Le Bris, C. et Lelièvre, T. (2006). Mathematical Methods for the Magnetohydrodynamics of Liquid Metals.

[40] Descloux, J., Flueck, M. et Romerio, M. V. (1994). Stability in aluminum reduction cells: a spectral problem solved by an iterative procedure. Dans *Light Metals: Proceedings of Sessions, TMS Annual Meeting (Warrendale, Pennsylvania)*p. 275-281.

[41] Gerbeau, J. -., Lelièvre, T. et Le Bris, C. (2003). Simulations of MHD flows with moving interfaces. *Journal of Computational Physics,* volume 184, numéro 1, p. 163-191.

[42] Kadkhodabeigi, M. (2008). Two-dimensional model of melt flows and interface instability in aluminum reduction cells. Dans *TMS Light Metals*p. 443-448.

[43] Kohno, H. et Molokov, S. (2007). Finite element analysis of interfacial instability in aluminium reduction cells in a uniform, vertical magnetic field. *International Journal of Engineering Science,* volume 45, numéro 2-8, p. 644-659.

[44] Morris, S. J. S. et Davidson, P. A. (2003). Hydromagnetic edge waves and instability in reduction cells. *Journal of Fluid Mechanics,* numéro 493, p. 121-130.

[45] Sele, T. (1977). Instabilities of the metal surface in electrolytic alumina reduction cells. *Metallurgical Transactions B,* volume 8, numéro 4, p. 613-618.

[46] Segatz, M. et Droste, C. (1994). Analysis of magnetohydrodynamic instabilities in aluminum reduction cells. Dans *Light Metals: Proceedings of Sessions, TMS Annual Meeting (Warrendale, Pennsylvania)*p. 313-322.

[47] Ziegler, D. P. (2010). Hall cell MHD instability: Recent theoretical analyses and experimental support. Dans *TMS Annual Meeting*p. 401-414.

[48] Kiss, L. I. et Vékony, K. (2008). Dynamics of the gas emission from aluminum electrolysis cells. Dans *TMS Light Metals*p. 425-429.

[49] Levich, B. (1942). The theory of concentration polarisation. *Acta Phys. Chim.,* volume 17, p. 257-307.

[50] Fares, E. et Schröder, W. (2002). A differential equation for approximate wall distance. *International Journal for Numerical Methods in Fluids,* volume 39, numéro 8, p. 743-762.

[51] Chung, M. -. (2000). Numerical method for analysis of tertiary current distribution in unsteady natural convection multi-ion electrodeposition. *Electrochimica Acta,* volume 45, numéro 24, p. 3959-3972.

[52] Kee, R. J., Coltrin, M. E. et Glarborg, P. (2003). *Chemically Reacting Flow: Theory and Practice*. Wiley Hoboken, NJ,

[53] Ariana, M., Désilets, M. et Proulx, P. (2013). Numerical analysis of ionic mass transfer in the electrolytic bath of an aluminium reduction cell. Dans *TMS Light Metals*p. 695-699.

[54] Zoric, J., Thonstad, J. et Haarberg, T. (1998). Influence on current distribution by the initial shape and position of an anode and by the curvature of the aluminum in prebake aluminum cells. Dans *Light Metals: Proceedings of Sessions, TMS Annual Meeting (Warrendale, Pennsylvania)*p. 445-453.

[55] Zoric, J., Thonstad, J. et Haarberg, T. (1999). Influence of the initial shape and position of an anode and the curvature of the aluminum on the current distribution in prebaked aluminum cells. *Metallurgical and Materials Transactions B: Process Metallurgy and Materials Processing Science,* volume 30, numéro 2, p. 341-348.

[56] Zhang, Y. et Rapp, R. A. (2004). Modeling the dependence of alumina solubility on temperature and melt composition in cryolite-based melts. *Metallurgical and Materials Transactions B: Process Metallurgy and Materials Processing Science,* volume 35, numéro 3, p. 509-515.

[57] Zhang, Y., Wu, X. et Rapp, R. A. (2003). Solubility of alumina in cryolite melts: Measurements and modeling at 1300 K. *Metallurgical and Materials Transactions B: Process Metallurgy and Materials Processing Science,* volume 34, numéro 2, p. 235-242.

[58] Hiveš, J., Thonstad, J., Sterten, Å et Fellner, P. (1996). Electrical conductivity of molten cryolite-based mixtures obtained with a tube-type cell made of pyrolytic boron nitride. *Metallurgical and Materials Transactions B: Process Metallurgy and Materials Processing Science,* volume 27, numéro 2, p. 255-261.

[59] Ariana, M., Désilets, M. et Proulx, P. On the analysis of ionic mass transfer in the electrolytic bath of an aluminum reduction cell. *Canadian Journal of Chemical Engineering,* volume 92, numéro 11, p. 1951-1964.

[60] Solheim, A. et Sterten, A. (1999). Activity of alumina in the system NaF-AlF 3-Al 2O 3 at NaF/AlF 3 molar ratios ranging from 1.4 to 3. Dans *Light Metals: Proceedings of Sessions, TMS Annual Meeting (Warrendale, Pennsylvania)*p. 445-452.

[61] Robert, E., Olsen, J. E., Danek, V., Tixhon, E., Østvold, T. et Gilbert, B. (1997). Structure and thermodynamics of alkali fluoride-aluminum fluoride-alumina melts. Vapor pressure, solubility, and Raman spectroscopic studies. *Journal of Physical Chemistry B,* volume 101, numéro 46, p. 9447-9457.

[62] Bouyer, F., Picard, G. et Legendre, J. -. (1997). Computational and analytical chemistry: Methodology to study chemical reactions between sodium, calcium, and aluminum fluorides in molten cryolite. *International Journal of Quantum Chemistry,* volume 61, numéro 3, p. 507-514.

[63] Leistra, J. A. et Sides, P. J. (1988). Hyperpolarization at gas evolving electrodes-II. Hall/heroult electrolysis. *Electrochimica Acta,* volume 33, numéro 12, p. 1761-1766.

[64] Thonstad, J. (1969). Chronopotentiometric measurements on graphite anodes in cryolite-alumina melts. *Electrochimica Acta,* volume 14, numéro 2, p. 127-134.

[65] Issa, R. I. (1986). Solution of the implicitly discretised fluid flow equations by operator-splitting. *Journal of Computational Physics,* volume 62, numéro 1, p. 40-65.

[66] Jasak, H. (1996). Error analysis and estimation for the finite volume method with applications to fluid flows. *Error Analysis and Estimation for the Finite Volume Method with Applications to Fluid Flows,*